THE UNIVERSITY OF EDINBURGH

INSTITUTE OF ECOLOGY AND RESOURCE MANAGEMENT

CARBON AND WATER FLUXES IN A BOREAL FOREST ECOSYSTEM

MARK BRYCE RAYMENT

BSc. (Hons.) Bath

MSc. (Dist.) Essex

A THESIS SUBMITTED FOR THE DEGREE OF DOCTOR OF PHILOSOPHY

MAY 1998

EX BIBL. UNIV. EDINBURGH

Declaration

This thesis has been composed by myself.

The work this thesis describes is my own work, except where stated otherwise, and has not been submitted in application for any other degree.

Mark Rayment

May 1998

Dedication

I dedicate this thesis, as I dedicate everything, to my wife, Natalia. Without her, none of this would have been possible, or worthwhile.

And to Santiago, too small to realise how he's helped me over the last months.

Acknowledgements

It is a privilege to acknowledge my supervisor, Paul Jarvis. His tireless enthusiasm for all things has been inspirational.

Craig Barton, Jonathan Massheder and Steve Scott have each contributed significantly to everything I have done in Edinburgh, and for all the time that they have spend helping me, I thank them.

Many thanks are due to Alex, Davy, Eric and Peter in the University workshop, where they have been an inexhaustible supply of materials and good advice.

Thanks are also due to the BOREAS project staff who helped in many ways with the project infrastrucure.

This work was made possible through the award of a NERC studentship, through funding provided through the NERC TIGER programme, and through the NASA Mission to Planet Earth programme.

Thanks to Jon Massheder, Steve Scott, Pete Levy, Yadvinder Malhi, Mike Perks, Ford Cropley and John Moncrieff, all University of Edinburgh, and Andy Morse, University of Liverpool, for keeping the measurement systems running during absences from the field. Thanks to Dr. J. Norman, University of Wisconsin, for his part in the inter-comparison described in Chapter 2. Thanks to Paula Pacholek, Parks Canada, for measuring the organic matter thickness described in Chapter 3. Thanks to Andy Gray, University of Edinburgh, for undertaking the nutrient analyses described in Chapters 4 & 5. The shoot gas exchange measurements described in Chapter 5 represent an equal contribution of myself and Dr. D. Loustau, INRA, Bordeaux. Thanks are also due to Dr. D. Loustau for much helpful discussion concerning that chapter. The eddy covariance data described in Chapter 5 is largely the work of J. Massheder, University of Edinburgh. Thanks to Belinda Medlyn for her help using and modifying the MAESTRA model, described in Chapter 6.

Thanks to everyone who has made my time in Edinburgh funnier and more interesting than it would have in their absence.

Publications

PAPERS IN REFEREED JOURNALS

Rayment, M.B. and Jarvis, P.G. (1997) An improved open chamber system for measuring soil CO_2 effluxes in the field. *Journal of Geophysical Research-Atmospheres* **102**, 28779-28784.

Norman, J.M., Kucharik, C.J., Gower, S.T., Baldocchi, D.D., Crill, P.M., **Rayment, M.**, Savage, K. and Striegl, R.G. (1997) A comparison of six methods for measuring soil-surface carbon dioxide fluxes. *Journal of Geophysical Research-Atmospheres* **102**, 28771-28777.

Jarvis, P.G., Massheder, J.M., Hale, S.E., Moncrieff, J.B., **Rayment, M.** and Scott, S.L. (1997) Seasonal variation of carbon dioxide, water vapour, and energy exchanges of a boreal black spruce forest. *Journal of Geophysical Research-Atmospheres* **102**, 28953-28966.

Lavigne, M.B., Ryan, M.G., Anderson, D.E., Baldocchi, D.D., Crill, P.M., Fitzjarrald, D.R., Goulden, M.L., Gower, S.T., Massheder, J.M., McCaughey, J.H., **Rayment, M.** and Striegl, R.G. (1997) Comparing nocturnal eddy covariance measurements to estimates of ecosystem respiration made by scaling chamber measurements at six coniferous boreal sites. *Journal of Geophysical Research-Atmospheres* **102**, 28977-28985.

PRESENTATIONS AT CONFERENCES AND WORKSHOPS

Rayment, M.B. & Kruijt, B. (1995) Sub-canopy scale carbon fluxes in BOREAS. *XXth EGS conference*. Hamburg, Germany, April 1995.

Rayment, M.B. (1997) Photosynthesis and respiration of black spruce branches in BOREAS. *BOREAS scientific workshop*. Annapolis, USA, March 1997.

Rayment, M.B. (1997) Understanding the component fluxes of net ecosystem exchange. *XXIInd EGS conference*. Vienna, Austria, April 1997.

Jarvis, P.G., Massheder, J.M., **Rayment, M.**, Moncrieff, J.B., and Scott, S.L. (1997) Seasonal variation of carbon dioxide, water vapour, and energy exchanges of a boreal black spruce forest. *XXIInd EGS conference*, Vienna, Austria, April 1997.

Rayment, M.B. (1997) An open chamber system for measuring soil CO_2 efflux. *Euroflux soil respiration workshop*. Uppsala, Sweden, July 1997.

Rayment, M.B. (1997) Night-time corrections to eddy covariance data using chamber methods. *Comparative study on tower-based data between several forests in the world* (Workshop). Hiroshima, Japan, September 1997.

Abstract

To obtain a better understanding of the functioning of a globally important biome, the BOREAS project set out to make measurements of the interactions between a number of boreal ecosystems and the atmosphere. This study is concerned with measurements made in one such ecosystem, the old-growth black spruce (OBS) site of the BOREAS Southern study area (SSA), located in Saskatchewan, Canada, during the period 1993 – 1996. This thesis focuses on efforts to understand the net ecosystem exchange of CO_2 and water vapour in terms of the sub-component fluxes operating within the ecosystem. The component fluxes of primary interest are photosynthesis, respiration and evapotranspiration of foliage, and the efflux of CO_2 from the forest floor. Woody biomass respiration and changes in the storage of CO_2 in the air mass within the ecosystem are also considered. Methodologies were developed to study these fluxes on a continuous basis.

An "open" system gas exchange chamber for measuring soil CO_2 efflux was designed that eliminated the major problems that have been associated with this methodology in the past. The system was used to investigate temporal and spatial variation in soil CO_2 efflux at the field site. A scheme that integrated this temporal and spatial variation was used to estimate the CO_2 efflux from the forest floor for an entire year. Spatial variability in soil CO_2 efflux was high, and was related empirically to the thickness of the dead moss layer. Hour to hour variation was well described as an exponential function of soil temperature, and was significantly related to atmospheric turbulence. Seasonally, soil CO_2 efflux varied between low, but positive, rates before the springtime thaw and after the winter freeze, to rates as high as 14 $\mu mol\ m^{-2}\ s^{-1}$ in late summer. The total annual carbon efflux from the soil for 1996 varied from point to point between 152 and 1310 g (C) $m^{-2}\ yr^{-1}$, the total annual carbon efflux for the whole ecosystem was estimated to be 8.96 Mg (C) $ha^{-1}\ yr^{-1}$.

A "branch bag" methodology for studying the gas exchange of whole tree branches was developed and operated for an entire growing season. Daily maximum photosynthetic rates were zero at the beginning and end of the year and reached a maximum of $\approx 6\ \mu mol\ m^{-2}\ s^{-1}$. Night-time respiration reached a maximum rate of $\approx$

0.8 μmol g^{-1} s^{-1}. Maximum evapotranspiration rates rose rapidly from zero to a peak of ≈ 2 mmol m^{-2} s^{-1} as the upper soil layers thawed. Branch conductances reached a maximum of ≈ 35 mmol m^{-2} s^{-1}. Annual total daytime carbon uptake for individual branches ranged from 12.6 to 22.6 mol m^{-2} yr^{-1}, total night-time loss from 1.98 to 2.27 mol kg^{-1} yr^{-1} and total daytime transpiration from 1132 to 1947 mol m^{-2} yr^{-1}. Total annual gross photosynthesis for the canopy was estimated to be 9.60 Mg (C) ha^{-1} yr^{-1}, total foliage respiration was estimated to be 2.16 Mg (C) ha^{-1} yr^{-1}, and total above ground autotrophic respiration was estimated to be 3.03 Mg (C) ha^{-1} yr^{-1}.

Physiological parameters were extracted from gas exchange measurements made at three scales, shoots, branches and the whole canopy. Coherence was found between parameters extracted at the different scales. Three estimates of net biotic flux (NBF) for the ecosystem were obtained from: (a) a summation of the chamber-based measurements, scaled to the whole ecosystem; (b) a detailed canopy model (MAESTRA) parameterised from canopy structure and shoot gas exchange data; (c) a "big-leaf" model parameterised from eddy covariance data. The "big-leaf" estimate was in good agreement with the NBF measured by eddy covariance plus the storage term. During the daytime, the chamber-based method overestimated the NBF and MAESTRA underestimated the NBF compared to the eddy covariance measurements. During the night-time, both the chamber-based method and MAESTRA overestimated the loss of carbon from the ecosystem compared to the measured flux. Comparison of chamber data with eddy covariance data suggests biological and physical factors underlying the observed reduction in NBF under low turbulence conditions. This in turn suggests that current means of "correcting" data during these periods may be flawed.

In 1996, the estimated annual net carbon uptake for the ecosystem was 0.33 Mg (C) ha^{-1} yr^{-1}. This was the small difference between a large inward flux (total gross photosynthesis, 12.19 Mg (C) ha^{-1} yr^{-1}) and a large outward flux (total respiration, 11.63 Mg (C) ha^{-1} yr^{-1}). The carbon source/sink strength of this ecosystem is thus very sensitive to changes in environmental conditions, and the boreal region may be the location of a large positive feedback on global climate change.

Table of Contents

List of Symbols and Abbreviations xi

Chapter One
Introduction

ECOSYSTEM FUNCTION 1
SOIL CO_2 EFFLUX 3
FOLIAGE PHOTOSYNTHESIS, RESPIRATION AND TRANSPIRATION 8
EDDY COVARIANCE MEASUREMENTS 10
THESIS AIMS AND STRUCTURE 11
To quantify fluxes associated with ecosystem sub-components
To look inside the ecosystem "green box"
To compare methods of estimating the net biotic flux of the ecosystem
THE BOREAS PROJECT 12
SSA OBS SITE DESCRIPTION 13
EQUIPMENT INSTALLATION 14

Chapter Two
An Improved Open Chamber System for Measuring Soil CO_2 Effluxes in the Field

METHODS 16
Chamber design - pressure characteristics
Chamber design - collars
Field tests
Comparison with a closed system
RESULTS 21
DISCUSSION 24
SUMMARY 26

Chapter Three
Temporal and Spatial Variation of Soil Respiration in a Canadian Boreal Forest

METHODS 27
Equipment description
Data analysis
RESULTS 30
Instantaneous CO_2 efflux
Spatial variation
Long term temporal variation
Total yearly efflux
DISCUSSION 39
Temporal variation
Spatial variation
Response to turbulence
SUMMARY 44

Chapter Four
Long Term Measurement of Photosynthesis, Respiration and Transpiration of Black Spruce (*Picea mariana*)
MATERIALS AND METHODS 46
Branch bag description
Gas exchange calculations
Branch measurements
Sources of errors
RESULTS 53
Photosynthesis & respiration
Transpiration & conductance
Branch carbon balance
DISCUSSION 62
SUMMARY 70

Chapter Five
Photosynthesis, Respiration and Conductance of Black Spruce at Three Organisational Scales: Shoot, Branch & Canopy
METHODS - GAS EXCHANGE 71
Shoot measurements
Branch measurements
Canopy measurements
MODEL PARAMETERISATION - PHOTOSYNTHESIS 73
Shoot measurements
Branch measurements
Canopy measurements
MODEL PARAMETERISATION – RESPIRATION 79
MODEL PARAMETERISATION – CONDUCTANCE 80
Shoot measurements
Branch measurements
Canopy measurements
RESULTS 82
Shoot photosynthesis
Branch photosynthesis
Canopy photosynthesis
Shoot respiration
Branch respiration
Canopy respiration
Conductance
DISCUSSION 98
Spatial variation
Temporal variation
Canopy photosynthesis
Variation in parameters between organisational scales
Conclusion
SUMMARY 105

Chapter Six
Estimating the Net Biotic Flux of a Boreal Forest Ecosystem
METHODS 106
Component summation estimate of NBF
MAESTRA estimate of NBF
BIG-LEAF estimate of NBF
Sensitivity of eddy covariance measurements to method of filling in gaps
RESULTS 109
Comparison of models with eddy covariance data
Sensitivity of eddy covariance measurements to method of filling in gaps
DISCUSSION 115
Comparison of model estimates with data
Low U_* corrections
Use of eddy covariance in long term studies of ecosystem function
SUMMARY 123

Chapter Seven
The Carbon Balance of a Boreal Forest Ecosystem
METHODS 125
Annual carbon balance for 1996
Sensitivity of 1996 annual carbon balance to temperature
RESULTS 127
Best estimate of annual carbon balance for 1996
Sensitivity of 1996 annual carbon balance to temperature
DISCUSSION 130
Sensitivity of ecosystem carbon balance to temperature
SUMMARY 131

Concluding Remarks 132

References 134

Appendix 142

List of Symbols and Abbreviations

	Description	Unit
A	Instantaneous photosynthetic CO_2 uptake rate	$\mu mol\ m^{-2}\ s^{-1}$
a	Soil CO_2 efflux turbulence response parameter	$s\ m^{-1}$
a_1	Empirical coefficient of Ball Woodrow Berry Leuning conductance model, Leuning (1995)	dimensionless
A_1	Respiration temperature response parameter	$\mu mol\ mol^{-1}$
A_j	RuBP regeneration (electron transport) limited rate of photosynthesis	$\mu mol\ m^{-2}\ s^{-1}$
A_r	Carbon allocation to below-ground parts	$Mg\ (C)\ ha^{-1}\ yr^{-1}$
A_v	Carboxylation limited rate of photosynthesis	$\mu mol\ m^{-2}\ s^{-1}$
BOREAS	Boreal ecosystem-atmosphere study	
C	Macronutrient concentration	$mg\ g^{-1}$
c	Solution concentration or	$mg\ dm^{-3}$
	Branch photosynthesis temperature response parameter	dimensionless
c_c	Chloroplastic CO_2 mole fraction	$\mu mol\ mol^{-1}$
c_i	Substomatal CO_2 mole fraction	$\mu mol\ mol^{-1}$
c_s	CO_2 mole fraction just outside the stomata	$\mu mol\ mol^{-1}$
D	Leaf to air mole fraction humidity deficit or	$mmol\ mol^{-1}$
	Air mole fraction humidity deficit	$mmol\ mol^{-1}$
d	Distance	m
D_0	Conductance humidity deficit response parameter	$mmol\ mol^{-1}$
D_{ag}	Above ground detritus production rate	$Mg\ (C)\ ha^{-1}\ yr^{-1}$
D_{ex}	Root exudate production rate	$Mg\ (C)\ ha^{-1}\ yr^{-1}$
D_m	Moss turnover rate	$Mg\ (C)\ ha^{-1}\ yr^{-1}$
D_r	Root detritus production rate plus fine root turnover rate	$Mg\ (C)\ ha^{-1}\ yr^{-1}$
E	Transpiration rate	$mmol\ m^{-2}\ s^{-1}$
E_0	Activation energy of respiration	$J\ mol^{-1}\ K^{-1}$
EC	Eddy covariance CO_2 flux	$\mu mol\ m^{-2}\ s^{-1}$
g_c	Conductance to CO_2 flux	$\mu mol\ m^{-2}\ s^{-1}$
g_w	Conductance to water vapour flux	$mmol\ m^{-2}\ s^{-1}$
g_{w0}	Minimum conductance to water vapour flux	$mmol\ m^{-2}\ s^{-1}$
g_{wmax}	Maximum conductance to water vapour flux	$mmol\ m^{-2}\ s^{-1}$
H_v	Activation energy of J_{max}, V_{max}, K_c or K_o	$J\ mol^{-1}\ K^{-1}$
H_d	Deactivation energy of J_{max} or V_{max}	$J\ mol^{-1}\ K^{-1}$
J_{max}	Maximal electron transport rate	$\mu mol\ e^{-}\ m^{-2}\ s^{-1}$
k	Respiration temperature response parameter ($\ln(Q_{10})/10$)	dimensionless
K_c	Michaelis constant for CO_2	$\mu mol\ mol^{-1}$
K_{c20}	Michaelis constant for CO_2 at 20 °C	$\mu mol\ mol^{-1}$
K_o	Michaelis constant for O_2	$mmol\ mol^{-1}$
K_{o20}	Michaelis constant for O_2 at 20 °C	$\mu mol\ mol^{-1}$
k_{PFD}	Conductance irradiance response parameter	dimensionless
n	Number	dimensionless
NBF	Net biotic flux	$\mu mol\ m^{-2}\ s^{-1}$
		$g\ (C)\ m^{-2}\ yr^{-1}$
NEE	Net ecosystem exchange	$\mu mol\ m^{-2}\ s^{-1}$

		g (C) m^{-2} yr^{-1}
NPP	Net primary productivity	Mg (C) ha^{-1} yr^{-1}
OBS	Old Black Spruce	Mg (C) ha^{-1} yr^{-1}
p	Thickness of peat layer	mm
P	Total ecosystem gross photosynthetic rate	Mg (C) ha^{-1} yr^{-1}
P_e	Net ecosystem exchange	Mg (C) ha^{-1} yr^{-1}
P_f	Foliage gross photosynthetic rate	µmol m^{-2} s^{-1}
		Mg (C) ha^{-1} yr^{-1}
PFD	Photon flux density	µmol m^{-2} s^{-1}
P_m	Moss gross photosynthetic rate	µmol m^{-2} s^{-1}
		Mg (C) ha^{-1} yr^{-1}
P_{max}	Asymptotic maximum photosynthetic rate	µmol m^{-2} s^{-1}
pO_2	Intracellular O_2 concentration	mmol mol^{-1}
Q	Photon flux density	µmol m^{-2} s^{-1}
Q_{10}	Respiration temperature response parameter	dimensionless
R	Gas constant (8.314) or	J mol^{-1} K^{-1}
	Total ecosystem respiration rate	Mg (C) ha^{-1} yr^{-1}
R_0	CO_2 efflux rate at 0 °C	µmol m^{-2} s^{-1}
R_{10}	CO_2 efflux rate at 10 °C	µmol m^{-2} s^{-1}
R_d	Daytime "dark" respiration rate	µmol m^{-2} s^{-1}
		Mg (C) ha^{-1} yr^{-1}
R_f	Foliage respiration rate	µmol m^{-2} s^{-1}
		Mg (C) ha^{-1} yr^{-1}
R_h	Heterotrophic respiration rate	Mg (C) ha^{-1} yr^{-1}
R_r	Root respiration rate	Mg (C) ha^{-1} yr^{-1}
R_{rg}	Root growth respiration rate	Mg (C) ha^{-1} yr^{-1}
R_{rm}	Root maintenance respiration rate	Mg (C) ha^{-1} yr^{-1}
R_s	Total soil respiration rate	Mg (C) ha^{-1} yr^{-1}
R_T	CO_2 efflux rate at temperature T	µmol m^{-2} s^{-1}
R_{Tav}	CO_2 efflux rate at T_{av}	µmol m^{-2} s^{-1}
R_w	Above-ground woody tissue respiration rate	Mg (C) ha^{-1} yr^{-1}
R_{wg}	Above-ground woody tissue growth respiration rate	Mg (C) ha^{-1} yr^{-1}
R_{wm}	Above-ground woody tissue maintenance respiration rate	Mg (C) ha^{-1} yr^{-1}
SSA	Southern Study Area	
S_v	Entropy term	J mol^{-1}
T	Leaf temperature	K
T_0	Respiration temperature response parameter	K
T_{av}	Daily average soil temperature	°C
T_l	Leaf temperature	K
T_{max}	High temperature at which conductance is g_{w0}	°C
T_{min}	Low temperature at which conductance is g_{w0}	°C
T_{opt}	Temperature at which conductance is g_{wmax} or	°C
	Temperature at which branch photosynthesis P_{max}	°C
T_{soil}	Soil temperature at 10 cm depth	°C
U_*	Friction velocity	m s^{-1}
V_{max}	Maximal velocity of carboxylation	µmol m^{-2} s^{-1}
V_{sol}	Volume of solution	dm^{-3}

W_{sample}	Mass of tissue sample	g
α	Apparent quantum efficiency of electron transport	$\mu mol\ \mu mol^{-1}$
Δ_{ag}	Above ground NPP	Mg (C) $ha^{-1}\ yr^{-1}$
Δ_r	Below ground NPP	Mg (C) $ha^{-1}\ yr^{-1}$
Δ_s	Change in soil organic matter pool	Mg (C) $ha^{-1}\ yr^{-1}$
ΔS	Storage flux	$\mu mol\ m^{-2}\ s^{-1}$
Γ^*	CO_2 compensation point in the absence of dark respiration	$\mu mol\ mol^{-1}$
ϕ	Apparent quantum efficiency of photosynthesis	$\mu mol\ \mu mol^{-1}$
θ	Convexity coefficient of the electron transport curve	dimensionless
Θ	Convexity coefficient of the irradiance dependence of photosynthetic CO_2 uptake	dimensionless
τ	Time constant	minutes
γ	Variogram dissimilarity measure	dimensionless
ε_t	Sum of environmental conditions at time t	dimensionless

Reference

Leuning, R. (1995) A critical appraisal of a combined stomatal-photosynthesis model for C_3 plants. *Plant Cell and Environment* **18**, 339-355.

Chapter One - Introduction

ECOSYSTEM FUNCTION

At the current rate of increase, the atmospheric CO_2 concentration will be more than double its pre-industrial level by the end of the 21st century (Houghton *et al.* 1995). This will repercussions throughout the global carbon cycle, but there are considerable uncertainties as to what the direct or indirect effects will be. A consensus of opinion exists that there will be a general global warming (Houghton *et al.* 1995), but how this warming will impact upon the biotic component of the earth-atmosphere system is a vital question, the answer to which is by no means clear. Because there are two-way interactions between the biosphere and the atmosphere, so that each affects the other in complex ways, it is possible that changes to one might feed back upon the other in a self-reinforcing, or, conversely, in a self-regulating way (Lashof 1989).

To be able to predict the future role of the biosphere in a changed climate, it is important that we begin by seeking to understand how the individual ecosystems that make up the biosphere function under present conditions. To obtain a better understanding of the functioning of a globally important biome, the boreal forest, the BOREAS project set out to make measurements of the interactions between a number of boreal ecosystems and the atmosphere. This work contained within this thesis is concerned with measurements made in one such ecosystem, the old-growth black spruce (OBS) site of the BOREAS Southern study area (SSA), located in Saskatchewan, Canada, during the period 1993 – 1996.

The ways in which ecosystems and the atmosphere interact may be regarded as either biophysical or biogeochemical in nature. To the former belong physical properties such as albedo and surface roughness, and the fluxes of heat and momentum. To the latter belong nutrient and carbon pool properties and fluxes of trace gases such as CO_2 and CH_4. Most experiments designed to investigate ecosystem-atmosphere interaction, have adopted a hierarchical approach, incorporating measurements made at a number of scales (e.g. Sellers 1994), from global inversion models (e.g. Keeling, Piper & Heimann 1996) and remote sensing (e.g. Cihlar, Chen & Li 1997) at the largest scale, through boundary-layer budgets (e.g. Denmead *et al.* 1996) and isotope

techniques (e.g. Ciais *et al.* 1995) at the regional scale, to net ecosystem exchanges of specific ecosystems at the stand scale, using, for example, the flux gradient and the eddy covariance techniques (e.g. Baldocchi *et al.* 1996; Moncrieff *et al.* 1997b). At the most local level, we can use enclosures or chambers to measure the fluxes of trace gases to and from specific components of an ecosystem. This thesis focuses on efforts to understand the net ecosystem exchange of CO_2 and water vapour in terms of the sub-component fluxes operating within an ecosystem, and draws on measurements made with a range of chambers, as well as with eddy covariance (Jarvis *et al.* 1997).

Chamber methods can be used to provide independent verification of measurements made by other techniques. For example, chamber measurements of leaf-scale photosynthesis or methane emissions from the soil may be compared to eddy covariance estimates of the ecosystem-scale fluxes of these gases. Chamber techniques can also be used to provide additional measurements, supporting the larger scale techniques listed above. As an example, to be able to use isotopic composition studies to integrate plant function to the canopy scale, it is necessary to identify the sources and sinks of trace gases within a canopy, and this is most conveniently done with chamber methods. Chamber-based measurements are also needed to supplement the eddy covariance technique. For example, in order to separate out the CO_2 exchange of a vegetation canopy from the CO_2 exchange of the whole ecosystem, chamber measurements of the soil CO_2 efflux can be subtracted from the net ecosystem flux, leaving the canopy flux as the residual. Additionally, there may be circumstances in which the eddy covariance technique does not give a reliable indication of ecosystem function (Moncrieff, Malhi & Leuning 1996), and in such situations, chamber measurements of trace gas exchange can be used to fill in gaps in the data.

To predict changes in ecosystem-atmosphere interactions in a changed climate, it is necessary to produce, from our measurements models of ecosystem function. Empirically based models of ecosystem function, such as "big leaf" models at the stand scale derived from eddy covariance measurements, can provide useful tools for integrating ecosystem function to larger scales. Because these models are generally

not mechanistic, however, there are potential problems when extrapolating their behaviour to conditions outside the range of natural variation from which they were derived. Chamber measurements of the individual components of net ecosystem flux, can be used to derive and validate models that are more closely related to the biological processes underlying ecosystem function, and may therefore be more robust in their predictive capabilities.

SOIL CO_2 EFFLUX

Current estimates put the total terrestrial soil carbon pool at over 1500 Gt C. This is the second largest pool of the global carbon cycle after the deep ocean, and more than twice the estimated living biomass pool (Schimel 1995). Estimates of the global total carbon efflux from the soil lie between 50 and 75 Gt C yr^{-1} (Raich and Schlesinger 1992), similar to, but slightly smaller than, global gross primary productivity (Houghton and Woodwell 1989). Of particular importance are the soils of the boreal region, which make up the largest soil organic matter stock (Lashof 1989). Accumulation of carbon in these soils is primarily the result of low soil temperatures (Van Cleve, Barney & Schlentner 1981; Bonan 1992), and experimental manipulations of soil temperature have been shown to increase soil organic matter decomposition rates, thereby increasing the soil CO_2 efflux and resulting in a reduction of the soil organic matter store (Van Cleve, Oechel & Hom 1990). Net ecosystem exchange is often the residual between two large fluxes, similar in size but opposite in sign (i.e. photosynthetic carbon uptake and respiratory carbon loss) and consequently a relatively small increase in the rate of soil respiration may be sufficient to switch the ecosystem from carbon sink to carbon source (Oechel *et al.* 1993). There is therefore, at least potentially, a major positive feedback between the temperature increases expected as a consequence of radiative greenhouse forcing (predicted to be most severe in higher latitudes; Houghton, Jenkins & Ephraums 1990), and CO_2 emission from the soils of the boreal region (Lashof 1989).

Despite a long history of soil CO_2 efflux measurements (see for example Lundegårdh 1927), the efflux of CO_2 from the soil surface remains one of the most difficult ecosystem processes to measure in an accurate and appropriate manner. In practice,

four distinct approaches have evolved, each with several variations, and associated strengths and weaknesses. None, however, has become recognised as the "standard" methodology, and there remains no established procedure for determining the accuracy of any one (Norman, Garcia & Verma 1992).

Micrometeorological methods in general, and the eddy covariance technique in particular, have considerable advantage over other methods in that the soil system under observation remains completely undisturbed at all times, and the efflux measured is, therefore, likely to be an appropriate one (for example Baldocchi *et al.* 1986; Baldocchi & Meyers 1991). The problems with these approaches stem from the theoretical assumptions on which the techniques are based (such as a level and homogeneous upwind fetch, a zero mean vertical windspeed, and the absence of sources or sinks between the soil and the sensor) which may not be valid at or near the soil surface, particularly within a plant canopy.

Measurement of the CO_2 concentration within the soil profile can lead to an estimate of CO_2 efflux when combined with a knowledge of the diffusivity of the gas within the substrate, using a standard flux-gradient approach. This method has been used successfully to determine CO_2 efflux from snow packs (Somerfeld, Mosier & Musselman 1993) and may provide the only satisfactory method of partitioning the CO_2 source between different soil horizons. However, the practical difficulty in determining accurately soil diffusivities in heterogeneous soil systems limits applicability of this approach to all but the most simple of "soil" systems (Nakayama 1990).

The two remaining methodologies both employ some form of enclosure or chamber set upon the soil surface, and measure either the rate of accumulation of CO_2 or the instantaneous efflux of soil CO_2 (i.e. the so-called closed and open systems, respectively). Earlier closed systems typically employed an alkaline compound to absorb CO_2 evolving into the chamber over a period of some hours. Subsequent weighing or chemical titration enabled the total amount of CO_2 absorbed by the alkali to be determined, and consequently also the average CO_2 efflux (Monteith,

Szeicz & Yabuki 1964). More recently, the use of infra-red gas analysis (Parkinson 1981; Norman, Garcia & Verma 1992) has enabled the accumulation rate to be determined over much shorter time periods. This is desirable for two distinct reasons. Firstly, in order to relate soil CO_2 efflux to environmental variables, it is necessary to make measurements at the same temporal scale as changes in the driving variables, since otherwise transient responses might pass unnoticed (in the case of short term variability) or correlations might be misleading (in the case of non-linear responses). Secondly, during the course of taking a measurement with a closed system, there is necessarily a rise in the CO_2 concentration within the chamber, and unless careful attention is paid to screening the correlation coefficients of the concentration increase over time, this may lead to an underestimation of the natural flux as the result of a continuously decreasing CO_2 concentration gradient between the soil and chamber (Nakayama 1990).

A very short measurement period, however, introduces a number of complications. As Jury *et al.* (1982) have pointed out, the efflux should be measured over a sampling period of days rather than of minutes, depending upon where within the soil profile most of the CO_2 is being produced. Denmead and Raupach (1993) also concluded that in order to account for changes in the diffusion properties of the soil profile, the minimum period for measurement of soil efflux should be 24 hours. Such a period also facilitates expression of the measured efflux in relation to environmental variables when there is a lag period between a change in the driving variable and a corresponding change in CO_2 efflux.

Considering these points, a satisfactory means of making a temporally meaningful measurement is to sample the soil efflux, and driving variables, *continuously* and in such a way as to have minimal effects on the conditions of the soil. A promising system that achieves this is the automated closed chamber. With this system, an area of soil normally open to the atmosphere is temporarily enclosed, the rate of concentration increase determined as with a simple closed system, and finally the chamber is removed. This is carried out by some means of mechanical actuation (for example Eckardt's system, described and illustrated in Chapter 2, Šesták, Catsky and

Jarvis 1971). Since the soil is enclosed for only a short period (for example 10 minutes every hour) this system has a major advantage over permanent enclosures in that the microclimatic conditions (for example the energy balance) of the sample area are more likely to be representative of non-enclosed areas. In addition to the systematic errors associated with using closed chambers for measuring soil CO_2 efflux, a drawback of this system is the mechanical complexity.

According to Denmead and Raupach (1993), the most useful option for chamber based measurements is within an *open* system. Open system gas exchange techniques have found widespread application in the measurement of CO_2 fluxes in biological systems. Air is passed through a chamber enclosing the system under observation, and any change in the CO_2 concentration of the air leaving the chamber (the analysis air-stream) compared to air entering the chamber (the reference air-stream) is the result of an efflux or an uptake of CO_2 within the chamber. The general design requirements of an open system are that the flow rate of air through the chamber and the change in CO_2 concentration of the in-flowing and out-flowing air should be measured accurately, and that the chamber interior should be isolated from the ambient environment so that CO_2 concentration changes in the air stream are solely caused by the plant or soil under observation.

In addition, two further features are required of any chamber used to measure continuously the CO_2 efflux from soils. Firstly, the chamber should allow transmission of fluctuations in atmospheric pressure through to the soil surface, since the exchange of CO_2 from the soil to the atmosphere is to some extent driven by the "pumping" action of these pressure fluctuations (Kimball & Lemon 1971; Baldocchi & Meyers 1991). Secondly, there should be minimal pressure difference between the chamber interior and the atmosphere, eliminating any mass flow of air into or out of the chamber, through the soil pores.

Construction of a chamber to isolate the soil *in situ* from its gaseous environment is, however, difficult because of the porous nature of soil, and it is inevitable that the chamber will be leaky. Where leaks are unavoidable, it is possible to isolate the

chamber contents by employing an air seal providing the air within the chamber is well mixed (Šesták *et al.* 1971). Air seals have usually been achieved by maintaining a slight positive pressure within the chamber, ensuring that ambient air does not enter the chamber and dilute the chamber air, but may equally well be created with a slight negative pressure within the chamber, drawing in ambient air and ensuring that no chamber air is lost. Moreover, the use of a chamber "open" to the atmosphere, but "closed" with an air seal also ensures that there is minimal impedance to the transfer of atmospheric pressure fluctuations to the soil surface.

Criticism has in the past been directed toward open systems used to measure soil CO_2 efflux, on account of the pressure differentials created between the inside and outside of the chamber. Some pressure differential is inevitable, even in re-circulating closed systems, since without this there could be no flow of air through the chamber. Pressures measured inside chambers in the field, however, have shown that soil effluxes measured under a positive pressure of 1 Pa can be as much as an order of magnitude lower than effluxes measured under a negative pressure of 2.5 Pa (Kanemasu, Powers & Sij 1974). This effect is the result of an induced mass flow of air between the chamber and the atmosphere through the soil pores, carrying with it CO_2-poor air from the chamber when under positive pressure, or CO_2-rich air from the soil when under negative pressure. In either case, the mass flow of air acts to create an apparent CO_2 flux that is quite different from that occurring with no pressure differential. If open chambers are to be used successfully in the field, measurements of soil CO_2 efflux should be made only after careful consideration has been given to minimising the pressure differential. One approach (Fang and Moncrieff 1998) is to use two pumps simultaneously to pump air into and out from the chamber. Chapter two reports the design and usage of a simple robust soil efflux measurement system, capable of continuous measurement at multiple sites. The use of the system in the field is illustrated with a preliminary dataset made during 1994 at the BOREAS Southern Study Area Old Black Spruce site located towards the southern limit of the boreal forest in northern Saskatchewan, Canada. A comparison between this system and five other methods for measuring soil surface CO_2 fluxes is given by Norman *et al.* (1997). Chapter three describes the results of a chamber

study of soil CO_2 efflux over two years at the BOREAS Southern Study Area Old Black Spruce site.

FOLIAGE PHOTOSYNTHESIS, RESPIRATION AND TRANSPIRATION

The extraction of physiologically meaningful parameters from measured flux data is an essential part of modelling land-atmosphere interactions because it helps us understand how mass and energy fluxes can be scaled up in space and time. Analysis of physiological parameters may also help in the understanding of more specifically biological questions. For example, is the variation in the growth rates of branches at different heights in the canopy a straight-forward consequence of differing incident photon (400 to 700 nm) flux density (PFD), or do branches become physiologically acclimated to their differing light environments. Similarly, part of the seasonality observed in ecosystem behaviour may be a function of biological changes in the biosphere and not simply a reflection of seasonality in the climate. Physiological parameters also provide a basis for a quantitative comparison of ecosystem function between different ecosystem types.

Physiological understanding of photosynthesis and respiration has typically been gained through gas exchange measurements made on single leaves or single shoots (e.g. Walcroft *et al.* 1997). From this understanding inferences may be made about the behaviour of the population of leaves/shoots with tree crowns and forest canopies (e.g. Harley & Baldocchi 1995). This type of measurement, however, is labour intensive, and the subsequent process of integration to the whole canopy requires considerable and detailed information about the physical structure of crowns and canopy. Secondly, the time constants of biological control processes vary from minutes to years and longer, and understanding the time-varying properties of vegetation canopies is essential for predicting their future behaviour. Thus, model parameterisations based upon short-term measurements of physiological behaviour may not be appropriate for the whole photosynthetic season. This is particularly true of ecosystems subject to strongly seasonal climates such as the boreal forest, where these problems are further confounded by changes in leaf/shoot physiology resulting from dramatic changes in temperature and the availability of water, nutrients and

PFD. Such situations require that biological function be monitored throughout the year and perhaps over a number of years. Two previous studies of the "seasonal" variation in gas exchange of black spruce made measurements on small shoots over eight days between July & October (Zine El Abindine *et al.* 1995) and 22 days between June & August (Vowinkel, Oechel & Boll 1975). A more convenient and convincing way of achieving this for foliage in a forest ecosystem is through the use of automated branch bags, measuring the gas exchange of whole branches through infra-red gas analysis over the growing season (Dufrêne, Pontailler & Saugier 1993; Saugier *et al.* 1997). Using data collected over a long period, it is possible to extract model parameters by regression against natural variation in the driving environmental variables.

Taking the branch as the unit of observation greatly simplifies extrapolation to the whole tree, and thereafter to the entire canopy, since a tree may be considered as being made up of a relatively small number of branches, each of which is largely autonomous in terms of its carbon budget (Sprugel, Hinckley & Schaal 1991). Moreover, direct measurements of whole branch CO_2 exchange provide an already integrated measure that may be used as a means of validating procedures for integrating needle or shoot measurements to higher organisational levels.

Conventional methods of characterising the ecophysiolocal functions of a canopy (for example stomatal behaviour or photosynthetic capacity) typically operate at the tissue or organ scales, and the results are then "scaled-up" to the whole canopy. In practice, the procedures used for this "scaling" between scales of organisation are seldom, if ever, validated. This is primarily because measurements of net ecosystem exchange made, for example, with the eddy covariance technique, measure the summation of all exchange processes within an ecosystem, of which canopy CO_2 exchange is but one. Before net ecosystem exchange can be used for validating "scaling" methods, the other biotic processes (notably heterotrophic respiration in the soil) need to be taken into account.

It may be possible, however, to "scale-up" measurements made, say, at the shoot "scale" to some intermediate "scale" (e.g. the branch), enabling validation of these procedures against direct measurements at "a range of scales". Success in scaling

from the leaf to the branch will then give the confidence to apply these procedures to scaling from the leaf to the entire canopy.

Chapters four and five describes a study of the CO_2 and water exchange of the most common Canadian boreal forest tree species, black spruce (*Picea mariana* [Mill.] B.S.P.), using measurements made at three organisational scales: the shoot, the branch and the canopy. The variation of physiological parameters over the course of a year and between organisational scales is investigated.

EDDY COVARIANCE MEASUREMENTS

The eddy covariance method is a widely used technique for measuring the net ecosystem exchange (NEE) of energy and trace gases between ecosystem and atmosphere, and is a powerful tool for understanding of how changes in the global climate might lead to changes in the biosphere (e.g. Baldocchi *et al.* 1996). The key to predicting ecosystem response to climate change, however, is understanding the controls on the component energy and trace gas fluxes that together make up the net biotic flux (NBF) between the ecosystem and the atmosphere. Eddy covariance directly measures turbulent transport between the land surface and the atmosphere. In highly turbulent conditions where there is no horizontal advection of air, most of the transport between the ecosystem and the atmosphere is turbulent transport, and NEE measured by eddy covariance is, therefore, numerically identical to NBF. These conditions are not, however, always satisfied (Moncrieff, Malhi & Leuning 1996). For example, night-time turbulence is sometimes insufficient to guarantee the functioning of the eddy covariance technique, and during these times measured NEE systematically underestimates NBF. Adding the storage flux, ΔS, (i.e. the change in the amount of a gas stored in the volume of air below the eddy covariance sensor (Baldocchi, Hicks & Meyers 1988)) to the eddy covariance measurements can in theory (and often in practice) correct for the loss of turbulent transport at night, and give an estimate of NBF from NEE (e.g. Grace *et al.* 1996). The storage flux cannot, however, correct for situations where horizontal advection of air (caused, for example, by sloping terrain or large-scale convective structures) causes an apparent "loss" of flux from the system. These situations tend to occur systematically at night (under conditions of stable stratification of the atmosphere) when respiratory carbon

effluxes dominate the NBF. Therefore, in obtaining the continuous long-term data-sets necessary to identify ecosystem responses to weather and climate, it is imperative that we also have recourse to other means of estimating NBF at such times. Moreover, if other means of estimating NBF are based on processes of which we have some mechanistic understanding, it is possible to attempt to investigate, *a priori*, the sensitivity of the ecosystem to climate change.

This thesis is not concerned primarily with the measurements of NEE *per se* (that being largely the concern of other group members) but it is concerned with the use of chamber measurements (and measurement of the storage term) that, used in conjunction with eddy covariance measurements, can greatly improve our understanding of this problem.

Chapter six estimates the NBF of carbon for a boreal ecosystem using three methods:- summing the chamber-based measurements of the ecosystem component fluxes, using a detailed radiation absorption, photosynthesis and respiration model – MAESTRA, and using an aggregated, "big-leaf", canopy model. These estimates are then compared to a "direct" measurement of NBF using eddy covariance data corrected for the storage flux. The sensitivity of the estimated annual ecosystem carbon balance to the method used to fill gaps in the eddy covariance data is investigated. The chamber-based component summation method is then expanded into a complete carbon budget for the ecosystem in Chapter seven, and the sensitivity of the annual carbon balance to temperature is considered.

THESIS AIMS AND STRUCTURE

To quantify fluxes associated with ecosystem sub-components

This thesis aims to identify and measure the most important component fluxes of an ecosystem in a globally important biome, the boreal forest. Methodologies are developed to measure the gas exchange of the forest floor and of the above-ground parts of the forest. From these measurements, and from other data, a carbon budget for the ecosystem is prepared and the annual net ecosystem carbon balance is estimated.

To look inside the ecosystem "green box"

To gain a better understanding of the "physiology" of the ecosystem, process-based models of the important component fluxes of the ecosystem are derived. From these models a mechanistic model of the annual net carbon balance of the ecosystem is constructed, and the temperature sensitivity of the annual net carbon balance is investigated.

To compare methods of estimating the net biotic flux of the ecosystem

To help verify estimates of the net biotic flux of the ecosystem made by the eddy covariance technique and to help validate estimates of the net biotic flux generated by a "big leaf" model and a detailed canopy model, these data are compared to estimates of the time integrated net biotic flux based on chamber measurements. Consideration is given to the sensitivity of the net biotic flux to the method of filling gaps in eddy covariance data.

Chapters two and three are concerned with the forest floor CO_2 efflux. Chapters four and five are concerned with the gas exchange of the above ground parts of the ecosystem. Chapters six and seven bring the four preceding chapters together to provide a complete description of the carbon balance of the ecosystem.

THE BOREAS PROJECT

This work was done within the framework of the BOREAS project. The boreal forest is the circumpolar forest above 48 °N. It occupies about 21 % of the forested land surface, and contains about 13 % of the carbon stored in biomass and about 43 % of the carbon stored in soils (Sellers *et al.* 1997). It is therefore an important component of the global carbon cycle. Furthermore, many model predictions of global warming suggest that warming will be most pronounced at these high latitudes, particularly within continental interiors. The Boreal Ecosystem Atmosphere Study (BOREAS) was an international multi-scale experiment conducted between 1993 and 1996 in Saskatchewan and Manitoba, Canada. The stated aim of BOREAS was to improve our understanding of the interactions between the boreal forest biome and the atmosphere in order to clarify their roles in global change. Measurements were made over an area of 1000 by 1000 km, with most of the focus being at two main study

areas, approximately 100 by 100 km, one at the southern, and one at the northern limit of the boreal forest. A detailed description of the project may be found in Sellers *et al.* (1997). The boreal forest biome is a mosaic of large areas of fen, lakes and forests. In this region, the forests are largely black spruce (*Picea mariana* (Mill.) BSP.), jack pine (*Pinus banksiana* Lamb.), aspen (*Populus tremuloides* Michx.), white spruce (*Picea glauca* (Moench) Voss) and tamarack (*Larix laricina* (Du Roi) K. Koch), with old-growth black spruce forest being the most extensive of these, occupying around half of the total area (Ogunjemiyo *et al.* 1997).

SSA OBS SITE DESCRIPTION

The BOREAS Southern Study Area Old Black Spruce (SSA OBS) site lies toward the southern boundary of the boreal forest, approximately 100 km north of Prince Albert, Saskatchewan, Canada, at 53.99 °N, 105.12 °W. The stand was predominantly black spruce of fairly uniform age (around 115 years) and height (between 10 and 11 m). Tamarack, jack pine, and mixed poplars made up less than 5 % of the trees, although some tamarack were emergent, reaching up to 16 m in height. Diameter at breast height varied from 3 to 20 cm, with a mode of *ca.* 10 cm. There were *ca.* 5900 stems per hectare, and total basal area was *ca.* 30 m^2 ha^{-1}. The projected leaf area index of the site averaged 4.4, however the crowns were very narrow, typically less than 2.5 m diameter, and the foliage was extremely clumped around the branches and trunk, resulting in columnar structure rather than a continuous canopy. A sparse understorey of mixed herbaceous shrubs reached a height of up to 1.5 m in the more open areas.

The black spruce-peat moss community (muskeg) is the dominant community of the North American boreal region, and is characterised by cold, nutrient poor and frequently waterlogged soils (Larsen 1980). Low rates of organic matter decomposition in such soils lead to the build up of a thick layer of acidic peaty organic matter. This in turn leads to reduced soil temperature, increased soil moisture and a further reduction in decomposition rate, until this process is interrupted when the forest floor is consumed by fire (Bonan 1992).

There was a pronounced hummock-hollow microtopography in the forest floor, which was mainly peat moss (*Sphagnum* spp.), with some mixed feather mosses (*Hylocomium splendens, Pleurozium schreberi* and *Ptilium crista-castrensis*) in the drier areas. Immediately below the living moss was a layer (2 - 10 cm) comprising a light brown mat of dead moss, overlying a thick layer (2 - 10 cm) of dense peat. The peat became increasingly humic deeper into the soil profile. Vascular plant roots were mainly confined to a narrow (2 - 3 cm) transitional zone between the most humic peat and the underlying waterlogged clay. In some areas, standing water was visible throughout the time that the soil was unfrozen. A full description of the site is given by Jarvis *et al.* (1997).

Black spruce is the dominant tree species throughout the North American boreal region and occurs from latitudes as high as 70 °N in western Canada to nearly 40 °N in the eastern US. This large range reflects the species' ability to grow on a wide variety of mineral and organic soils, but black spruce is particularly well adapted to grow under conditions of very low nutrient availability, such as areas with cold, frequently waterlogged soils, where it successfully out-competes most other tree species (Lamhamedi & Bernier 1994).

The black spruce-peat moss community (muskeg) is the dominant community of the North American boreal region, and is characterised by cold, nutrient poor and frequently waterlogged soils (Larsen 1980). Low rates of organic matter decomposition in such soils lead to the build up of a thick layer of acidic peaty organic matter. This in turn leads to reduced soil temperature, increased soil moisture and a further reduction in decomposition rate, until this process is interrupted when the forest floor is consumed by fire (Bonan 1992).

EQUIPMENT INSTALLATION

Two eddy covariance systems were installed, one above the crowns, at 27 m, and one at 2 m height. An automatic weather station was installed at 26 m and additional meteorological measurements were made at 2 m height. Profiles of CO_2 and water vapour concentration and temperature were measured at eight heights through the canopy, and temperature sensors were also positioned in the foliage, in the trunks and

at five depths in the soil profile. An array of 15 quantum sensors was positioned below the canopy, and four quantum sensors were positioned within the crowns. Soil CO_2 efflux was measured at a total of 45 locations, shoot gas exchange was measured on 20 shoots, branch gas exchange was measured on four branches, and woody tissue respiration was measured on 18 tree stems. Four sap flow sensors and eight cavitation sensors were also installed at the site for a period. A full description of the equipment installed on the site is given by Jarvis *et al.* (1997) and in the relevant chapters.

Chapter Two - An Improved Open Chamber System for Measuring Soil CO_2 Effluxes in the Field

The aim was to design an "open" chamber for the continuous measurement of soil CO_2 efflux that was not leaky and allowed atmospheric pressure fluctuations to be experienced at the soil surface.

METHODS

Chamber design - pressure characteristics

An "open" chamber is open to the ambient environment in as much as it is connected through the inlet or the outlet aperture which is sealed by a flow of air. It is the pressure drop across the length of tube associated with this aperture and the throughflow of air, that determines the internal chamber pressure. The difference between internal and external pressure is a function of the flow rate of air and the length and cross-sectional area of the tube.

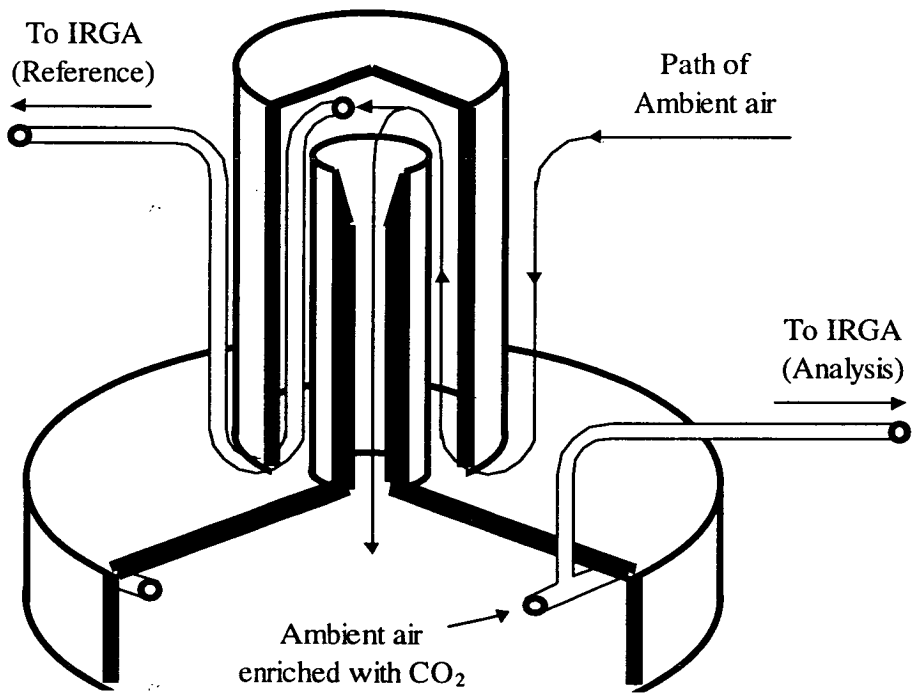

Figure 2.1. Schematic diagram of a section through an open system soil CO_2 efflux chamber.

To investigate this relationship further, a closed cylindrical chamber of diameter 0.28 m and height 0.15 m was constructed (see Figure 2.1). Ambient air enters the

chamber through a centrally mounted inlet tube, the cross-sectional aperture of which could be varied between 0 and 500 mm^2 (0 - 25 mm diameter). Air was pumped from the chamber through a peripherally mounted perforated tube and a mass flow controller (Tylan FC-260, Tylan general (UK) Ltd., Swindon.) at 1 dm^3 min^{-1} (± 1%). The pressure difference between the inside and outside of the chamber was measured with a micro-manometer (Furness Controls Ltd. (UK), low pressure transducer FCO40), capable of resolving pressure differentials down to 0.004 Pa, for inlet apertures in the range of 0 to 500 mm^2 (Figure 2.2). With apertures larger than 320 mm^2 the pressure differential was less than the resolution of the micro-manometer.

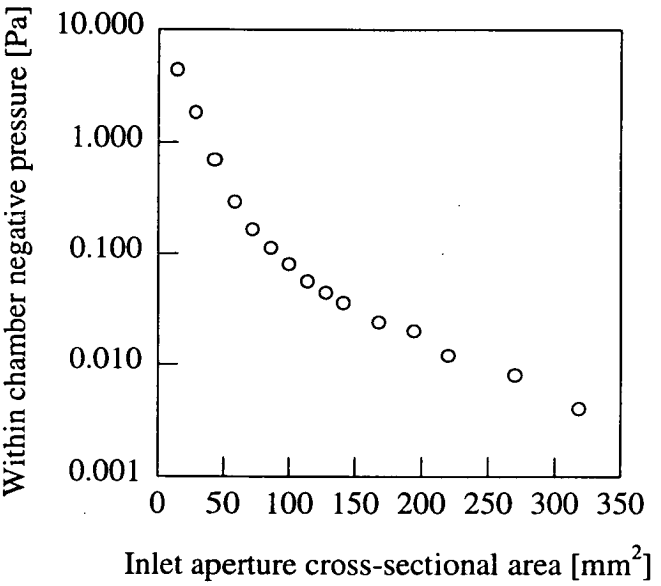

Figure 2.2. Effect of inlet aperture on internal chamber negative pressure (with respect to atmospheric pressure) at 1 dm^3 min^{-1} flow rate.

To characterise the effectiveness of the seal between the chamber interior and ambient air, a quantity of humus was enclosed in the chamber as a source of CO_2, and the whole apparatus placed within a freely ventilating enclosure. Ambient air was drawn through the chamber at flow rates of 0.25, 0.5, 0.75 and 1.0 dm^3 min^{-1}. Ambient air sampled at the open end of the intake tube, and air drawn through the chamber were analysed for CO_2 concentration using an infrared gas analyser (Li 6252, LICOR Inc., Lincoln, Nebraska, USA.) in differential mode. As aperture

diameter was increased from (just above) zero, the CO_2 concentration differential remained constant, until an aperture was reached at which it rapidly but irregularly tailed off, indicating that CO_2 from inside the chamber was being sampled in the reference air stream. It was at this aperture, therefore, that the volume flux density down the tube was no longer sufficient to prevent CO_2 from escaping up the tube, against the mass flow of incoming air. The maximum inlet aperture size above which a loss of CO_2 occurred was found to be a linear function of flow rate (Figure 2.3), the gradient of which gives the critical flow velocity of air through the inlet tube necessary to prevent outward diffusion of CO_2. This velocity was calculated to be 48 mm s^{-1}, rather more than the diffusion coefficient of CO_2 in air (14.7 mm s^{-1}). This discrepancy is possibly because the velocity of air through the tube is not uniform across its width, but is lower closer to the tube walls.

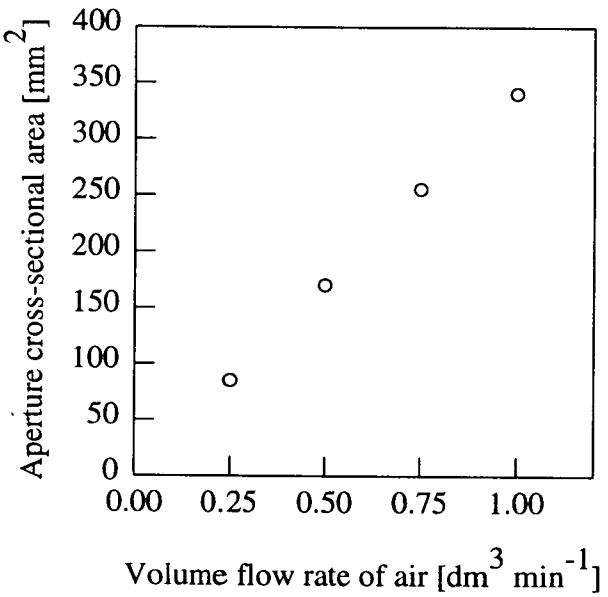

Figure 2.3. Effect of flow rate on the maximum intake aperture area above which a loss of CO_2 occurred against the mass flow of air into the chamber.

For field use a flow rate of 1 dm^3 min^{-1} was chosen, setting the maximum aperture area possible at 340 mm^2, corresponding to a pressure difference between the interior of the chamber and the ambient atmosphere of no more than 0.004 Pa (Figures 2.3 and 2.2). To make the chamber more robust for use in the field, the variable aperture intake tube was replaced with a fixed circular intake tube of length 150 mm and

internal cross-sectional area 340 mm^2. A rigid cover was constructed to fit over the intake tube to prevent any horizontal movement of air across the end of the tube inducing a venturi suction of air out of the chamber, a gap of 10 mm between the bottom of this cover and the chamber lid allowed free passage of ambient air to the intake inlet. Internal - external pressure difference was measured at flow rates of 0 to 5 dm^3 min^{-1}. At flow rates of 1 dm^3 min^{-1} and less, differential pressure was at or near the resolution of the micro-manometer and did not increase above 0.01 Pa until the flow rate exceeded 4 dm^3 min^{-1}.

Chamber design - collars

The chamber used in the field was designed in two pieces, a steel collar inserted into the ground, and a removable flat lid of clear acrylic, fitted with a vertically mounted aluminium inlet tube and a peripherally mounted perforated outlet tube as described above (Figure 2.1). The use of a flat lid reduced the chamber volume as far as possible, ensuring that the system had a minimal flushing time and a rapid response to changes in CO_2 efflux rate. A silicon rubber gasket was used to ensure a gas-tight seal between the collar and lid which was held in position with four spring clips (Protex Fasteners Ltd., Redditch, UK.).

Edge effects were minimised through the use of round collars of diameter covering a ground area of 616 cm^2, well above the 400 cm^2 recommended as a minimum by Monteith *et al.* (1964). The length of the collars, and the depth to which they are inserted should be varied from site to site, depending on the soil type and surface vegetation being investigated. Collars should be inserted deep enough to minimise influx of ambient air into the chamber but damage to roots should be minimised also as this has been found to result in a reduction of soil CO_2 efflux (Wildung, Garland and Buschbom 1975), attributed to a reduction in root respiration by severed roots.

Field tests

Extensive field tests were carried out at the Southern Study Area Old Black Spruce site of the BOREAS project in Saskatchewan, central Canada during 1994 and again

in 1996. Collars were inserted into the highly decomposed lower region of the peat layer, the exact depth depending upon the thickness of the moss layer. Collars projected between around 2 to 7 cm above the soil surface, which was low in relation to their diameter of 28 cm, and unlikely to cause micrometeorological effects at the soil surface resulting from changes in the lateral surface wind flow. Once inserted, the collars were left for at least one day for the soil system to re-equilibrate with ambient conditions. The chamber lid was then placed in position and the CO_2 efflux from the collar was measured over two or three diurnal cycles using infra-red gas analysis (Li 6252, LICOR Inc., Lincoln, Nebraska, USA.). Following this period, the lid was removed and placed on another collar. Six collars were inserted at randomly chosen locations, two remained in the same location for the entire study, the rest were measured on two, three or four occasions (separated by a minimum of 6 days) before being moved to a new location. Sample periods of longer than three diurnal cycles were not considered satisfactory due to the tendency for evaporation to condense out on the chamber lid, this was particularly a problem in early summer when melting soil ice led to waterlogged soils, which, combined with warm days and cool nights, created conditions of heavy dew formation, and the low flow rate through the chamber was not sufficient to prevent condensation building up.

A solenoid-based, gas-switching system enabled two collars to be sampled alternately, each chamber being sampled for 5 minutes, with the first minute of each measurement being ignored to allow for total flushing of the tubing and IRGA. Ambient air was drawn through both chambers at all times, irrespective of which collar was being measured for CO_2 efflux. Drying columns (anhydrous $CaSO_4$, "Drierite", Aldrich Chemical Co., Gillingham, UK.) were fitted at the chamber end of both the reference and analysis air lines to prevent condensation of water vapour in the lines and to minimise any errors resulting from cross-sensitivity to water vapour in the gas analyser. Simultaneous measurements were made of the soil temperature at the surface and at 5, 10, 20, 50 and 100 cm depth within 6 m of the collar being measured, and this and the gas analysis data were logged to a Campbell Scientific 21X data logger (Campbell Scientific, Shepshed, UK.), which also controlled the switching of the solenoids.

Comparison with a closed system

For the purposes of consistency between the study sites within the BOREAS project, an inter-comparison between the system described here and the prototype of a commercially available closed system (LICOR Inc., Lincoln, Nebraska, USA.) was made in collaboration with J. M. Norman (University of Wisconsin, Madison, Wisconsin USA). The LICOR system is a dynamic closed system, in which air is re-circulated between the chamber and an infrared gas analyser, and efflux is measured as a rate of rise of internal CO_2 concentration (Norman *et al.* 1992). For this comparison, six pairs of collars were inserted along a 10 m transect, and simultaneous measurements of soil efflux were made by both systems (for a full description of this inter-comparison see Norman *et al.* 1997).

RESULTS

During the period 11 August 1994 to 9 September 1994, 27 diurnal observations were made. Figure 2.4(a) shows a typical time course of CO_2 efflux, illustrating the continuous nature of the measurement. For each diurnal observation at each location, forest floor CO_2 efflux was fitted to an exponential function of soil temperature measured at 5 cm depth (for example Figure 2.4(b)). The coefficients of the linear regression of ln(efflux) against soil temperature for each set of diurnal observations provided a single estimation of the two parameters describing the exponential response of CO_2 efflux to temperature: a basal rate describing the predicted efflux rate at 0 °C (R_0) and a temperature coefficient defined as the efflux rate at temperature (t + 10 °C) divided by the efflux rate at temperature t (Q_{10}).

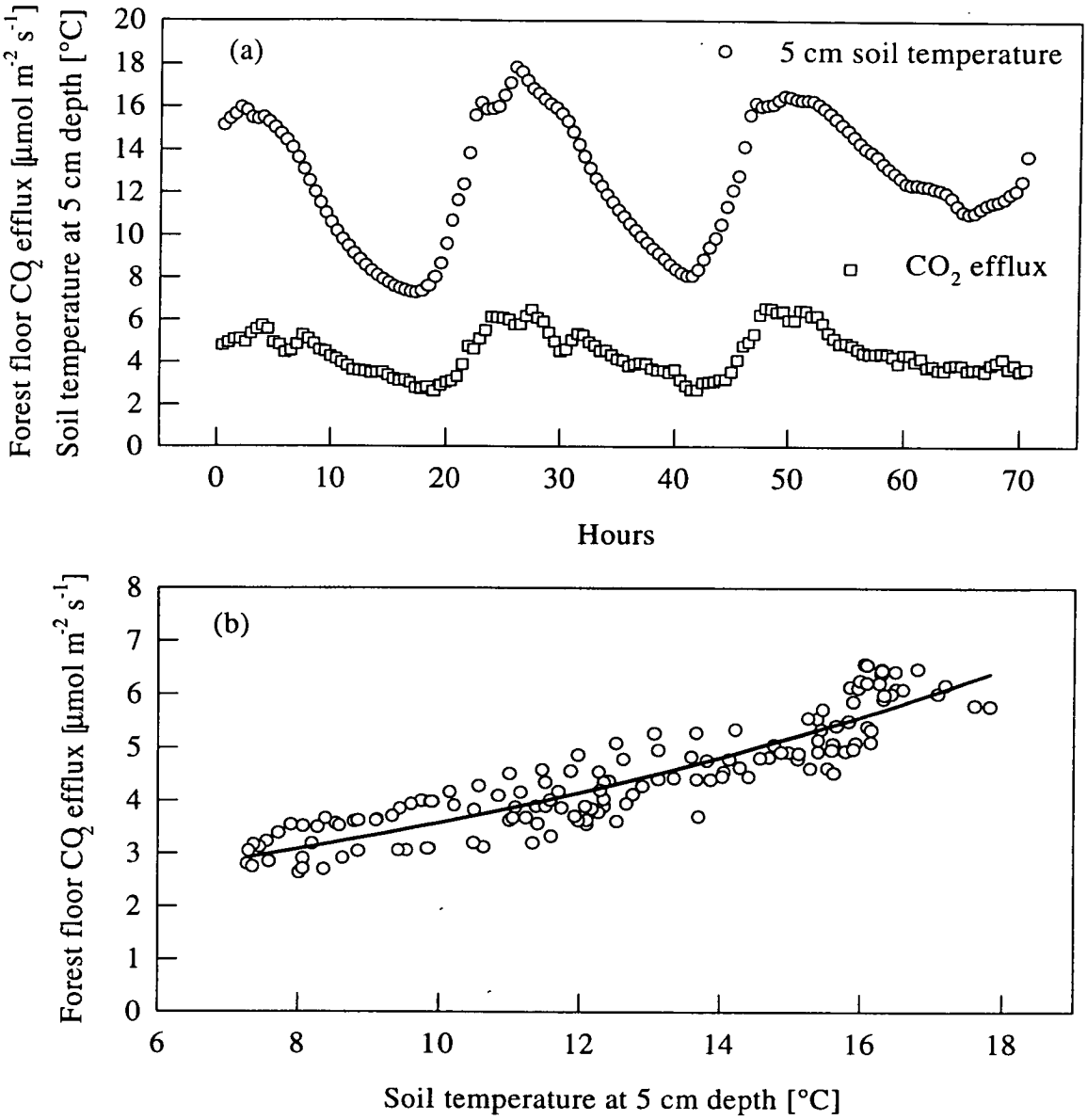

Figure 2.4. (a) Three day long time course of forest floor CO_2 efflux (squares) and soil temperature at 5 cm depth (circles) and (b) same data with efflux plotted as a function of temperature, and fitted exponential function.

Considerable spatial variability was found in CO_2 efflux over distances of only a few meters. Basal rates of forest floor efflux (R_0) ranged from 0.25 µmol m^{-2} s^{-1} to 3.6 µ mol m^{-2} s^{-1}, with a mean value of 1.72 µmol m^{-2} s^{-1} and a standard deviation of 0.12 µmol m^{-2} s^{-1} (Figure 2.5(a)). Temperature coefficients ranged from 1.8 to 3.8, with a mode of 2 - 2.25 (Figure 2.5(b)). The diurnal range of soil temperature varied between 4.7 and 12.2 °C. The response function is less well defined at the smaller of these ranges, and accounts for some of the variability in the Q_{10}. Care must be taken

when comparing quoted values of Q_{10}, since the same area would appear to exhibit a smaller Q_{10} when this is derived from the soil surface temperature (where there is a wide diurnal variation in temperature) than when the Q_{10} is derived from the temperatures deeper within the soil (where diurnal variation in soil temperature is attenuated). In this case temperature at 5 cm depth was chosen as it minimised hysteresis in the response of efflux to temperature.

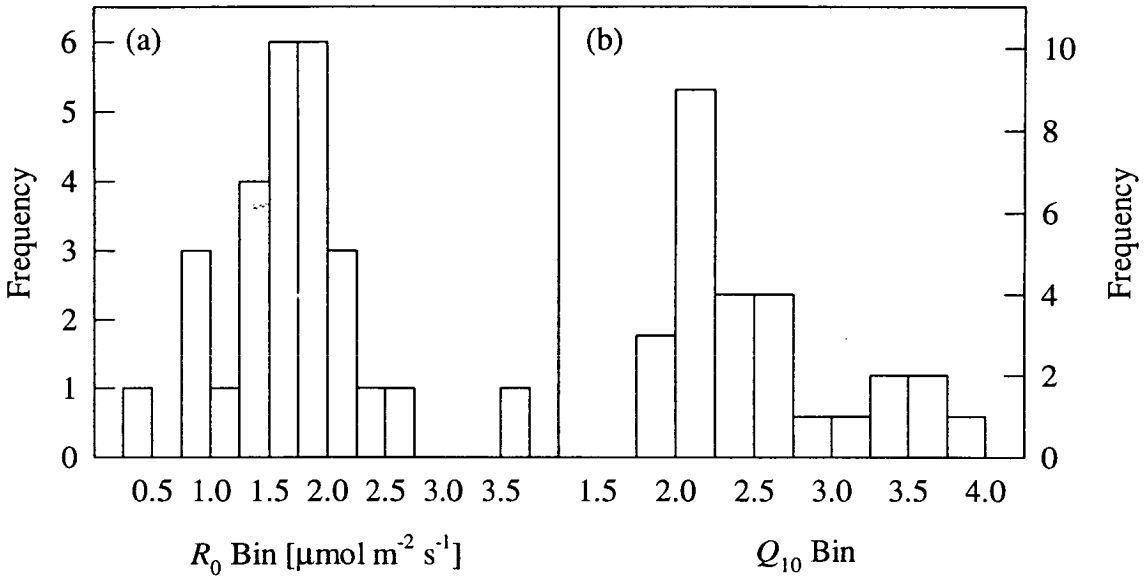

Figure 2.5. Spatial heterogeneity of (a) calculated basal rate and (b) temperature quotient of forest floor CO_2 efflux measured over a four week period at the BOREAS Old Black Spruce site in summer 1994.

Results from the methodological inter-comparison showed that there was a trend for the instantaneous effluxes measured with the open system to be up to 10% larger than those measured with the closed dynamic methodology (Figure 2.6), however due to the small sample size (n = 6 locations) this difference was not statistically significant (at the 95% level) (*cf.* Norman *et al*, 1997).

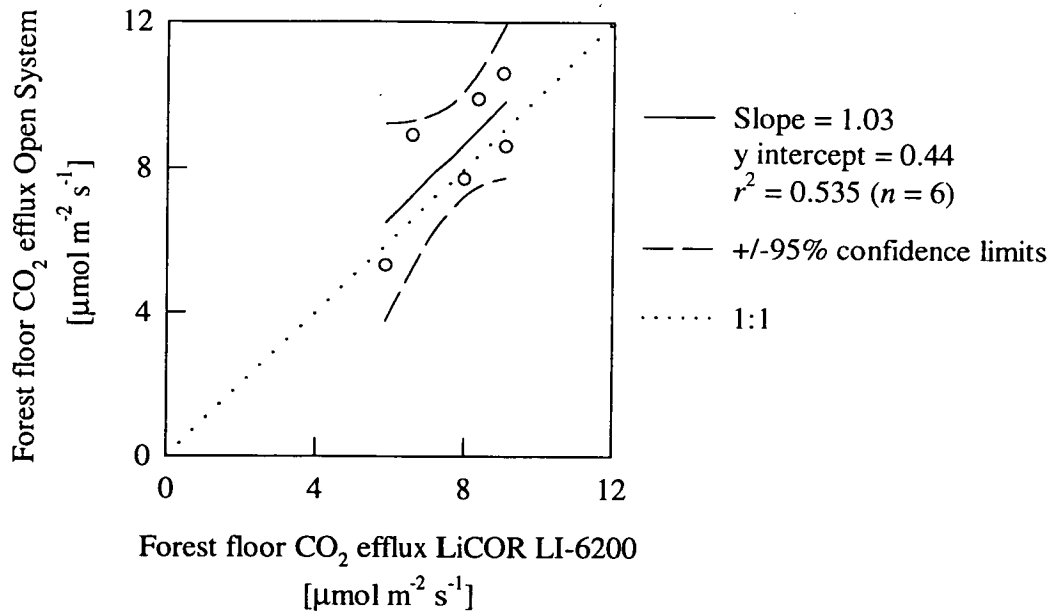

Figure 2.6. Comparison of forest floor CO_2 efflux as measured using the open system technique described here and using the LICOR soil chamber (see text for details).

DISCUSSION

The open chamber system described here was operated continuously for three months, and provided a large amount of high quality data for the efflux of CO_2 from the forest floor. Having no moving parts, the system was robust and aside from collar placement and insertion, the only maintenance necessary was the renewal of the drying columns and calibration of the IRGA.

Having eliminated the pressure problems that have previously beset open system measurements of soil CO_2 efflux, the agreement between open and closed systems is encouraging, particularly since the open system provides a means of making time series measurements in a much less labour-intensive way than is possible with a manually operated closed system. It is difficult, however, to be conclusive with such a small inter-comparison sample size as reported here.

The means of the six inter-comparison values recorded nevertheless show that generally the open system gave results slightly higher than the closed system (see also Norman *et al.* 1997). This is not inconsistent with the view of Dr. R. Striegl (US

Geological Survey, Denver, CO.) that mathematical models of gas movement in soils suggest that chamber measurements are subject to around a 10% underestimation of the natural soil efflux, and a similar underestimation has also been demonstrated under laboratory conditions (Nay, Mattson & Bormann 1994). One possible cause for this underestimation is the reduction or compete curtailment of the pumping action of atmospheric pressure fluctuations at the soil surface that is inevitable in closed systems and in conventional open chamber systems where the intake pump is positioned between the atmosphere and the chamber. The chamber system described here is designed such that the large aperture intake tube presents a negligible impedance to the transfer of pressure fluctuations from the atmosphere to the soil surface, and as such presents the soil with turbulence conditions as close as possible to those experienced in natural conditions. There is another reason why closed soil chambers are expected to systematically underestimate the magnitude of the flux of CO_2 from the soil surface. The flux calculated in a closed system is proportional to the rate of change in the CO_2 concentration and the chamber volume, and whereas the nominal chamber volume is easily determined, the "effective" volume of the chamber includes the air-filled pore spaces in the soil, the CO_2 concentration within which is also increasing during measurement. Since the air filled porosity of most soils is between 40 and 50 % by volume, the effective chamber volume can be significantly higher (up to 10 %, Rayment, unpublished data) than the nominal chamber volume, and consequently the "true" rate of CO_2 production may well be larger than that calculated using this technique.

A factor possibly contributing to the apparently higher rates measured with the open system has been suggested to be the reduction in the drying out of the moss layer due to decreased evapotranspiration, or more correctly, a re-wetting of the moss by water condensing out on the chamber lid, and dripping back onto the moss surface. There was some evidence that this might have occurred at one of the two chamber locations that remained unchanged for the entire field season, however the removal of chamber lids for a minimum of six days between measurements and the re-positioning of collars after a maximum of four measurement periods served to ensure that even if there had been some dripping of condensation this would be insignificant in relation

to the total fluxes of water (inward and outward) over the measurement period. Moreover, at the time the inter-comparison was made, the volumetric water content of the soil was low (0 - 0.15 m 9%, 0.15 - 0.3 m 26% and 0.3 - 0.6 m 32%. Data courtesy of Dr. R. Cuenca, Oregon State University, OR.), and no condensation occurred within the freshly positioned chambers.

SUMMARY

Soil respiration is an important component of the global carbon budget, yet no single means of measuring soil CO_2 efflux has become universally accepted as a standard methodology. Chamber systems have found widespread use, but have been criticised for two reasons. Firstly, within chamber pressure differentials are often large enough (in the order of Pascals) to generate an additional mass flow of CO_2 into of out of the chamber, masking the natural diffusive or turbulent flow. Secondly, the "pumping" action of pressure fluctuations at the soil surface has been shown to be important in the exchange of CO_2 between the soil and the atmosphere, and these pressure fluctuations cannot be transferred through to the soil surface when closed chambers are used. An "open" chamber for the measurement of soil CO_2 efflux has been designed which utilises an air seal to maintain chamber pressure within 0.004 Pa of atmospheric pressure, eliminating any mass flow and ensuring that atmospheric pressure fluctuations are transferred through to the soil surface. The system was used at the BOREAS Southern Study Area Old Black Spruce site through the 1994 and 1996 field campaigns and was found to be robust and simple to use in the field. Consistency was found between soil CO_2 effluxes measured with this system and a closed dynamic chamber system.

Chapter Three - Temporal and Spatial Variation of Soil Respiration in a Canadian Boreal Forest

METHODS

Equipment description

A full description of the open chamber gas exchange system methodology is given in Chapter two (see also Rayment and Jarvis 1997). A solenoid-based, gas-switching system enabled multiple locations to be sampled alternately. Two soil respiration chambers were used in 1994, four in 1996. Each chamber was sampled for five minutes, with the first minute of each measurement being discarded, allowing for total flushing of the previous sample from the tubing and IRGA. In 1994, each chamber was sampled every 10 minutes, and three samples were combined to calculate half hour averages. In 1994 each chamber was sampled every 20 minutes. Ambient air was drawn through both sample and reference lines of all chambers at all times, irrespective of which collar was being measured for CO_2 efflux. Sample air flow was measured and controlled using mass flow controllers (Tylan FC-260, Tylan general (UK) Ltd., Swindon.) at 1 dm^3 min^{-1} (± 1%). Reference air flow is not used in the calculation of CO_2 efflux but was set with a needle valve to 1 dm^3 min^{-1}, ensuring that there was no pressure difference between the sample and reference sides of the gas analyser. Reference and sample CO_2 concentrations were measured using an infrared gas analyser (LI-6252 in 1994, LI-6262 in 1996, LICOR Inc., Lincoln, Nebraska, USA.) in differential mode. In 1994 drying columns (anhydrous $CaSO_4$, "Drierite", Aldrich Chemical Co., Gillingham, UK.) were fitted at the chamber end of both the reference and analysis air lines to minimise any errors resulting from cross-sensitivity to water vapour in the gas analyser. Drying columns were not necessary in 1996 as the LI-6262 measures and corrects for water vapour concentration. The gas analysers were calibrated at weekly intervals, using compressed air bottles whose CO_2 concentrations were determined through comparison with BOREAS project prime standard bottles. Simultaneous soil temperature measurements were made at 5, 10, 20, 50 and 100 cm depth within 6 m of the collars during the measurement period in 1994 and from November 1995 until December 1996. Soil temperature and CO_2 efflux data were transmitted via a multiplexer (AM416, Campbell Scientific (UK) Ltd., Shepshed, Leics.) and recorded

with a datalogger (Campbell CR21X), which also controlled the switching of the solenoids.

To facilitate making measurements on the moss-covered forest floor, metal collars (28 cm diameter) were inserted through the moss into the peat layer. The depth to which they were inserted depended upon the thickness of the moss layer, but all collars projected between 2 to 7 cm above the moss surface. Once inserted, the collars were left uncovered for at least one day before measurement in order for the soil system to re-equilibrate with ambient conditions. In 1994, six collars were installed at randomly chosen locations. Two collars remained in the same location for the entire study, the others were measured on two, three or four occasions (separated by a minimum of 6 days) before being moved to a new location. In total, 37 locations were measured over 102 days from day 151 to 253 of 1994. Eight collars were installed at random locations in November 1995, and were measured weekly throughout the spring, summer and autumn of 1996, from day 100 to 332.

Data analysis

Two typical sets of soil surface CO_2 efflux measurements are shown in Figure 3.1.

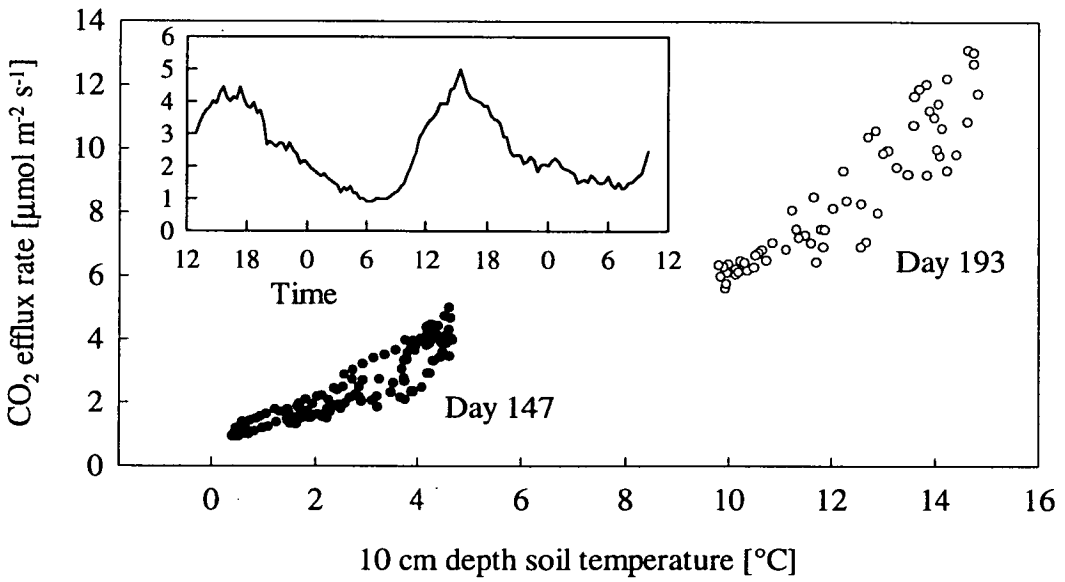

Figure 3.1. Two typical sets of soil CO_2 efflux data plotted against soil temperature. Each data point represents a single five minute efflux measurement, made every 20 minutes, and the twenty minute average 10 cm depth soil temperature. Inset is the time course of soil CO_2 efflux measured on day 147. Measurements were made at location 2 at the BOREAS SSA OBS site in 1996.

Most of the short term (i.e. hour to hour) variation in soil CO_2 efflux is a function of soil temperature (Rayment and Jarvis 1997). Two soil temperature response functions were fitted to each diurnal set of observations, a conventional exponential type response and an Arrhenius-type activation energy response. The exponential function was of the form,

$$R_T = R_0 \exp(kT) \tag{3.1}$$

where R_T is the CO_2 efflux rate at temperature T (°C), R_0 is the efflux rate at 0 °C (i.e. a basal rate) and k is a parameter describing the temperature sensitivity (related to Q_{10} by $Q_{10} = \ln(10k)$). The activation energy response followed the form of Lloyd and Taylor (1994),

$$R_T = A_1 \exp(-E_0 / (T - T_0)) \tag{3.2}$$

where R_T is the CO_2 efflux rate at temperature T (K), A_1 is a data-set-dependent parameter, T_0 is a temperature between T and 0 K and E_0 is analogous to a temperature dependent activation energy. The models were fitted using 5, 10 and/or 20 cm depth soil temperature as the driving variable.

The open chamber system used in this study is designed to allow the transfer of pressure fluctuations resulting from atmospheric turbulence through to the soil surface, since there is some evidence that the "pumping" action of these pressure fluctuations plays a role in the exchange of CO_2 between the soil and the atmosphere (Baldocchi and Meyers 1991). Therefore the temperature response function was modified to incorporate this effect. Because no high frequency atmospheric pressure data were available directly, friction velocity (the square root of the covariance between variations in vertical and horizontal windspeeds), U_*, was used to describe the degree of atmospheric turbulence (Oke 1987). The response of CO_2 efflux to turbulence was described as a simple linear function,

$$R = R_T (T) + aU_* \tag{3.3}$$

where R is the soil CO_2 efflux rate, R_t is the CO_2 production rate as a function of temperature t. The parameter a describes the response of CO_2 efflux to the friction

velocity, U_*, measured at 27 m height, such that higher values of a imply that CO_2 efflux is more sensitive to atmospheric turbulence.

All functions were fitted to the data by least squares analysis using the SAS NLIN procedure.

RESULTS

Instantaneous CO_2 efflux

In general, with both the exponential and the activation energy models, the best least squares fit to the data was given by the 10 cm depth temperature, although some individual observations were better described using 5 cm depth temperature. In order to compare response parameters between locations and times, it was necessary that the same environmental variables were used to drive both models. Changing the functions to describe the CO_2 efflux as the sum of two fluxes, one driven by 5 cm depth temperature and one by 10 cm depth temperature, resulted in a slightly higher average unadjusted r^2. When the r^2 was adjusted for the number of parameters, however, the single temperature models were found to provide a better description of the data across all locations and times. Therefore, for consistency, the 10 cm depth temperature alone was used as the driving variable for the short term (diurnal) response to temperature. Least squares fits of the models to the entire year's data showed that the exponential model and the activation energy model described diurnal data equally well, both having a total r^2 for all data of 0.75. Addition of the turbulence response parameter, a, made a significant ($p < 0.05$) improvement to the fit of the temperature response models to the data, increasing the total r^2 for all data to 0.80 in both cases. The average value of a for each sample location in 1996 was observed to be significantly ($p < 0.05$) and positively correlated with the thickness of the peat layer at that location (Figure 3.2).

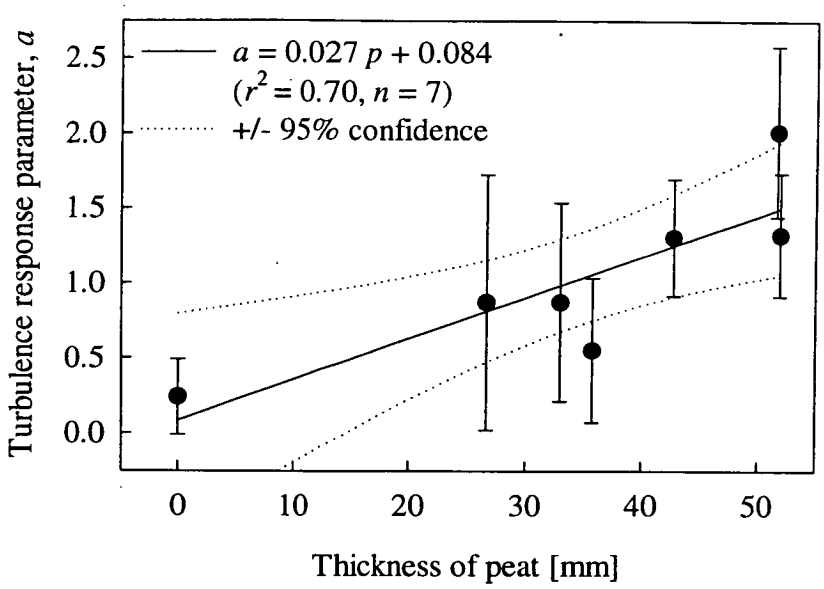

Figure 3.2. Relationship between the fitted turbulence response parameter, a, of soil CO_2 efflux and the thickness of the peat layer, p, for seven sample locations measured throughout 1996 at the BOREAS SSA OBS site.

Spatial variation

To assess the range of spatial variation in soil CO_2 efflux, the data sets collected between days 151 and 253 in 1994 were fitted to the simple exponential function described above (equation 3.1). Although there was a slight seasonal decrease in R_0 during this period, this trend was small in comparison to the total variation observed ($r^2 = 0.055$) and was not significantly different ($p > 0.05$) from the null hypothesis that there was no seasonal trend. Therefore fitted parameters from all the data sets collected during this period were combined to produce a spatial distribution of the basal rate of soil CO_2 efflux, R_0, and the temperature sensitivity coefficient, k (Figure 3.3).

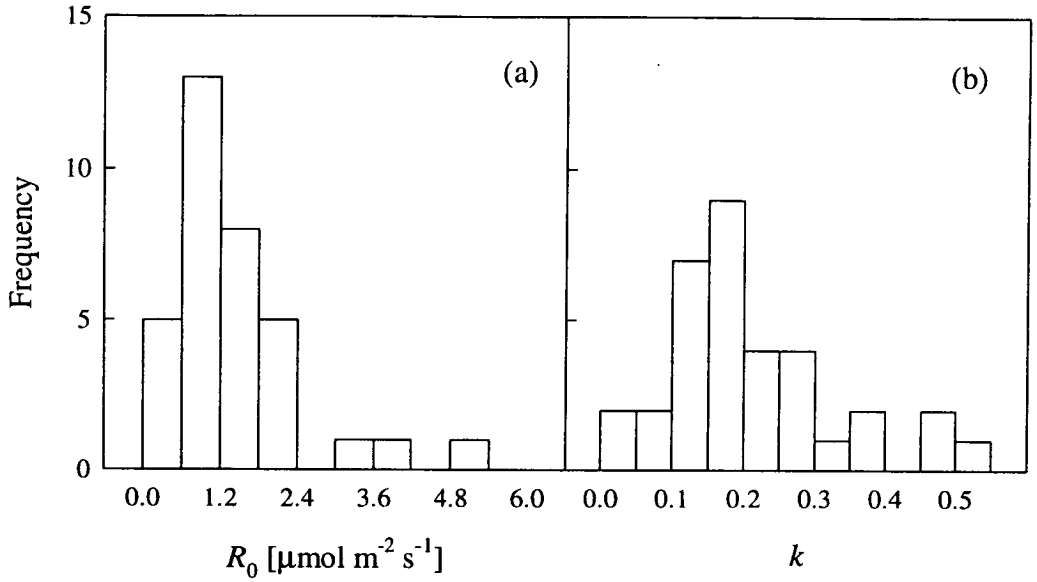

Figure 3.3. Frequency distribution of (a) basal rate, R_0, and (b) temperature sensitivity coefficient, k, of soil CO_2 efflux, measured at 34 locations at the BOREAS SSA OBS site between days 151 and 253 of 1994.

Variograms were constructed to show the scale of spatial heterogeneity of the locations sampled in 1994. γ is a measure of the dissimilarity between values of R_0 measured at two locations, i and j, separated by any distance class, d, given by,

$$\gamma(d) = 1/2\, n \sum (R_{0i} - R_{0j})^2 \qquad (3.4)$$

where n is the number of pairs of observations separated by d. There was a high degree of homogeneity between values of R_0 measured at locations separated by less than 1 m (Figure 3.4(a)). Spatial heterogeneity increased at distances larger than 1 m, but did not increase substantially as distances were further increased (Figure 3.4(b)).

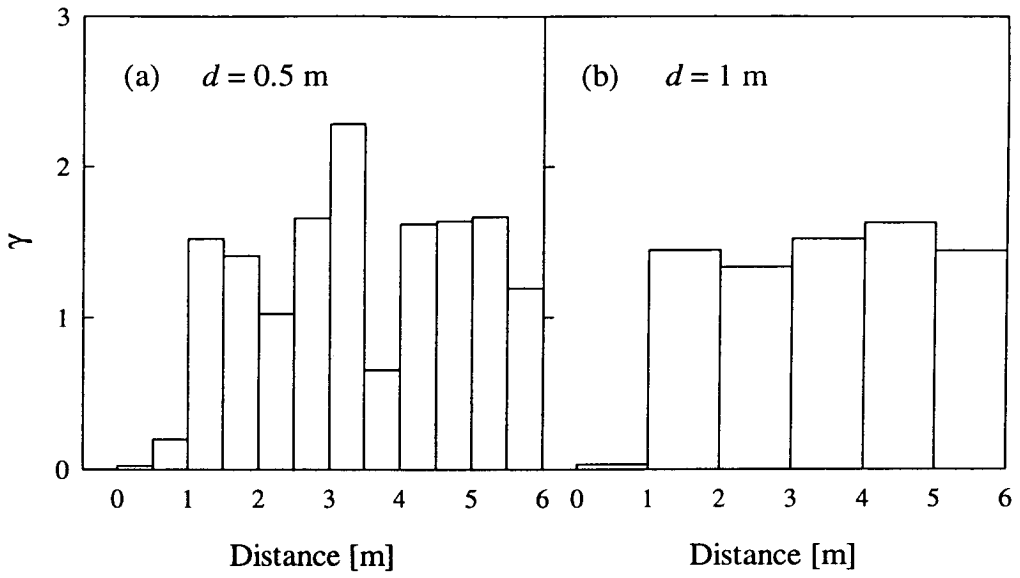

Figure 3.4. Variograms illustrating the scale of spatial heterogeneity of R_0 measured at the BOREAS SSA OBS site in 1994. See text for details.

To check that the eight locations chosen to study the long-term temporal variation in soil CO_2 efflux through 1996 (see below) were a representative spatial sample, a frequency distribution of R_0 was made for all data sets collected during the period of 1996 corresponding to the period of 1994 when measurements were made (i.e. days 151 through 253). Comparison of Figure 3.5 (1996 data) with Figure 3.3(a) (1994 data) indicates that the combined spatial and temporal variation in R_0 during 1996 was not less than during 1994, suggesting that the eight sample locations measured during 1996 were indeed a representative spatial sample. Moreover, the mean value of R_0 for this period in both years was found to be 1.28 μmol m^{-2} s^{-1}, indicating that there was no inter-annual variation in the basal rate of soil CO_2 efflux between these two years.

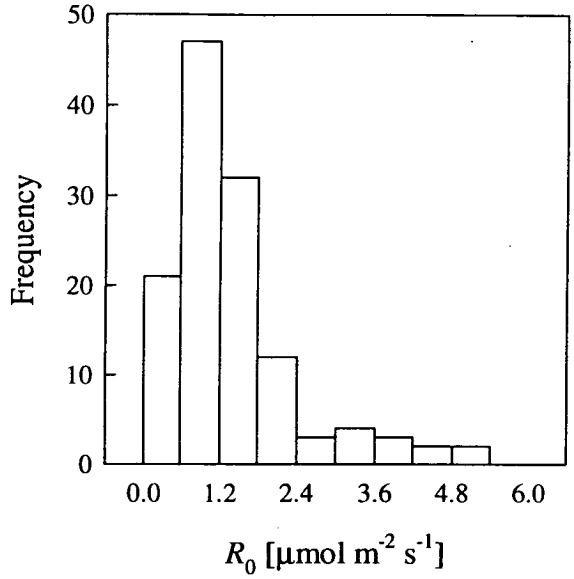

Figure 3.5. Frequency distribution of the basal rate, R_0, of soil CO_2 efflux, measured at 8 locations at the BOREAS SSA OBS site between days 151 and 253 of 1996.

Long term temporal variation

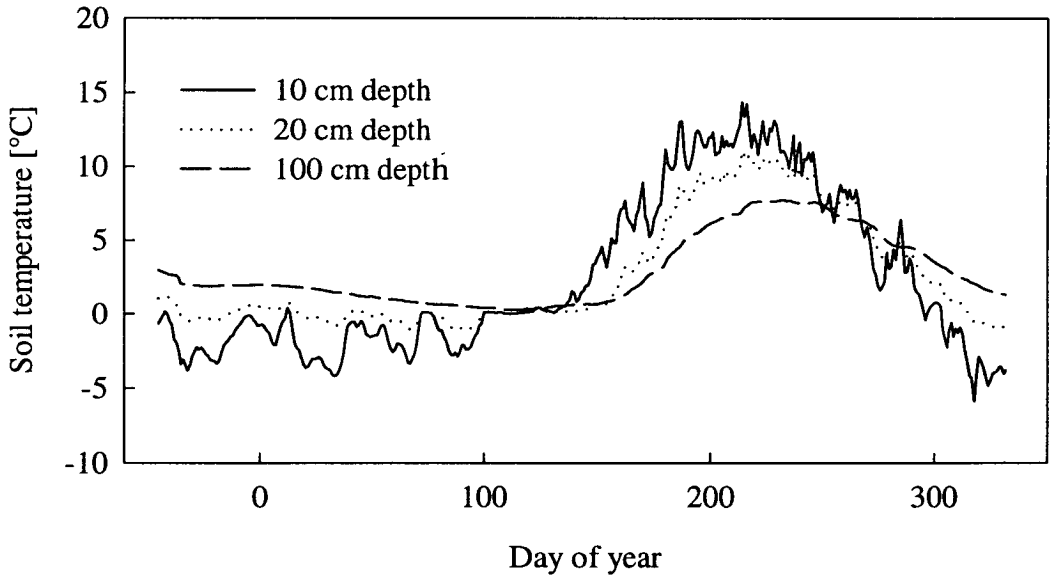

Figure 3.6. Soil temperatures measured through the soil profile at the BOREAS SSA OBS site from winter 1995 until winter 1996. Data are the mean of measurements made at four locations averaged over 30 minutes.

Because the short term (diurnal) variation in the soil CO_2 efflux rate resulting from short term changes in soil temperature was so large, patterns in the long term variation were investigated by exploring the way in which the temperature

insensitive rate and the temperature sensitivity parameters varied throughout the year. Figure 3.6 shows the soil temperature throughout the period from November 1995 to December 1996, for clarity only the 10, 20 and 100 cm depth temperatures are plotted. It is clear that the mean 10 cm depth soil temperature during the biologically active part of the year was considerably higher than 0 °C. If we estimate the instantaneous rate of soil CO_2 efflux by extrapolating from the efflux rate at 0 °C (i.e. R_0) using a temperature sensitivity (k) (equation 3.1), the sensitivity of the efflux to the value of k will increase as the measurement temperature increases above 0 °C, and any errors in the estimation of k will have an increasing impact on the estimated flux. In some cases, therefore, it is more appropriate to express the efflux in terms of a temperature insensitive rate at some temperature other than zero, falling within the temperature range over which the measurements were made (e.g. R_{10}). In this way, the instantaneous flux at any moment is estimated by interpolation within the measurement range, rather than by extrapolation. Because this study covered the entire seasonal variation in soil temperature, there was no single temperature that fell within the temperature range of every diurnal set of observations made. The exponential function fitted to each diurnal set of instantaneous fluxes was therefore re-written as,

$$R_T = R_{Tav} \exp[k\,(T - T_{av})] \qquad (3.5)$$

where R_T is the efflux rate at temperature T, k is the temperature sensitivity as described above, and R_{Tav} is the efflux rate at T_{av}, the daily average soil temperature during the time at which the observations were made. In this way, the temperature sensitivity, calculated from diurnal variation in the efflux rate, is used only to estimate diurnal variation around a basal rate appropriate to the prevailing soil temperature conditions.

Figure 3.7 shows the seasonal variation in R_{Tav} and k through 1996; for clarity only data from two locations are plotted. R_{Tav} increased from low rates at the start of the measurement period, reached a maximum between days 200 and 250, and declined back to very low rates late in the year. The temperature sensitivity parameter, k, was generally at its highest (i.e. CO_2 efflux rate was most sensitive to temperature) at the start of the year, declined rapidly until around day 200 and declined more slowly

afterwards. Observations where the fitted k was not significantly different to zero (i.e. there was no significant variation with temperature) occurred at the end of the measurement period, for these observations k was defined to be zero.

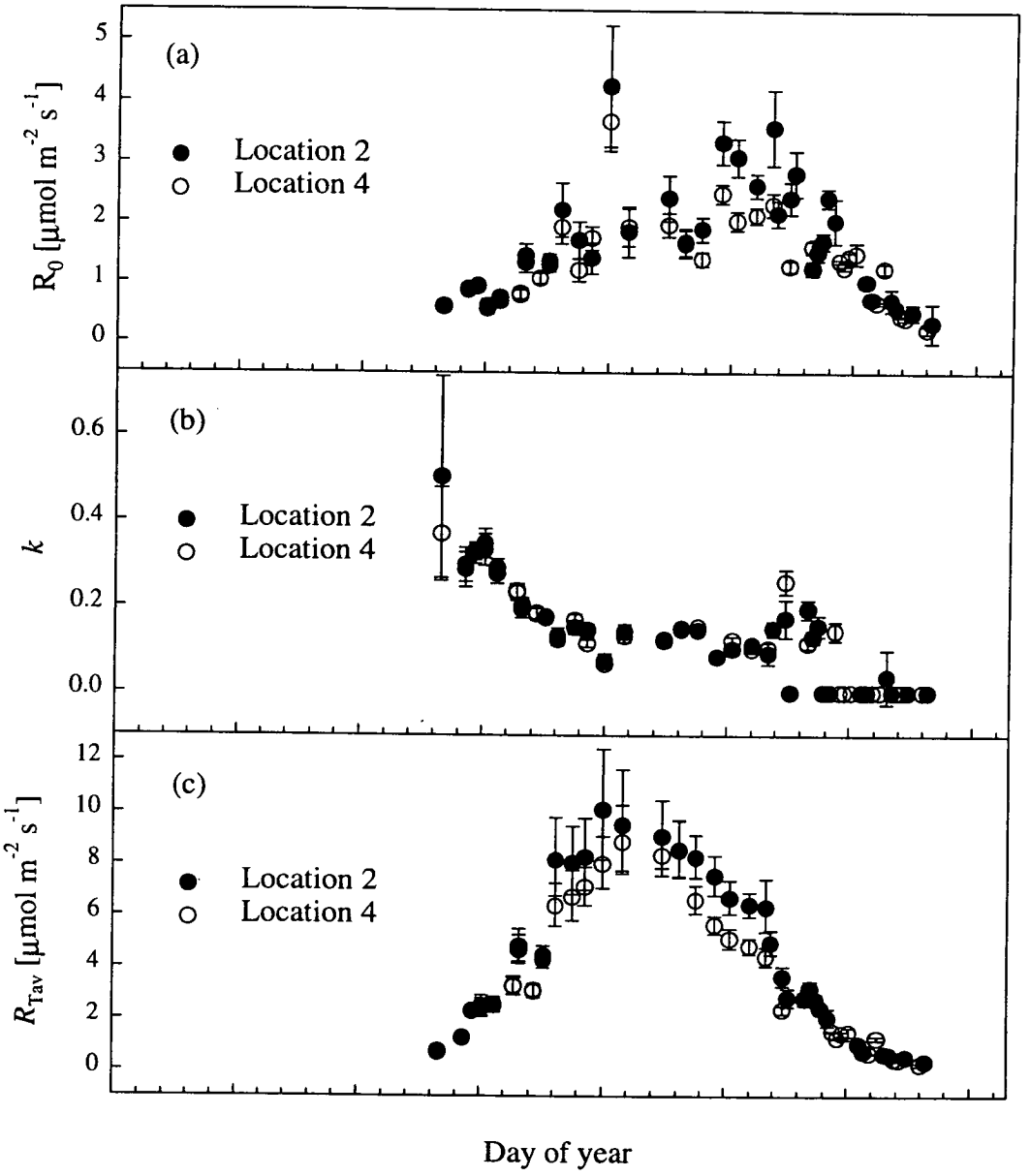

Figure 3.7. Seasonal variation of (a) basal rate, R_0, (b) the temperature sensitivity coefficient, k, and (c) R_{Tav} (see text for description) for soil CO_2 efflux at two locations at the BOREAS SSA OBS site during 1996. Each data point represents the least squares estimate of the parameter from a diurnal set of soil CO_2 efflux and 10 cm depth soil temperature measurements. Error bars are the ± 95% confidence limits for the parameter estimates.

Total yearly efflux

In order to estimate the total yearly carbon efflux from each measurement location, it was necessary to interpolate values of R_{Tav} and k between the observations plotted in Figure 3.7. Because the predicted efflux is relatively insensitive to the value of k when temperature variations are small (diurnal variation in soil temperature at 10 cm was typically around 6 °C when soil temperature was at its highest, and was lower when soil temperature was lower), daily values of k were estimated from a linear interpolation between measured values. Interpolation of the more important parameter, R_{Tav}, was based on the seasonal response of R_{Tav} to soil temperature (see Figure 3.8, for clarity data from two locations are plotted, and the ± 95% confidence limits for the parameter estimates are omitted). Most of the seasonal variation in R_{Tav} was explained by fitting R_{Tav} to an exponential temperature function (of the same form as equation 3.1) of daily average 10 cm soil temperature (average r^2 = 0.82 (excluding location 1, see below)).

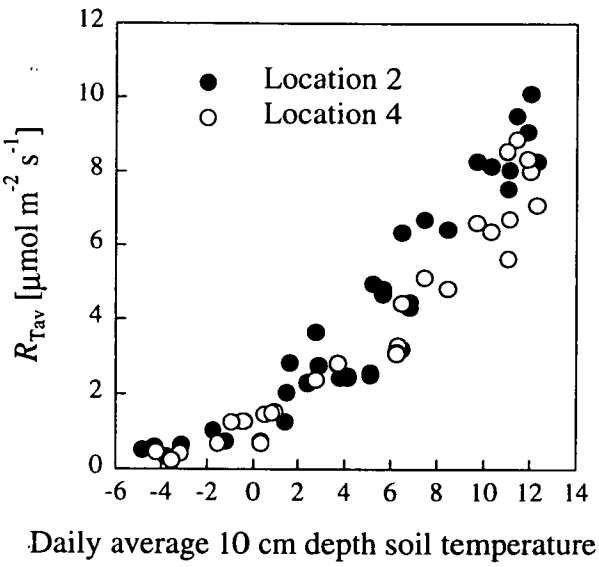

Figure 3.8. Relationship between the forest floor CO_2 efflux at the daily average 10 cm depth soil temperature, R_{Tav}, and the daily average 10 cm depth soil temperature for soil CO_2 efflux at two locations at the BOREAS SSA OBS site for the entire measurement period of 1996.

The estimated cumulative carbon efflux for the eight locations measured during 1996 is shown in Figure 3.9. Assuming that the locations measured in 1996 data are a representative spatial sample (as discussed above), the spatially averaged total soil

carbon efflux for the BOREAS SSA OBS site in 1996 was 896 g (C) m^{-2}, or 8.96 Mg (C) ha^{-1}. Confidence limits for this total were estimated from predictions using the upper or lower 95% confidence limits of the individual parameters (R_{Tav} and k) used in the calculations. The upper 95% confidence limit of the spatially averaged total soil carbon efflux was 1026 g (C) m^{-2} (10.26 Mg (C) ha^{-1}), the lower 95 % confidence limit was 786 g (C) m^{-2} (7.86 Mg (C) ha^{-1}).

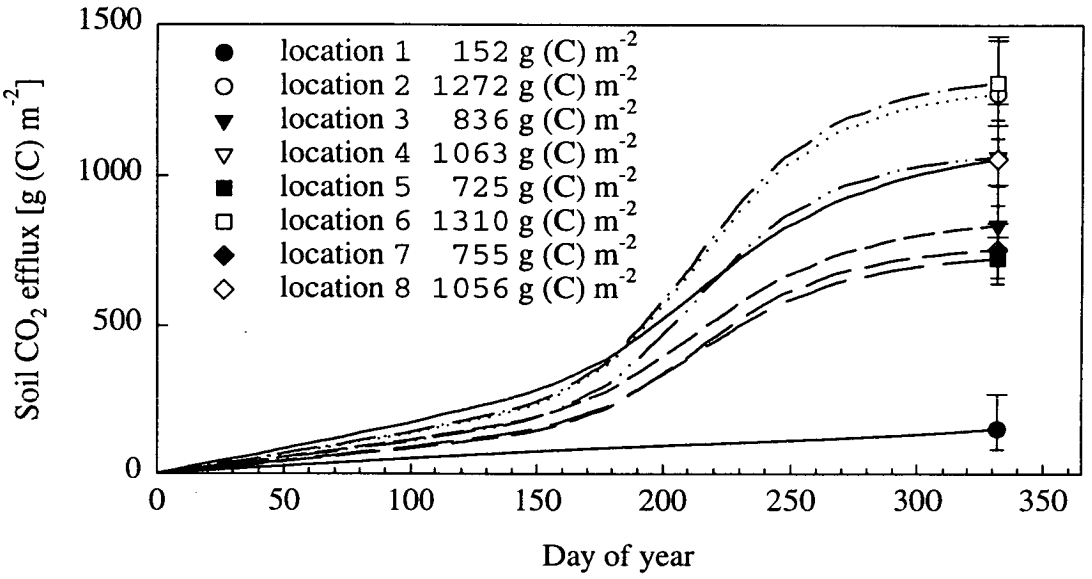

Figure 3.9. Predicted cumulative soil carbon efflux for the eight sample locations measured at the BOREAS SSA OBS site from the start of 1996 until the end of temperature measurements in December of that year. Data given are the predicted total annual carbon efflux at each location, and error bars are upper and lower 95% confidence limits based on predictions using either the upper or lower 95% confidence limits of the individual parameter estimates.

A good relationship was found between the predicted total annual carbon efflux and the thickness of the light brown mat of dead peat moss between the living moss and the darker, more humic peat underneath (Figure 3.10).

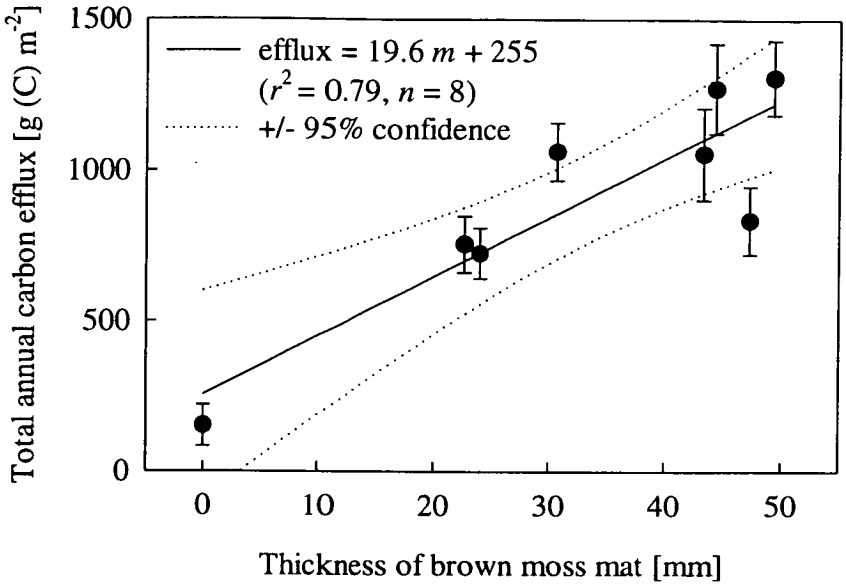

Figure 3.10. Relationship between the estimated total annual carbon efflux and the thickness of the light brown mat of dead peat moss for eight sample locations measured throughout 1996 at the BOREAS SSA OBS site. The relationship is described by the equation efflux [g (C) m^{-2}] = 19.6 × thickness [mm] + 255.2, r^2 = 0.79, n = 8.

DISCUSSION

The yearly total CO_2 efflux from the forest floor at this site was estimated to be 8.96 Mg (C) ha^{-1}. That this is an order of magnitude larger than, and of opposite sign to, the net ecosystem uptake estimated for this period (Chapter 6) highlights the importance of quantifying this component of the net ecosystem flux. A study of soil carbon cycling conducted near this site in 1995 (Nakane *et al.* 1997) estimated the total yearly CO_2 efflux from soil to be 2.83 - 3.68 Mg (C) ha^{-1} yr^{-1}, about one third of the estimate calculated from this study. Part of this inconsistency may relate to the different sample locations used in each study. The major difference between these two studies however, was that Nakane *et al.* employed the alkali absorption method to measure soil CO_2 efflux. This method (and static chambers in general) are known to underestimate soil CO_2 efflux, particularly when effluxes are large (e.g. Nay, Mattson & Bormann 1994) and consequently their extrapolated yearly flux is also likely to be an underestimate.

The large amount of variability observed in the forest floor CO_2 efflux rate, both diurnally (Figure 3.1) and seasonally (Figure 3.7(a)), illustrates the importance of

making measurements that span and resolve differences over these different time-scales, and demonstrates the strength of the dynamic open system used here. The high degree of spatial variability (Figures 3.3 & 3.5), found at all but the smallest scales (Figure 3.4), further demands that measurements are made at sufficiently large number of locations to provide an adequate spatial sample.

Temporal variation

The short term (hour-to-hour) variation in instantaneous soil CO_2 efflux was well described by a simple, two parameter, exponential function of a single soil temperature, where the parameters were allowed to vary with each set of observations collected. This description was not improved by using the three parameter activation energy type function proposed by Lloyd and Taylor (1994). This latter model did, however, produce a better description (i.e. a higher r^2) of the variation in the instantaneous soil CO_2 efflux when all the data collected at a particular location over the entire year were fitted to the function with a single set of parameters. This is because the Lloyd and Taylor (1994) model is, in effect, an exponential function where the temperature sensitivity coefficient increases with decreasing temperature. An increased temperature sensitivity at low temperatures has been observed elsewhere (Kirschbaum 1995; Blanke 1996; Winkler, Cherry & Schlesinger 1996; Nakane *et al.* 1997), and comparison of Figure 3.7(b) with Figure 3.6 illustrates that as soil temperature increases between days 150 and 200, k does indeed decrease. At the start of the growing season, only the uppermost part of soil profile (where temperature is well coupled to air temperature and diurnal variation is consequently high) is biologically active. As a result, the sensitivity of soil CO_2 efflux to temperature variation is high. As the season progresses, average temperatures deeper in the soil profile increase, and an increased depth of soil becomes active. The magnitude of the diurnal variation in soil temperature is, however, attenuated deeper in the soil profile, and as a consequence the sensitivity of the rate of CO_2 production to diurnal variations in temperature decreases, leading to a lower k. Late in the year, temperatures in the upper part of the soil profile are very low, and activity is concentrated in the lowest part of the soil profile where there is

very little diurnal temperature variation. At this time there appears to be little or no sensitivity of soil CO_2 efflux to diurnal temperature fluctuations.

The seasonal variation in R_{Tav} (or in the daily average soil CO_2 efflux rate which follows a similar seasonal trend) can be attributed, in part, to the volume of soil that is biologically active. In the early part of the year, the volume of active soil is restricted both by the high water table resulting from the limited drainage of melt water caused by frozen soil deeper in the soil profile, and by low temperatures so that only the uppermost part of the soil is warm enough for microbial decomposition to proceed. Conversly, in the latter part of the year, as the upper layers of soil become frozen, it is only the lower part of the soil profile that is active.

In addition, that part of the soil CO_2 efflux deriving from growth respiration associated with the production of new roots is highly seasonal. Average daily fine root growth in boreal trees has been shown to be exponentially correlated with 10 cm soil temperature (Tryon & Chapin 1983) and when measured at this site was found to follow a similar seasonal pattern to R_{tav} (Steele *et al.* 1997).

Because variations in soil temperature accounted for most of the variation in soil CO_2 efflux both at the short and long time-scales, it is likely that soil temperature predominately limited CO_2 production and that other factors, such as soil moisture, had little effect. Similar results have been found in other ecosystems (Moore 1985; Alvarez 1995; Son & Kim 1996). Decomposition rates in black spruce forests are unaffected by soil moisture contents in the range 100 to 250 %, and only become sensitive to soil moisture at contents below 75 % (Schlentner & Van Cleve 1985). Measured soil moisture contents at this site were found to vary between 150 and 250% (Nakane *et al.* 1997). Thus there was no reason to believe that soil CO_2 efflux at this site was ever limited by lack of soil moisture, although waterlogged soil conditions early in the year may have limited soil CO_2 efflux by reducing the active soil volume at this time.

Approximately one eighth of the estimated yearly total CO_2 efflux was lost from the soil before measurements were started on day 100 (Figure 3.9). This estimate must represent the upper limit to the total winter-time soil CO_2 efflux, since it was based

on a temperature response function derived largely from data collected at the end of the season, when the lower parts of the soil profile were yet to reach their yearly temperature low. The deep layer of snow accumulating in the winter insulates the soil from very low air temperatures, and has been shown to produce conditions whereby microbial respiration can continue throughout the winter (Mariko 1995; Sommerfeld Mosier & Musselman 1993). The estimated daily average wintertime CO_2 efflux rate from the forest floor at this site was 1.1 μmol m^{-2} s^{-1}, over twice the estimate of ~ 0.4 μmol m^{-2} s^{-1} for heterotrophic respiration alone generated by a modelling study for the colder BOREAS NSA OBS site (Frolking *et al.* 1997).

Spatial variation

Reported studies of the spatial variability of soil CO_2 efflux are few. Hanson (1993) found coefficients of variability for daytime forest floor CO_2 efflux rates of between 0.28 and 0.42 in a deciduous oak forest, somewhat less than the 0.87 found in this study, although no indication of the spatial scale of this variability is given. Similarly, Goulden *et al.* (1996) describe extensive heterogeneity in soil CO_2 efflux at the Harvard forest, with rates varying between 3.8 and 7.5 μmol m^{-2} s^{-1}, although the area over which this variation occurred was not reported. Nakayama (1990) reported that soil CO_2 efflux rates may vary by up to 100% at locations 1 m apart, suggesting a similar scale of variability to that found here, where locations separated by 1 m showed as much intra-site variability as locations separated by larger distances (Figure 3.4).

Much of the spatial heterogeneity found in this study results from variations in micro-topography at the site, mediated through the depth of the peat layer. Thus, in relation to the hummocks, the hollows are wetter, consequently more prone to anaerobic conditions, and moss production and decomposition rates are lower. An extreme case of this is evidenced at location 1 (1996), which was located in a small gravel filled hollow, with no surface organic matter, and where the water table remained at the "soil" surface for most of the year. The soil CO_2 efflux rates at this location changed very little through 1996, and measured rates were not significantly different at the end of the measurement period to those observed in mid-summer.

Response to turbulence

The responsiveness of the soil CO_2 efflux measured with this chamber system to atmospheric turbulence supports the suggestion that pressure fluctuations at the soil surface play a role in the transfer of CO_2 between the soil and the atmosphere (Kimball & Lemon 1971). A similar argument, based on measurements made with the eddy covariance technique, has been put forward by Baldocchi & Meyers (1991). This finding has two important implications.

Firstly, chamber methods of measuring soil CO_2 efflux which do not allow the transfer of pressure fluctuations through to the soil surface (i.e. "closed" systems) will interfere with the transport of CO_2 from the soil. If the chamber were in place for a long enough period, the system would eventually reach a steady state when the diffusive transport of CO_2 from the soil would equal the CO_2 production rate. Chambers that calculate CO_2 efflux from the transient increase in CO_2 concentration within a closed volume, however, can only be left in position for short periods. During the measurement period, the curtailment of turbulent transport of CO_2 from the soil into the chamber is likely to cause an increase in the CO_2 stored within the soil volume, and will consequently result in a systematic underestimation of the flux that would have occurred in the absence of the chamber. The predicted CO_2 efflux, with and without the turbulence response term, was calculated from the model parameters extracted from the 1996 data. The fluxes estimated without the turbulence term were between 86 % and 98 % of the fluxes estimated when the turbulence term was included. The error associated with excluding the effect of turbulent exchange of CO_2 between the soil and the chamber was estimated by recalculating the predicted effluxes, leaving out the turbulence term. From this it was estimated that excluding the effect of turbulent exchange results in an average underestimation of the "true" efflux by 8.8 %. A comparison between methods of measuring soil CO_2 efflux showed that, compared to this method, a closed chamber system did indeed underestimate the flux (Rayment & Jarvis 1997; see also Norman *et al.* 1997). A similar underestimation has also been demonstrated under laboratory conditions (Nay, Mattson & Bormann 1994), and a mathematical model of gas movement in soils suggest that chamber measurements that restrict the transport of CO_2 from the

soil are subject to around a 10% underestimation of the natural soil efflux (Dr. R. Striegl US Geological Survey, Denver, CO.).

Secondly, the reduction of net ecosystem exchange (NEE) measured by the eddy covariance technique during periods of low turbulence ($U_* < 0.35$ ms^{-1}), especially at night, is generally considered to be a consequence of a reduction in the turbulent exchange of air from within the canopy volume to the atmosphere. At these times it is usual for the "storage" flux (that is the increase or decrease in the total amount of CO_2 stored within the canopy volume) to be added to the measured NEE, thus in principle generating a turbulence independent net "biotic" flux. Situations occur, however, when this composite biotic flux is not, in fact, independent of turbulence, and at these times it is typically assumed that this is the result of an advective loss of CO_2 from the system (e.g. Moncrieff, Malhi & Leuning 1996). For these situations, biotic flux estimates (NEE plus the storage flux) are often replaced with modelled estimates of NEE derived from eddy covariance measurements made under highly turbulent conditions ($U_* > 0.35$ ms^{-1}). The model used typically expresses NEE as a simple exponential function of temperature. The finding here, that the efflux of CO_2 from the soil surface is dependent on turbulence, carries the implication that this "correction" is based on an incorrect assumption, i.e. that NEE should be expected to be independent of turbulence. Making this low turbulence correction to NEE on the basis of temperature will, therefore, cause a systematic overestimation of the loss of CO_2 from the system at night, and consequently will result in a systematic underestimation of the daily CO_2 uptake by an ecosystem. What is needed, therefore, is some means to extend the storage flux to include also any change in the amount of CO_2 stored within the soil volume. The relationship between the effect of turbulence on the efflux and the thickness of the peat layer (Figure 3.2) suggests that this "within soil storage" of CO_2 may be more pronounced in organic soils with a high air filled porosity than denser mineral soils.

SUMMARY

The efflux of CO_2 from the soil surface is a key component of the carbon balance of any ecosystem. Quantifying this flux and understanding the factors that underlie the temporal and spatial variation in its magnitude are fundamental to our understanding

of the behaviour of the ecosystem as a whole and to our ability to predict the likely consequences of climatic change. Forest floor CO_2 efflux was measured at 45 locations over two years in a *Picea mariana* stand at the BOREAS Southern old black spruce (OBS) site. Spatial variability was high, and was related empirically to the thickness of the dead moss layer. Short term (hour to hour) variation was well described as a simple exponential function of soil temperature, and was significantly related to atmospheric turbulence. Seasonally, soil CO_2 efflux varied between low, but positive, rates before the springtime thaw and after the wintertime freeze, to rates as high as 14 μmol m^{-2} s^{-1} in late summer. The total annual carbon efflux from the forest floor for 1996 was estimated to be 8.96 Mg (C) ha^{-1} with 95% confidence limits of 7.86 Mg (C) ha^{-1} and 10.26 Mg (C) ha^{-1}. For individual sampling locations, both the total annual carbon efflux and the responsiveness of the efflux to atmospheric turbulence were significantly correlated with the thickness of the peat layer on the forest floor.

Chapter Four - Long Term Measurement of Photosynthesis, Respiration and Transpiration of Black Spruce (*Picea mariana*)

To quantify the annual carbon uptake by foliage at the BOREAS SSA OBS site, photosynthesis, respiration and transpiration of whole branches was measured over an entire growing season.

Materials and Methods

Branch bag description

Two branch bags were installed on each of two trees, labelled East and West in order to signify their position relative to the canopy access tower, at the BOREAS southern study area OBS site (Sellers *et al.* 1995) in early April 1996. Two bags were positioned in the Upper canopy (at 7.85 m (Bag 1, West) and 8.25 m (Bag 3, East) height) and two in the Lower canopy (at 5.22 m (Bag 2, West) and 5.48 m (Bag 4, East) height). The tree heights were 10.25 m (West) and 10.01 m (East), this represented the modal height for black spruce in this stand. Tree diameter at breast height was 10 cm and 9 cm respectively. The bags were supported in position by elastic ropes attached to the trunk above the bag and, where necessary, to a support projecting from the canopy access tower. This arrangement allowed the bags to move freely as the trees and branches moved with the wind. Each of the bags was positioned on a south facing branch thus minimising shading by the tower.

The bags (Figure 4.1) consisted of two 5 mm thick acrylic end pieces, ellipsoid in shape (600 mm major axis, 300 mm minor axis, 0.14 m^2 area), separated by five thin (5 mm diameter) stainless steel rods, covered with polypropylene film (ICI Propafilm, 34 µm thickness, ICI Propafilm, Dumfries), and sealed along the edges of the end pieces with silicone sealant. One end piece was made such that it could slide up or down the rods to adjust the bag length to suit the individual branch. An ellipsoid shape was chosen to minimise the dead volume within the bag, to minimise the bag's surface area to volume ratio (minimising any adsorption/desorption effects), to minimise attenuation of incoming light, to allow snow to slide off and to prevent water pooling on the top. The bottom of the bag was left unsealed to allow placement of the bag over the branch, whereafter it and the branch entry point were also sealed with silicone sealant.

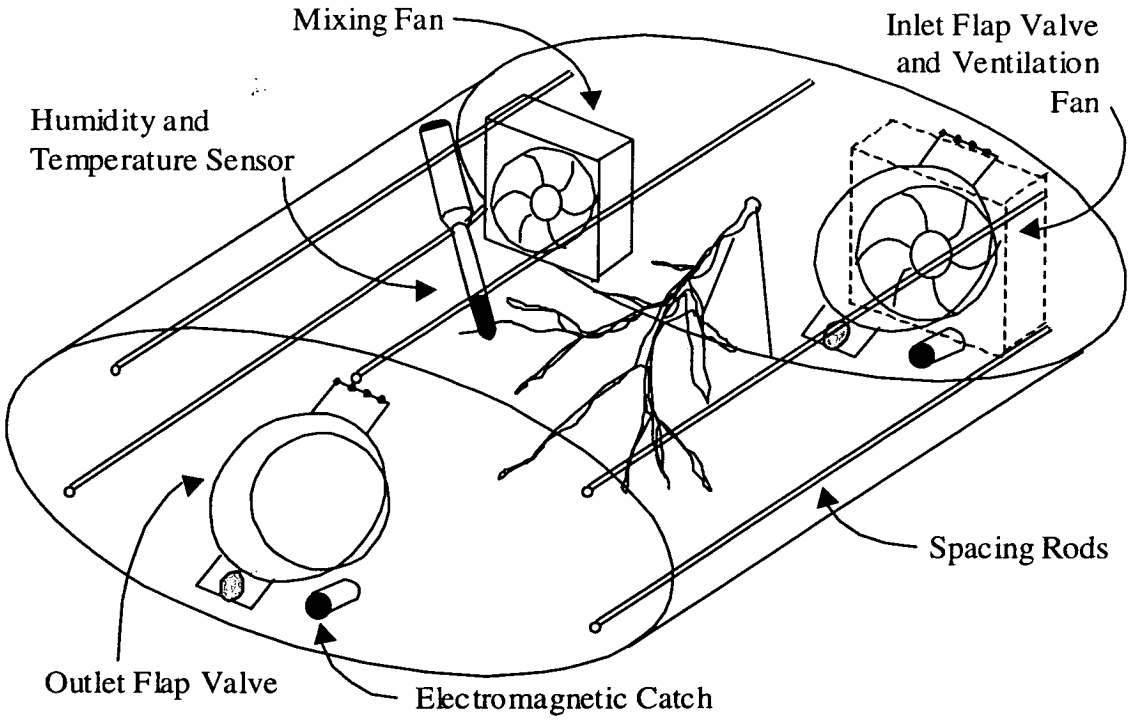

Figure 4.1. Schematic of branch bag construction.

A 12v electric fan (RS 583-050, RS Components Ltd., Corby) was mounted at the trunk end of each bag, and blew air at a high flow rate (40 dm^3 s^{-1}; approximately 18 to 26 air changes min^{-1}) through the bag via large shrouded inlet and outlet ports. When a gas exchange measurement was to be made, the ventilation fan was switched off and an internal circulating fan was switched on. Thin plexiglas flap valves dropped over the inlet and outlet ports and were shut tight with small electromagnetic catches. Air was circulated (5 dm^3 min^{-1}) continuously between all bags and a box containing the IRGA and control system (mounted nearby on the tower), at all times, through loops of tubing (5 mm i.d. Dekabon 1300, Furon, Gembloux, Belgium). At measurement time a small amount of air (0.2 dm^3 min^{-1}) was diverted from the appropriate loop to the IRGA (LI-6262, LI-COR Inc., Lincoln, Nebraska) operating in absolute mode.

Within each bag, relative humidity and air temperature were measured (Vaisala HMB 30A, Vaisala (UK) Ltd., Cambridge), as was leaf temperature (0.2 mm diameter Cu-Con thermo-junction referenced to the air temperature sensor) and, for a

period, bag internal vs. external temperature (Cu-Con thermocouple). Photon flux density (PFD) incident upon each branch was measured with a horizontal light sensor (SD101QV, Macam Ltd., Livingston) mounted directly onto the branch, midway along its length. Sensor outputs were transmitted via a multiplexer (Campbell AM416) and recorded with a datalogger (CR21X, Campbell Scientific (UK) Ltd., Shepshed, Leics.), which also initiated the measurement sequence. The gas analyser was calibrated at weekly intervals, using gas bottles of CO_2 in air with concentrations that were determined through comparison with BOREAS project prime standard bottles.

Gas exchange calculations

Each bag was closed for five minutes in turn, during which time the sensors were read every 20 seconds. Each bag was therefore measured every 20 minutes. Gas exchange was calculated from the slope of the regression of gas concentration against time and the volume of the system (106.3, 134.3, 91.9 and 106.3 dm^3 for bags 1 to 4, respectively). Data from the initial 40 s for CO_2 and the initial 80 s for H_2O vapour were excluded to ensure that the previous air sample was entirely flushed from the IRGA. The volume of air sample bled to the IRGA during the measurement period was negligible ($\approx$ 1 dm^3) compared to the bag volume, and was ignored in calculations. All bags were tested for leaks by shading the branch to its light compensation point, blowing into the bag to create a large internal/external concentration difference, closing the inlet and outlet ports and monitoring bag concentration. For example, the CO_2 concentration changed from 1607 to 1603 µmol mol^{-1} over the course of five minutes, demonstrating that leakage could be ignored over the period of measurement.

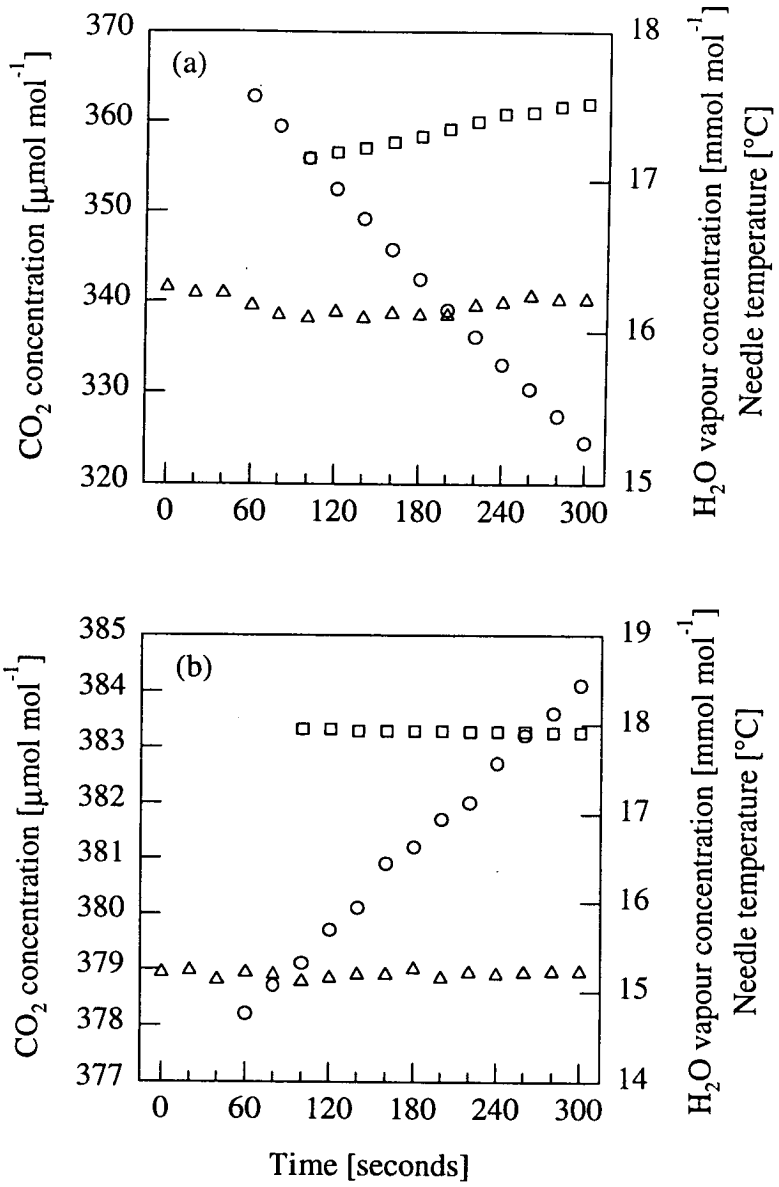

Figure 4.2. Typical time courses of branch bag measurements made during (a) the daytime (Bag 1, 12:00 local time, day 200) and (b) the night-time (Bag 1, 00:00 local time, day 200). o = CO_2 concentration, □ = H_2O vapour concentration, Δ = needle temperature.

Figure 4.2 shows that the changes in concentration over the measurement period were linear with time, even at night when the flux was small. This indicates that respiration measurements with a chamber of this type are possible when sufficient attention is paid to sealing the chamber and to ensuring that the inlet/outlet ports remain tightly closed during the measurement period. There was no evidence of any systematic change in the temperature regime during the course of a measurement period, but during the daytime the temperature within each bag was consistently

higher than the temperature immediately outside the bag. This effect was found to be a linear function of PAR incident on the bag ($r^2 > 0.9$ upper bags, $r^2 > 0.7$ lower bags), and was therefore more pronounced in the bags experiencing higher radiation at the top of the canopy than in those positioned lower down. Air temperatures inside the lower bags were within 1 °C of ambient temperature 90 % of the time and were exceptionally up to 3 °C warmer than the ambient air; inside the upper bags air temperatures were within 1 °C of ambient air temperature 75 % of the time, within 3 °C 90 % of the time and exceptionally were up to 6 °C warmer than the ambient air. Temperature elevation inside bags at the same height was similar, suggesting that the internal mixing fan was sufficient to minimise any differences in the boundary layer resistance of the branches resulting from their different sizes.

Daytime was defined as being the period between dawn and dusk when incident PFD was above 3 μmol m^{-2} s^{-1}. Branch conductance to water vapour, g_w, was calculated from the water vapour flux, E, and the leaf to air humidity deficit, D, (expressed as a mole fraction deficit) according to:

$$g_w = \frac{E}{D} \tag{4.1}$$

using only those data for which water vapour flux exceeded 0.025 mmol m^{-2} s^{-1} and the leaf to air humidity deficit exceeded 1 μmol mol^{-1}. The water vapour flux cut-off value was determined as the value below which the calculated fluxes were not significantly different to zero and corresponded to the value at which the regression line through the concentration measurements from which the flux was calculated fitted the data with an average r^2 value of less than 0.95. The humidity deficit cut-off point was chosen to eliminate spurious values when the denominator was very small. All averages referred to in the text (e.g. daily average branch conductances, Figure 4.6(c)) are the unweighted average of all the values measured. Daily and night-time totals (e.g. Figures 4.4(b) and 4.5(c)) were calculated only when all instantaneously measured values for that period were free from known error.

Small gaps in the data resulting from technical problems (IRGA failure, loss of power) were filled using multiple linear regression to relate daily total carbon uptake

or water loss to the entire set of meteorological data collected. Blind testing showed that predictions from this procedure fitted observed data with $r^2 > 0.95$ for all branches.

Branch measurements

After the end of the observation period (December 1996) the branches were cut off whole and photographed in three projections. Leaf area, needle and wood dry mass and chlorophyll and nutrient contents of current year and previous years needles were measured. Projected needle area was measured with a LI-COR 3100 area meter; needle and wood dry mass was measured following 24 hours drying at 70 °C in a ventilated oven; chlorophyll content was measured on a sub-sample of the needles (following Porra, Thompson & Kriedemann 1989); N, P, K, Ca & Mg were measured on finely ground sub-samples of the oven-dried needles using the method described by Allen (1989) with some modifications. Organic matter was oxidised using an acid oxidation process prior to analysis: 2 cm^3 of concentrated H_2SO_4 were carefully added to 100 (± 10) mg of plant material in a test tube followed by H_2O_2 (2 × 75 cm^3). The sample tubes were then heated at 320 °C for 6 hours, cooled and made up to 100 cm^3 with distilled water. N concentration was determined by a gas diffusion method using a flow injection analyser (Fiastar, Tecator, Wilsonville, Oregon, USA). Total P was determined by a molybdenum blue method using the flow injection analyser as described in the application note ASN 60-04/83 (Perstorp Analytical Ltd., Maidenhead, Berkshire, UK). K, Ca and Mg were determined by atomic absorption spectrometry (919 Atomic Absorption Spectrometer, UNICAM, Cambridge, UK). Based on 100 mg of dried sample made up to a fixed volume of 100 cm^3, the macronutrient concentration, C, was calculated as:

$$C = \frac{c \times V_{sol}}{W_{sample}} \qquad (4.2)$$

where c is the concentration of the solution (mg dm^{-3}), V_{sol} is the volume of the solution (0.1 dm^3) and W_{sample} = original mass of the sample (0.1g). Although the data are not presented here, nutrient contents, water potentials and single shoot measurements of gas exchange were measured on adjacent branches at intervals

EX BIBL. UNIV. EDINBURGH

during the growing season. Sapflow and cavitation sensors were also installed in the trees for a period.

Sources of errors

Errors in calculated fluxes are directly proportional to errors in leaf area and bag volume measurements. Repeated, independent measurements showed that these systematic errors were less than ± 1 % of the quoted values. The LI-COR IRGA is a very stable instrument, nevertheless, if the calibration of the analyser were to drift by 1 $\mu mol\ mol^{-1}$ during the course of a five minute measurement, this would correspond to an error of less than 0.05 $\mu mol\ m^{-2}\ s^{-1}$ in the calculated rate of photosynthesis.

Measurements of water vapour flux (and branch conductance) are subject to errors arising from any adsorption of water vapour onto the inside of the bags as the water vapour concentration rises during the measurement period, leading to systematic underestimation of transpiration. The use of Propafilm (having a low susceptibility to water adsorption/desorbtion) as the material for the bags, together with the bags' high volume to surface area ratios, should have reduced this effect as far as possible.

The small temperature increases observed inside the bags compared with the ambient air temperature may have affected CO_2 and water vapour exchange, both directly (i.e. by acting on the biochemical activity of the branch) and indirectly (e.g. by increasing the humidity deficit of the air). Using the a simple light and temperature response model (Table 4.2) and a relationship between the temperature elevation inside each bag and the radiation incident upon it, it was possible to make a first degree estimate of the effect of the temperature increases on branch CO_2 exchange. Comparing the annual carbon uptake total calculated with and without the temperature correction, it was estimated that the total carbon uptake for the upper bags would have been *reduced* by 1.7 % in the absence of the temperature elevation. There was negligible difference (< 0.1 %) between the estimates of annual carbon uptake of the lower branches with and without the temperature correction.

RESULTS

Figure 4.3 shows diurnal time-courses of gas exchange and concurrent environmental variables during and following a cloudless day in June for an upper canopy and a lower canopy branch. On this particular day, calculated branch conductance at the start of the morning was similar for the two branches but the higher PFD on the upper branch resulted in higher photosynthetic and transpiration rates. By late morning branch conductance of the lower branch had increased whereas conductance of the upper branch remained more or less constant, possibly because of the higher leaf temperature and humidity deficit in the upper canopy. This, combined with a PFD at the lower branch that was comparable with that at the upper branch (and typically above the value required for light saturation of photosynthesis, (Yue & Margolis 1993; see also Chapter 5)), resulted in larger water and carbon fluxes through the afternoon than in the morning. PFD on the lower branch was typically lower and more variable than on the upper branch as a result of the shade cast by the branches higher up. Night-time respiration rates in this instance were similar for the two bags shown, and declined in concert with temperature as the night progressed.

A full discussion of the seasonal variation in the instantaneous measured values and derived physiological parameters and a comparison of these with published literature is given in Chapter 5.

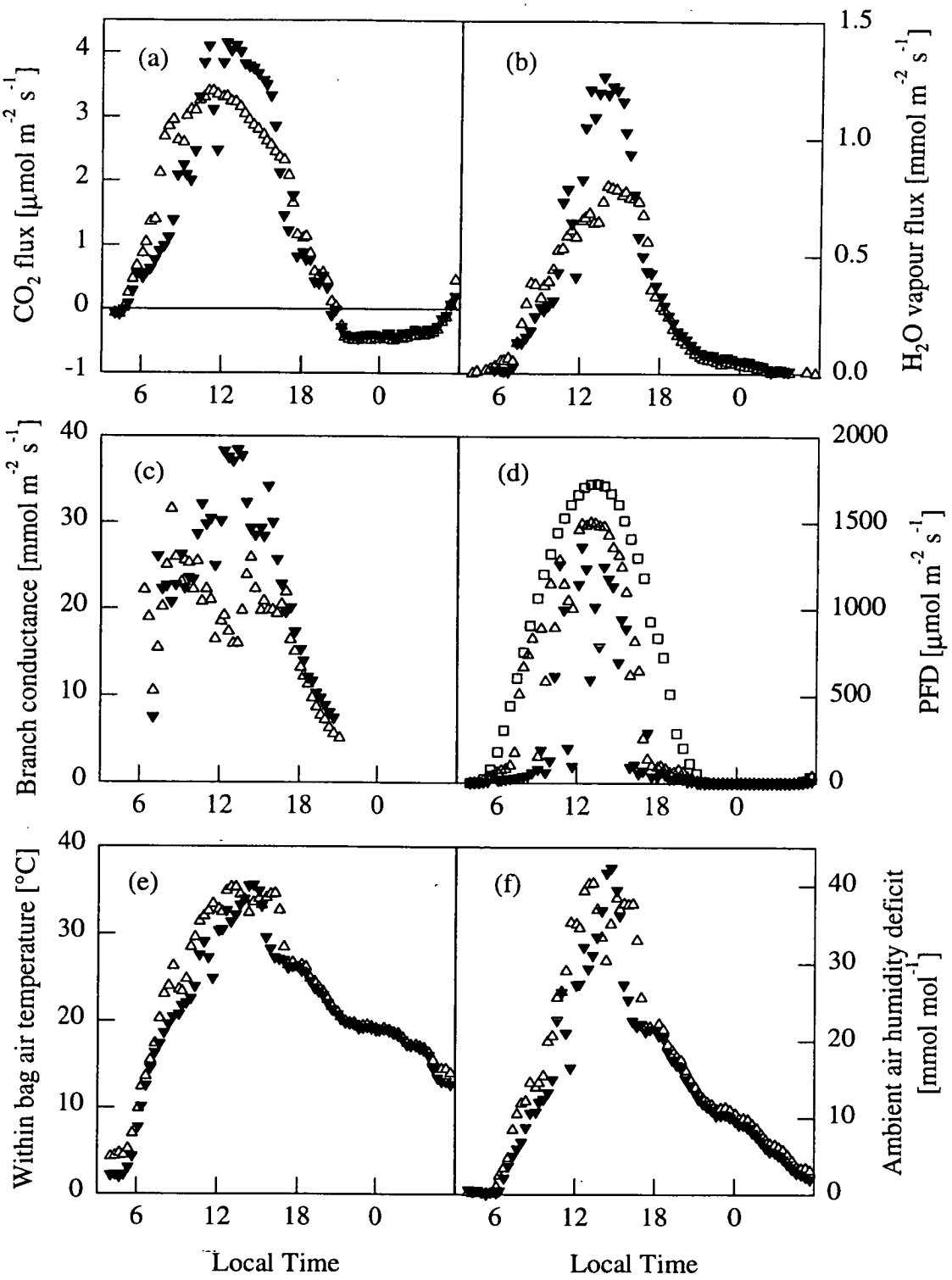

Figure 4.3. Diurnal time-courses of (a) CO_2 exchange, (b) water vapour exchange, (c) calculated branch conductance to water vapour, (d) PFD, (e) air temperature and (f) air humidity deficit during and following a cloudless day in June for an upper canopy and a lower canopy black spruce branch at the BOREAS SSA OBS site. Δ = Branch 1, Upper West, ▼ = Branch 2, Lower West, = Above canopy.

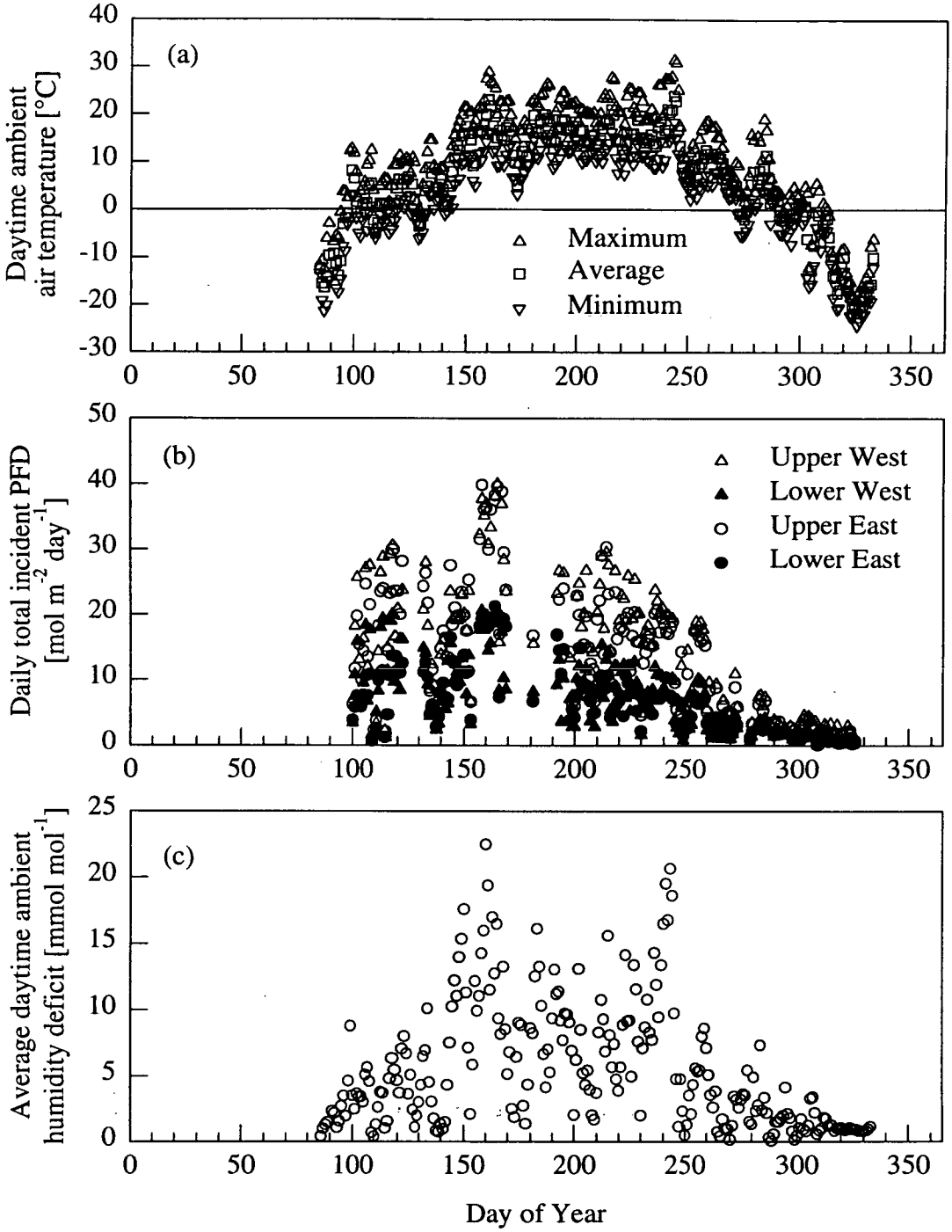

Figure 4.4. Seasonal variation in major environmental variables controlling the gas exchange of foliage at the BOREAS SSA OBS site in 1996. (a) minimum, average and maximum air temperature, measured above the canopy, (b) daily total PFD incident on each bag, and (c) the average daytime humidity deficit measured above the canopy.

Photosynthesis & respiration

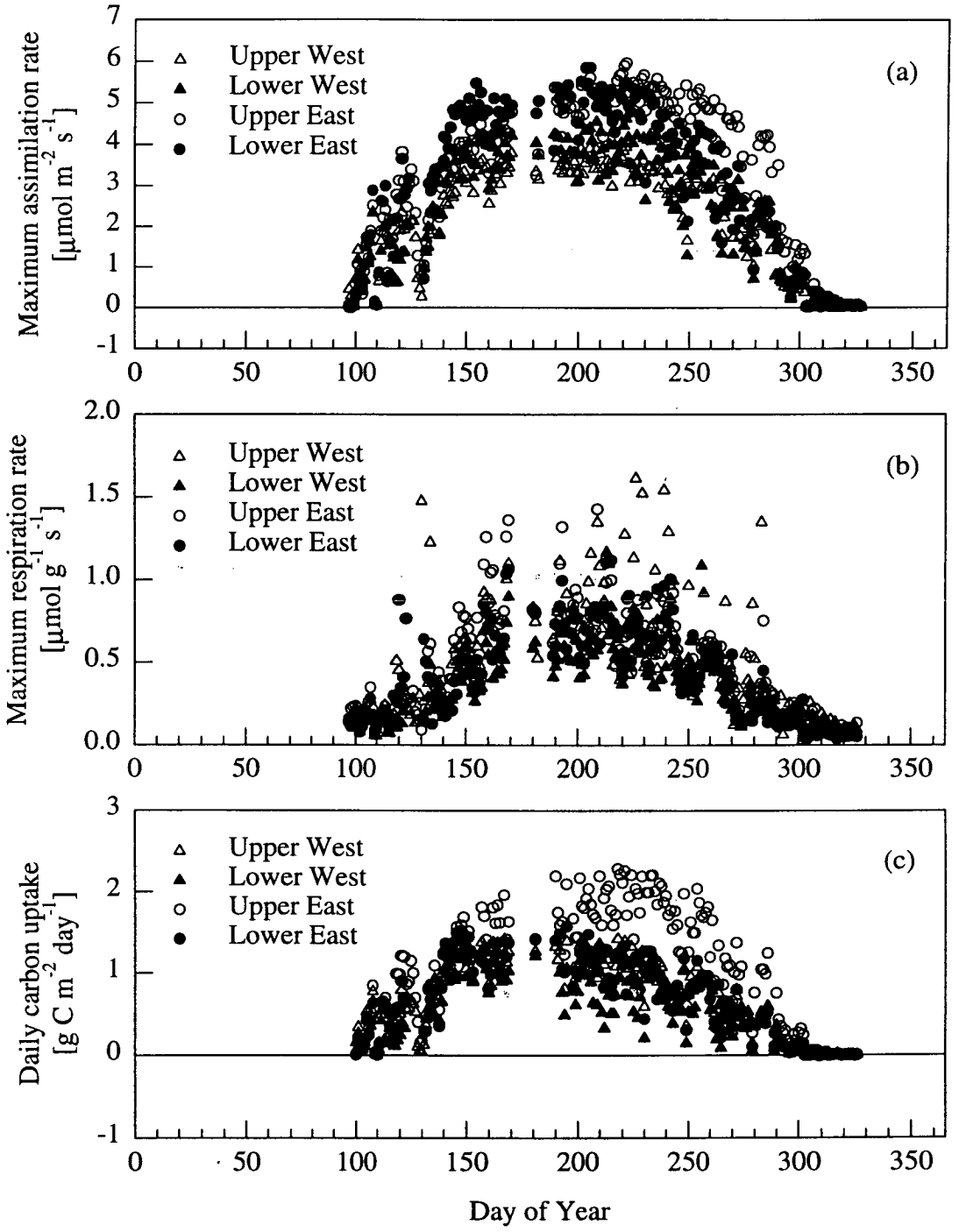

Figure 4.5. Seasonal variation in (a) the daily maximum instantaneous CO_2 assimilation rate, (b) the daily maximum instantaneous CO_2 efflux rate, and (c) the daily total carbon uptake rate of four black spruce branches at the BOREAS SSA OBS site in 1996.

Figure 4.4 shows the seasonal variation in the environmental variables that are most important in driving photosynthesis and transpiration and Figure 4.5 shows the

seasonal variation in the CO_2 exchange characteristics of each of the branches. The daily maximum assimilation rate was zero at the start of the observation period, day 97, and increased rapidly thereafter. Daily average air temperature within the bags first rose above zero on day 98 (see Figure 4.4), the same day that the maximum air temperature exceeded 5 °C for the first time. Two subsequent periods when average air temperature was below zero (days 109 to 111 and days 128 to 131) reduced both the maximum assimilation rate and the daily total carbon uptake to near zero. It is, therefore, reasonable to conclude that there was no significant uptake of carbon by the foliage before the bags were installed. The maximum instantaneous assimilation rates measured in each bag were 4.0, 4.7, 6.0 and 5.8 $\mu mol\ m^{-2}\ s^{-1}$ for branches 1, 2, 3 and 4 on days 221, 154, 221 and 205, respectively. Daily total carbon uptake reached maximum rates of 1.4, 1.3, 2.3 and 1.6 g C m^{-2} (projected leaf area) day^{-1} on days 218, 149, 218 and 195 for branches 1 to 4, respectively. Maximum air temperature within the bags rose above 5 °C for the last time on day 307, and after that day there was no significant photosynthetic carbon uptake by any of the branches. For all branches small daily respiratory losses of carbon were recorded both at the very start and at the very end of the measurement period of between 0.005 and 0.007 g C m^{-2} (projected leaf area) day^{-1}.

No differences were found between the maximum assimilation rates of the upper and lower branches of either individual tree, but large differences were evident between the two trees. Treating daily values as independent data, the maximum assimilation rates of the East tree were significantly higher than those measured on the West tree, both for the upper ($p << 0.001$) and for the lower ($p < 0.001$) branch. Night-time respiration rates (expressed on a wood plus needle dry mass basis) showed no difference between branches on the two trees at the same height, but rates measured on the upper branch were significantly higher than those measured on the lower branch for both trees ($p < 0.001$ and $p < 0.1$ for the West and East trees, respectively). Significant differences were found in the daily total carbon uptake, both between branches on the same tree (upper > lower, $p < 0.005$ and $p << 0.001$ for the West and East trees, respectively) and between the trees (East > West, $p << 0.001$ and $p < 0.005$ for upper and lower branches, respectively). These differences were

such that there was no significant difference between the upper branch on the West tree and the lower branch on the East tree.

Transpiration & conductance

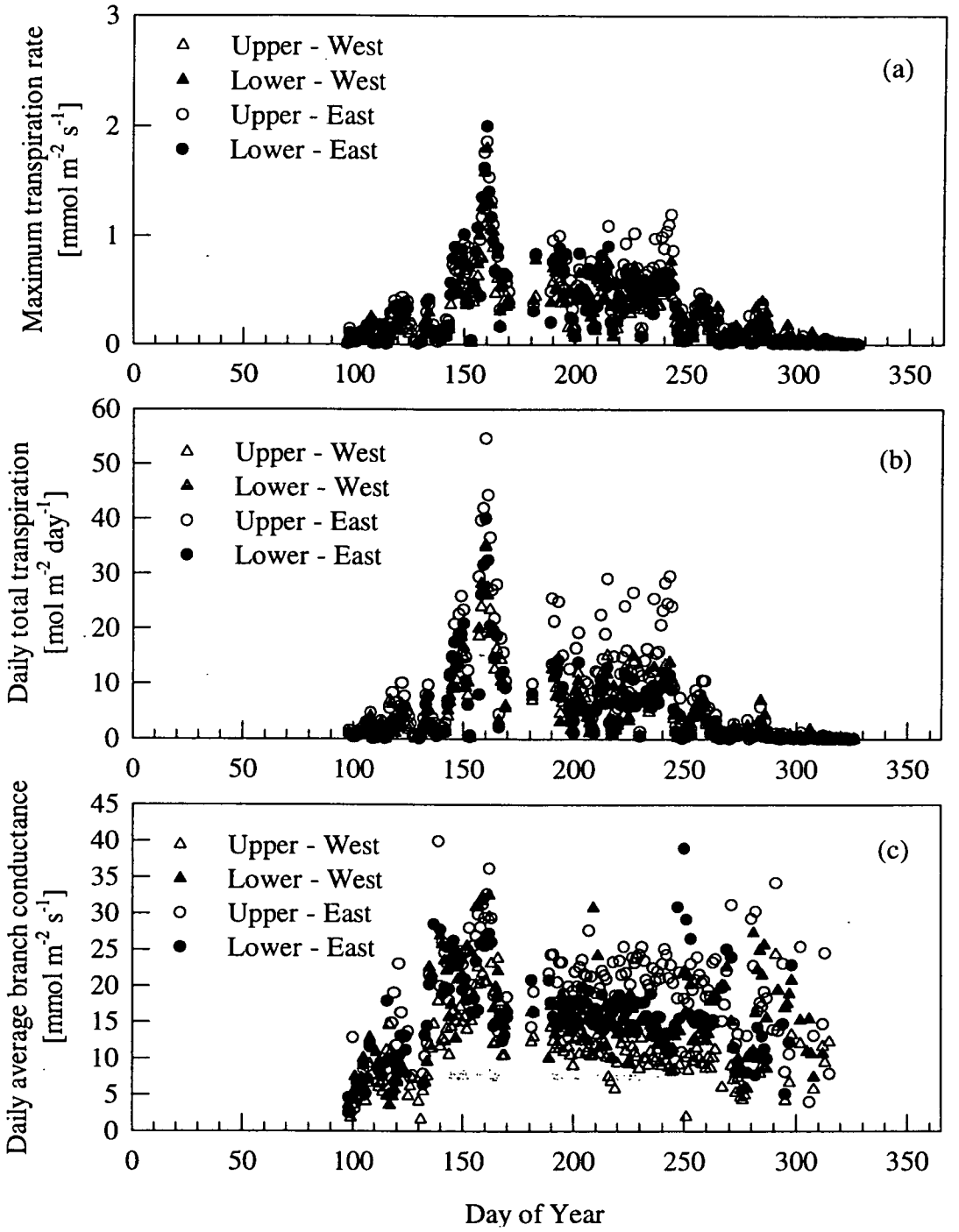

Figure 4.6. Seasonal variation in (a) the maximum transpiration rate, (b) the daily total transpiration, and (c) the daily average branch conductance to water vapour of four black spruce branches at the BOREAS SSA OBS site in 1996.

Figure 4.6 shows the seasonal variation in the transpiration of each branch. Both the daily maximum transpiration rate and the daily total transpired water were zero at the beginning and end of the measurement period. This was probably the result of low air temperature and the consequently low humidity deficits. Transpiration rates were reduced to zero during two episodes, centred around days 110 and 130, when average air temperature was below zero, as described for carbon uptake. Further periods of very low transpiration rates were observed throughout the year, coincident with periods of low radiation and humidity deficit (see Figure 4.4). Daily maximum transpiration rate reached a peak on day 160, with rates of 1.3, 1.8, 1.9 and 2.0 mmol m^{-2} s^{-1} for branches 1, 2, 3 and 4, respectively. Day 160 was also the day that incident PFD and humidity deficit both reached their yearly maxima (Figure 4.4).

Treating daily values as independent data, daily total transpiration rates of the upper branch on the East tree were significantly higher than all other branches ($p < 0.001$), but the maximum transpiration rates of this branch were significantly different only to those of the upper branch on the West tree. There were no significant differences ($p > 0.05$) between the maximum transpiration rates of branches on the same tree, or between the rates of the two lower branches.

Figure 4.6(c) shows the seasonal variation in the daily average of the total branch conductance to water vapour, calculated as the unweighted average of the instantaneous conductances as detailed above. At the start of the measurement period soil temperatures were below zero throughout the soil profile and conductances were close to zero. On day 98, as the snow covering the forest floor started to melt, soil temperatures in the upper 10 cm increased to zero, and remained at this value until *ca.* day 130. Conductances during this period remained below 10 mmol m^{-2} s^{-1} but as soil temperatures started to increase above zero, daily maximum branch conductances increased rapidly, reaching a yearly maximum value on day 160. Thereafter, daily maximum conductance declined slowly from ≈ 15 mmol m^{-2} s^{-1} to ≈ 10 mmol m^{-2} s^{-1} around day 280 for all branches except the upper branch on the East tree. There was considerable scatter in the calculated values of branch conductance towards the end of the measurement period as a consequence of dividing low

transpiration rates by very low humidity deficits, and these data should therefore be viewed with caution.

Treating daily values as independent data, maximum branch conductances were significantly higher in the upper branch of the East tree than in all other branches ($p < 0.001$) whereas maximum conductances in the upper branch of the West tree were significantly lower than in all other branches ($p < 0.001$). There was no significant difference ($p > 0.05$) between the maximum conductances measured on the two lower branches.

Branch carbon balance

Figure 4.7(a & b) shows the cumulative daytime carbon uptake and night-time carbon loss for each branch for the entire measurement period of 231 days, from day 97 to day 327 (small gaps in the data having been filled as described above). At the end of the year daytime carbon uptake by the Upper branch on the East tree was *ca.* 80 % more than by the Lower branch on the West tree, and *ca.* 50 % more than by the other two branches. Night-time carbon loss was similar for all four branches. Figure 4.7(c) shows the cumulative transpiration observed during the measurement period. Total transpiration by the Upper branch on the East tree was *ca.* 70 % than by the other three branches. A summary of the physical and gas exchange characteristics of each branch is given in Table 4.1.

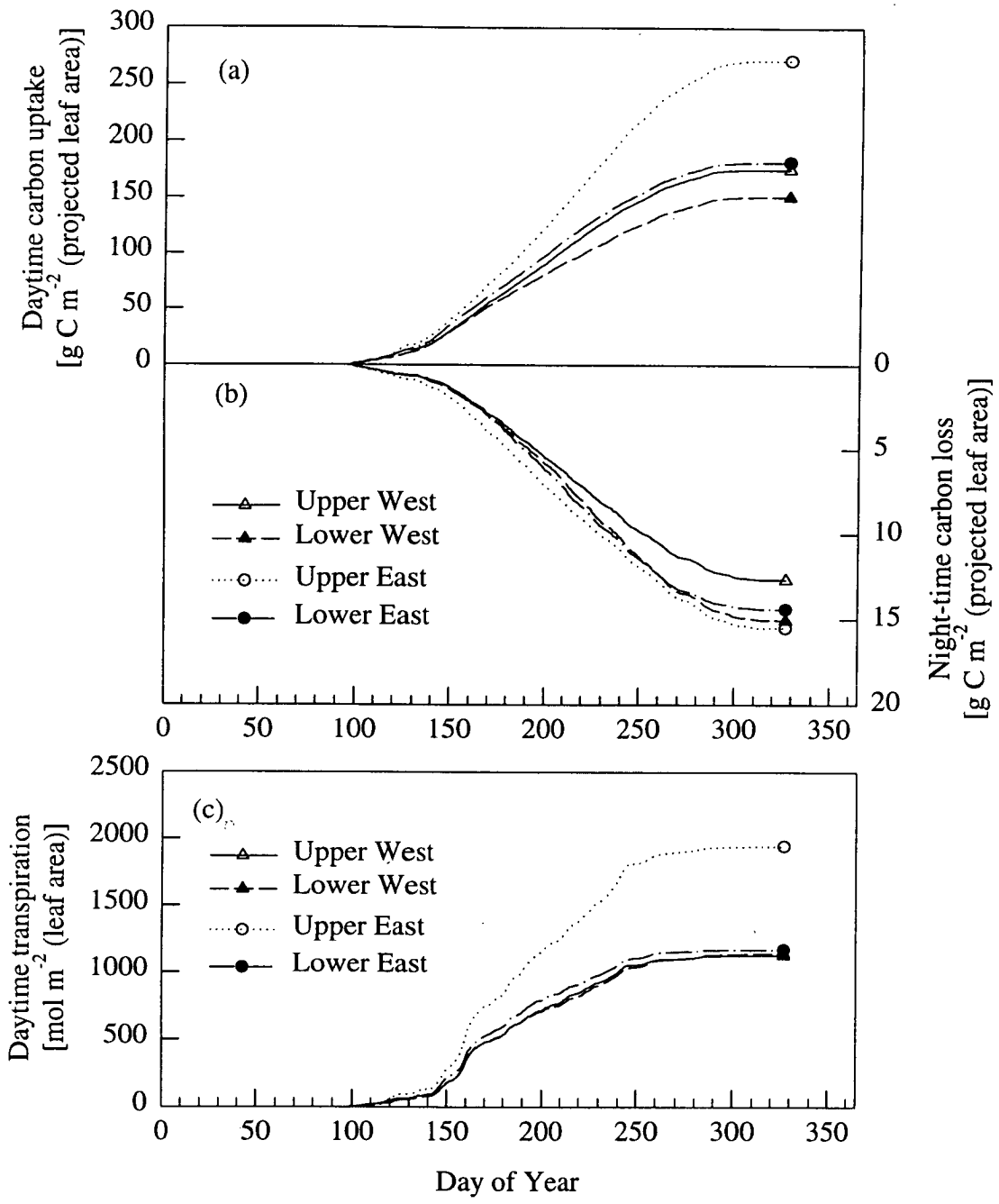

Figure 4.7. Cumulative (a) daytime carbon uptake, (b) night-time carbon loss and (c) transpiration measured over 231 days on four branches at the BOREAS SSA OBS site in 1996. Note that the scales of the two *y*-axes of (a) and (b) are not the same.

Table 4.1. Summary physical and gas exchange characteristics of four black spruce branches at the BOREAS SSA OBS site measured for the entire growing season of 1996, from day 97 to day 327. Nutrient and chlorophyll contents of needles are expressed on a needle dry mass basis, relative growth is calculated as the ratio of the current year increment in biomass to the total biomass of the branch, and water use efficiency is calculated as the amount of carbon gained per unit of water lost over the whole period.

		Tree 1 - West		Tree 2 - East	
Characteristic	Unit	Upper	Lower	Upper	Lower
Projected needle area	[m^2]	0.312	0.201	0.166	0.234
Total dry mass	[kg]	0.166	0.134	0.094	0.151
Nitrogen	[mg g^{-1}]	6.87	7.42	7.10	6.20
Phosphorus	[mg g^{-1}]	0.612	0.635	1.006	1.025
Total chlorophyll	[µg g^{-1}]	1031	1498	1365	1302
Total daytime carbon uptake	[g C m^{-2}]	174.8	150.6	271.1	181.4
Total night-time carbon loss	[g C m^{-2}]	12.7	15.1	15.5	14.4
Total night-time carbon loss	[g C kg^{-1}]	23.7	22.6	27.3	22.4
Relative growth	[mg g^{-1}]	52	32	81	67
Total water transpired	[kg m^{-2}]	20.38	20.63	35.04	21.15
Water use efficiency	[mol mol^{-1}]	0.013	0.011	0.012	0.013
Total incident PFD	[mol m^{-2}]	3299	1656	3184	1614

DISCUSSION

The pronounced seasonality observed in the daily maximum assimilation rate, stomatal conductance and transpiration were consistent with those observed in black spruce by Zine El Abindine *et al.* (1995) although their measurements were made only during the latter part of the year (between days 198 and 280) and showed a monotonic decline with time. The lack of seasonal variation in maximum photosynthetic rate observed in black spruce by Vowinkel *et al.* (1975) is similarly consistent with the data presented here, since their measurements were made sometime during June, July and August (day 152 at the earliest, day 243 at the latest) during which time there was also little evidence of variation in the maximum carbon assimilation rate at this site (see Figure 4.5 (a)).

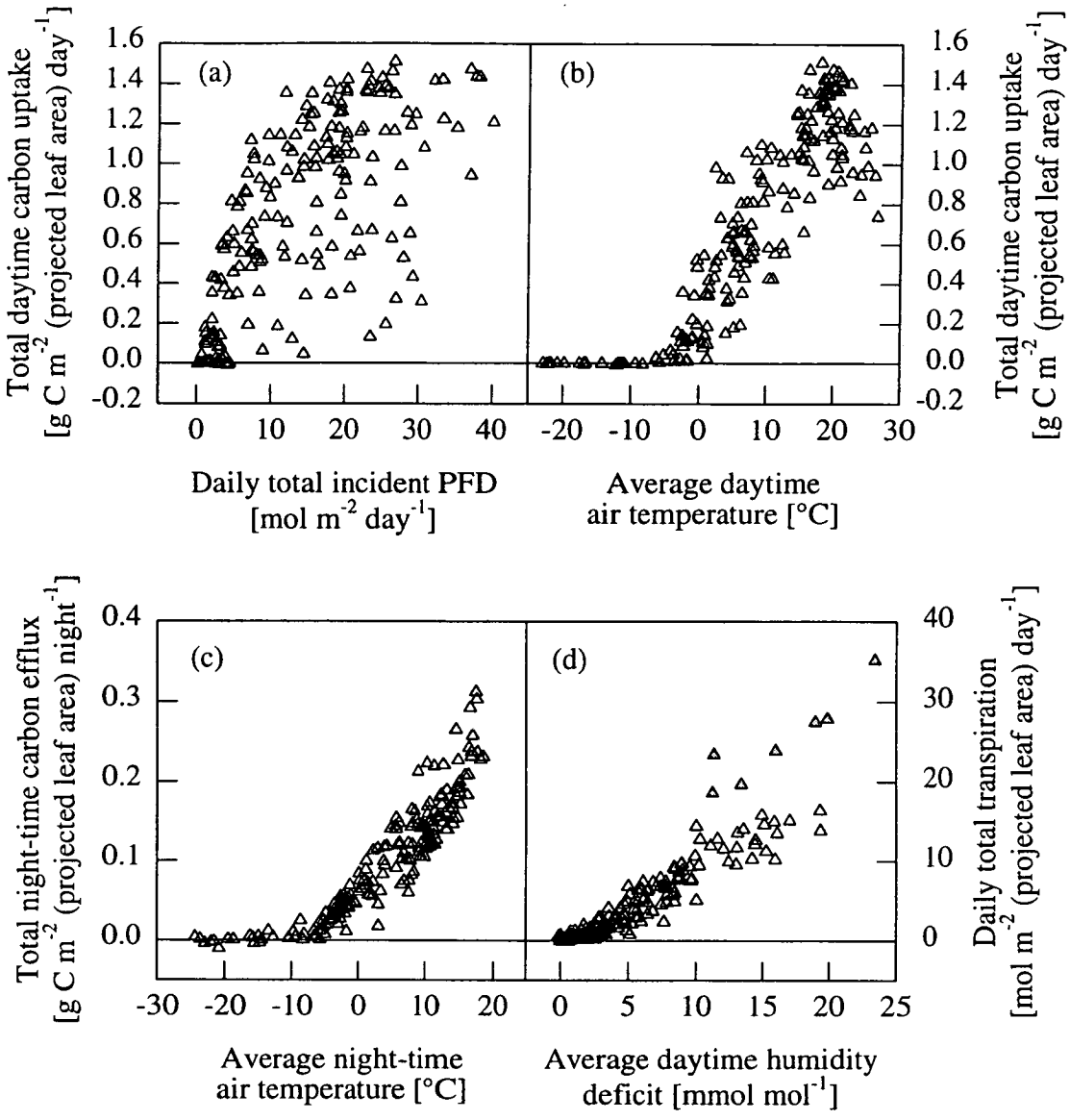

Figure 4.8. Relationships between the daily daytime carbon uptake and (a) daily total incident PFD and (b) average daytime within bag air temperature, between total night-time carbon efflux and average night-time within bag air temperature (c) and between daily total transpiration and average daytime humidity deficit (d) of branch 1 (Upper West) at the BOREAS SSA OBS site in 1996.

Relationships between the CO_2 uptake, transpiration and some key environmental variables are illustrated in Figure 4.8; for clarity data from only one branch (branch 1, the Upper branch on the West tree) are shown. An upper bound envelope (Jarvis 1976) drawn around the points of Figure 4.8(a) reveals that total daily daytime carbon uptake responded to *daily total* incident PFD in a manner similar to the way in which instantaneous photosynthesis responds to instantaneous incident PFD. Carbon uptake increases linearly with increasing incident PFD, then becomes

asymptotic as PFD increases beyond a "saturating" PFD. This can be described as a non-rectangular hyperbola. That daily carbon uptake does not continue to increase as daily total incident PFD increases argues against the assertion by Vowinkel *et al.* (1975) that daily total photosynthetic accumulation in the summer months is limited solely by PFD. Data points falling below this upper bound were from days when carbon uptake was primarily limited by variables other than light, for example, temperature. Figure 4.8(b) shows that carbon uptake by branches was almost completely suppressed when the average daytime temperature was below -6 °C, was at a maximum when the average daytime temperature was between 18 and 20 °C, and declined at higher average daytime temperatures.

Table 4.2. Parameters of combined light and temperature response model as fitted to daily carbon uptake for four black spruce branches at the BOREAS SSA OBS site. ϕ, P_{max} and Θ are respectively the initial slope, asymptote and convexity of a non-rectangular hyperbolic PFD response. c is the coefficient of the second order term and T_{opt} the optimum temperature of a quadratic function describing how daily carbon uptake varies with temperature. The low temperature cut-off point for daily carbon uptake was fitted by eye and set to -6 °C.

		Tree 1 - West		Tree 2 - East	
Parameter	Unit	Upper	Lower	Upper	Lower
n	-	231	231	231	231
r^2	-	0.89	0.80	0.84	0.86
ϕ (daily basis)	[g C mol PAR^{-1}]	0.29	0.36	0.41	0.36
S.E. of ϕ estimate	[g C mol PAR^{-1}]	0.10	0.08	0.09	0.07
P_{max} (daily basis)	[g C day^{-1}]	1.37	1.12	1.92	1.54
S.E. of P_{max} estimate	[g C day^{-1}]	0.08	0.06	0.06	0.11
Θ	-	0.50	0.82	0.94	0.68
c	-	0.0020	0.0028	0.0014	0.0028
T_{opt} (daily basis)	[°C]	19.1	15.1	22.3	15.6
S.E. of T_{opt} estimate	[°C]	0.94	0.71	2.03	0.62

Daily carbon uptake data were fitted to a model combining a PFD response and a temperature response. The PFD response was described as a non-rectangular hyperbola with the form,

$$A(Q) = \frac{\phi Q + P_{max} - \sqrt{(\phi Q + P_{max})^2 - 4\Theta\phi Q P_{max}}}{2\Theta} \qquad (4.1)$$

where $A(Q)$ is the daily total carbon uptake [g C m^{-2} (projected area) day^{-1}] as a function of Q, the incident PFD [mol quanta m^{-2} day^{-1}]. ϕ is the apparent quantum

efficiency of daily carbon uptake [g C mol^{-1} quanta], P_{max} [g C m^{-2} day^{-1}] is the asymptotic maximum daily carbon uptake and Θ is the convexity coefficient describing the smoothness of the curve.

The temperature response was described as zero carbon uptake for temperatures below -6 °C and a quadratic with a temperature optimum for temperatures above -6 °C, i.e.,

$$A(T) = 0 \qquad T < -6\ °C \qquad (4.2)$$

$$A(T) = A(Q).[1 - c\,(T - T_{opt})^2] \qquad T \geq -6\ °C \qquad (4.3)$$

where $A(T)$ is the daily total carbon uptake [g C m^{-2} (projected area) day^{-1}] as a function of T, the daily average daytime air temperature. T_{opt} is the daily average daytime temperature at which $A(T)$ is at a maximum and c is a coefficient describing the shape of the curve.

The models were fitted to the data using the SAS NLIN procedure. The derived parameters and relevant statistical information are given in Table 4.2.

For all branches, the parameterised model provided a good description of the measured data, accounting for most of the between-day variation in daily carbon uptake. Although it is hard to make definitive statements based on only four branches, it is noteworthy that the temperature optima estimated for the upper branches were significantly higher than those estimated for the lower branches. This may be evidence of some acclimation of the upper branches to the larger input of radiation, and hence higher temperatures, in the upper canopy (see total incident PFD, Table 4.1).

seven days centred around day 160 (shaded grey in 4.8(d)) when air temperature, air humidity deficit and incident radiation were all at their yearly maxima.

Daily photosynthesis and respiration rates have been plotted against the daily average of the driving environmental variables in Figure 4.8. Physiologically more meaningful descriptions, however, may result if the minimum or maximum of the environmental variable was used. For example, the low temperature at which daily carbon uptake is zero could be better described by relating carbon uptake to the daily *maximum* temperature, since the *daily* total carbon uptake may be above zero if the temperature rises above the low temperature cut-off point for photosynthesis even for a short period during the day, and, in the case of black spruce, net photosynthesis continues (albeit at a low rate) down to temperatures as low as -2 °C (Chapter 5). A certain amount of scatter in Figure 4.8 is the result of within-day variation in the driving environmental variables, since any evidence of such variation is lost when data are combined into daily average values yet the effects of any extreme values will be carried through into the daily total carbon or water fluxes. This is always the case when the physiological response to an environmental variable is non-linear, as in the response of photosynthesis to PFD and to temperature, but will be particularly pronounced when the within-day variation in these variables is large. At this site, variation in the daytime air temperature above the black spruce canopy was up to 17 °C and variation in daytime leaf temperature exceeded this.

The measurement period of 231 days covered the entire period of the year when the air temperature was above zero and the branches were biologically active. Although frost hardening enables certain spruce species to photosynthesise at temperatures as low as -5 °C (Ludlow, Neilson & Jarvis, 1972), and the photosynthetic apparatus of black spruce is undamaged by temperatures as low as -30 °C (Bigras and Margolis 1997), no frost hardening has found in black spruce when foliar N concentration is as low as found in this study (*ca.* 7 mg g^{-1}, Table 4.1) (Bigras *et al.* 1996). It is unlikely therefore that any photosynthetic uptake occurred outside the measurement period. Likewise, even though a small daily loss of carbon during the 135 days of winter when measurements were not made could reduce the annual carbon balance of the branches, the respiratory fluxes measured at the start and end of the measurement

period were so small (< 0.007 g (C) m^{-2} (leaf area) day^{-1}, Figure 4.5(c)) that even if this rate were to persist for the entire winter (rather than diminishing as temperatures dropped still further) the total carbon lost would still be less than 1 g (C) m^{-2} (leaf area), i.e. 0.4 to 0.6 % of the total annual uptake.

The most active branch (branch 3, the Upper branch on the East tree) took up nearly twice as much carbon and lost nearly twice as much water as each of the other three branches. The consistency found between the three others was particularly striking: during the course of the measurement period, the upper branch on the West tree received twice as much incident PFD as the lower branches yet took up only 16 % more carbon than the lower branch on the same tree and 3 % less carbon then the lower branch on the other tree. This apparent insensitivity to total incident PFD occurs because on typical days the PFD incident at the top of the canopy is well above that needed to saturate photosynthesis (Chapter 5; Yue & Margolis 1993; see also Figure 4.8(a)). Moreover, the narrow, highly clumped crown structure of the trees at this site allowed diffuse light to penetrate well into the "canopy" where the lower bags were situated, and diffuse light is used more efficiently in canopy photosynthesis than direct sunlight (Lloyd *et al.* 1995a; Wang & Jarvis 1990).

The high rates of photosynthesis found in branch 3 (Upper East) may be the result of this branch receiving the most light in the morning, when humidity deficits are low and stomatal conductances are consequently high. However, the lack of any large differences between the water use efficiencies of the different branches suggests that this is not the sole factor underpinning the higher photosynthetic activity of this branch. Both the total night-time carbon losses and the water vapour conductances were consistently higher for this branch than for the other branches (see Figures 4.6(c) and 4.4(b) above), indicating generally higher physiological activity by this branch than the others. This was the youngest branch (25 years old at its base, compared to 34 years for the other upper branch and 42 and 43 years for the two lower branches), and it was located within the top quarter of the tree crown. There was a reasonably good relationship between an indirect estimate of physiological activity (calculated as the yearly total carbon uptake) and a direct estimate of the relative growth of the branches (calculated as the ratio of the current year increment

in biomass to the total biomass of the branch) ($r^2 = 0.78$). All branches had a positive annual carbon balance, i.e. (daytime uptake) - (night-time loss) - (biomass increase) > 0, indicating that all branches were net exporters of carbon during the year.

The marked difference in foliar phosphorus concentration between the two trees (Table 4.1) further supports the suggestion that there was more active synthesis and growth in the East tree (with almost twice the P concentration of the West tree) than the West tree. The foliar phosphorus concentrations of both the current and all previous years' foliage for both branches of the East tree were the same as those found by Hom & Oechel (1983) in the most actively growing current-year foliage of black spruce in Alaska, whilst the concentrations of P in the West tree were less than those found in the oldest (13 years) needle age class sampled in Hom & Oechel's study. The main effect of phosphorus deficiency is to decrease the ATP content of photosynthetic tissue. This leads to a reduction in the rate of RuBP regeneration and hence to a reduction in the PFD-saturated photosynthetic rate (Lewis, Griffen, Thomas & Strain 1994). This may account for the higher carbon uptake rates found in the East tree compared to the West tree. Even the highest P concentrations found here are, however, something short of the 1.4 mg g^{-1} minimum critical needle concentration for black spruce referred to by Lamhamedi & Bernier (1994), and therefore all branches must, to a certain extent, be considered P deficient.

There seemed to be no relation between the concentration of nitrogen in the needles and the annual total carbon uptake, or between the concentrations of nitrogen chlorophyll, chlorophyll a:b ratio and the amount of incident radiation received. Thus, despite the very low foliar N concentrations, indicating that the trees were very N deficient (concentrations were half that considered optimum for black spruce, Lamhamedi & Bernier 1994), there was no evidence for any optimisation of nutrient allocation in response to PFD within the tree. This observation is consistent with the notion that these trees have not adapted to nutrient stress through changes in their use of N and P (Chapin & Kedrowski 1983).

SUMMARY

A system of large cuvettes was used to measure whole branch CO_2 and H_2O vapour exchange of four black spruce (*Picea mariana* [Mill] BSP) branches at the BOREAS southern study area OBS site. Measurements were started before the onset of the spring thaw and were continued until after the winter freeze up (i.e. day 97 through day 327). Daily maximum photosynthetic rates were zero at the beginning and end of the season and reached a maximum of ≈ 6 μmol m^{-2} s^{-1} (on a projected leaf area basis) around day 200. Night-time respiration reached a maximum rate of ≈ 0.8 μmol g^{-1} s^{-1} (dry mass basis) at around the same time. Maximum evapotranspiration rates rose rapidly from zero to a peak of ≈ 2 mmol m^{-2} s^{-1} (projected leaf area basis) as the upper soil layers thawed then dropped to ≈ 0.5 mmol m^{-2} s^{-1}. Maximum evapotranspiration remained fairly constant at this level between days 160 and 240, then fell back to zero as the soil water re-froze in the winter. Branch water vapour conductances were calculated from the H_2O vapour flux and the humidity deficit of the air and reached a maximum of ≈ 35 mmol m^{-2} s^{-1} (projected leaf area basis) around day 160. This pronounced seasonality could be explained in terms of the large seasonal variation in environmental variables, in particular temperature and PFD. A simple model combining light and temperature responses accounted for 80 to 90% of the day to day variation in daytime carbon uptake throughout the measurement period. Total daytime carbon uptake calculated for each branch for the entire growing season ranged from 12.6 to 22.6 mol m^{-2} (projected leaf area basis). Total night-time loss ranged from 1.06 to 1.29 mol m^{-2} (projected leaf area basis), or 1.98 to 2.27 mol kg^{-1} (total branch dry mass basis). Total daytime transpiration ranged from 1132 to 1947 mol m^{-2} (projected leaf area basis).

Chapter Five - Photosynthesis, Respiration and Conductance of Black Spruce at Three Organisational Scales: Shoot, Branch & Canopy

This chapter describes a study of the CO_2 and water exchange of the most common Canadian boreal forest tree species, black spruce (*Picea mariana* [Mill.] B.S.P.), using measurements made at three organisational scales: the shoot, the branch and the canopy. The variation of physiological parameters over the course of a year and between organisational scales is investigated.

METHODS - GAS EXCHANGE

Shoot measurements

In July and October 1996, measurements were made on shoots in the upper, mid or lower crown of four trees. Each shoot had a total needle area of approximately 70 cm^2 and comprised four to seven needle age classes. One intracellular CO_2 (c_i) and one PFD (Q) response curve of net CO_2 assimilation rate, transpiration and stomatal conductance was made for each of 14 shoots in July and six shoots in October using an open gas exchange system with climate control (Compact Minicuvette System, Walz, Effeltrich, Germany). Shoots were placed in a horizontal plane within the cuvette and received bilateral illumination from two fibre-optic illuminators (Walz, Effeltrich, Germany) composed of 200 parallel optical fibres applied to the glass lid of the cuvette at a distance of 3 cm from the needle surface. Intracellular CO_2 (c_i) response curves were determined by varying ambient CO_2 mole fraction (c_a) from 1500 ppm to 0 ppm under saturating PFD (Q = 1500 µmol m^{-2} s^{-1} at the needle surface). PFD response curves were determined by varying PFD from 1100 µmol m^{-2} s^{-1} to 0 µmol m^{-2} s^{-1} with ambient CO_2 mole fraction set to 1500 µmol mol^{-1}. Air temperature was set at 17.5 °C, and dew point temperature was set at 8 °C. Gas exchange was calculated on an illuminated needle area basis.

In July, temperature responses of gas exchange were determined for five shoots both in the dark and at an irradiance of 1200 µmol m^{-2} s^{-1}. These measurements were repeated on six different shoots in October. After several hours acclimation to 20 °C, each shoot was placed in the cuvette at 30 °C. When gas exchange reached a steady-state, the data were recorded. These measurements were repeated as the cuvette

temperature was decreased from 30 to 5 °C, by 5 °C steps. Each temperature step required approximately 40 minutes equilibration time. The temperature response of shoot respiration was determined using the same protocol with the cuvette enclosed in aluminium foil.

After completion of the gas exchange measurements, the shoots were cut off. The needles of each shoot were dried at 65 °C and weighed according to their age-class. Their total surface area was estimated using the values of specific needle area estimated from 30 samples of five needles the total areas of which were calculated from their length and width assuming a rhomboidal cross-section with a shape factor of 2.54. A different specific needle area was applied according to needle age class, but no significant difference in specific needle area was found with respect to needle location in the crown. The total N and P contents of the needles were determined after digestion in hot sulphuric acid by Kjeldahl digestion and molybdate ascorbate method, respectively, using an automated analyser (Autoanalyser II, Technicon, Dublin, Ireland). In October, sub-samples of fresh needles of each shoot were frozen in the field and brought back to the laboratory for chlorophyll analysis. The lengths and widths of a sample of four needles per shoot were measured, in order to determine their area and shape factor.

Branch measurements

The ventilated closed-system branch bags used followed a methodology developed at the Université Paris Sud-Orsay (Dufrêne, Pontailler & Saugier 1993) which has been described fully in Chapter 4, and will here be discussed only briefly. On each of two trees two branch bags were installed, one positioned in the upper canopy (8 m height) and one in the lower canopy (5.3 m height). Modal tree height was *ca.* 10.2 m. CO_2 and water vapour exchange was measured on each branch every 20 minutes, together with air and leaf temperature, incident PFD and relative humidity. At the end of the year the branches were cut down whole and needle area, needle and wood dry mass and chlorophyll and nutrient contents were measured for current and all previous years' needles (a full discussion of the methodology used is given in Chapter 4).

Canopy measurements

An eddy covariance flux measuring station was installed with the anemometer and gas analyser intake positioned at 27 m height. The system comprised a closed path infrared gas analyser (LI-6262, LI-COR Inc. Lincoln, NE), an ultrasonic anemometer (Solent A1012R, Gill Instruments Ltd., Lymington, England) and Edinburgh EdiSol software. The full technical specification is described in detail by Moncrieff *et al.* (1997a). An automatic weather station mounted close to the eddy flux system recorded a full suite of meteorological data. A complete description of the equipment installation is given by Jarvis *et al.* (1997).

The tree canopy CO_2 exchange was extracted from the net ecosystem flux by correcting for the simultaneous fluxes of CO_2 from soil respiration and moss photosynthesis. The measurement and spatial integration methodologies used to determine soil respiration are described in Chapers 2 and 3. The moss photosynthetic rates were predicted from data obtained from Dr. L.B. Flanagan (Carlton University, Ottawa, ONT.). The fluxes measured at the canopy scale were distinct from the measurements made at the shoot and branch scales in that the data represented measurements averaged over a 30 minute period, rather than discrete measurements at a point in time.

MODEL PARAMETERISATION - PHOTOSYNTHESIS

Shoot measurements

Net CO_2 assimilation rate (A) [μmol CO_2 m^{-2} s^{-1}], transpiration (E) [mmol H_2O m^{-2} s^{-1}], stomatal conductance for water vapour (g_w) [mmol H_2O m^{-2} s^{-1}], and for CO_2 (g_c) [mmol CO_2 m^{-2} s^{-1}] and substomatal CO_2 mole fraction (c_i) were calculated according to von Caemmerer and Farquhar (1981). Two photosynthesis models were fitted to the datasets, a simple non-rectangular hyperbola photon flux density (PFD) response (e.g Ögren and Evans 1993) and the more mechanistic Farquhar model (Farquhar *et al.* 1980). The simple model was of the form,

$$A = \frac{\phi Q + P_{max} - \sqrt{(\phi Q + P_{max})^2 - 4\Theta\phi Q P_{max}}}{2\Theta} - R_d \qquad (5.1)$$

where A is the instantaneous photosynthetic rate [μmol CO_2 m^{-2} s^{-1}], Q is the incident PFD [μmol quanta m^{-2} s^{-1}], ϕ is the apparent quantum efficiency of photosynthesis [μmol CO_2 μmol^{-1} quanta], P_{max} [μmol CO_2 m^{-2} s^{-1}] is the asymptotic maximum photosynthetic rate, Θ is the convexity coefficient describing the smoothness of the transition between PFD limited and PFD saturated rates of photosynthesis and R_d [μmol CO_2 m^{-2} s^{-1}] is the daytime "dark" respiration rate (the day respiration). ϕ was obtained from the slope of the initial (linear) part of the photosynthetic PFD response curve. This parameter was then prescribed and the other parameters were obtained by fitting the eq. 5.1 to the PFD response data. All model parameters were extracted from the data using the SAS NLIN or REG procedures.

Maximal velocity of carboxylation (V_{max}), observed maximal electron transport rate (J_{max}) [μmol e^- m^{-2} s^{-1}], daytime "dark" respiration (R_d) [μmol CO_2 m^{-2} s^{-1}] and apparent quantum efficiency of electron transport (α) [μmol e^- μmol^{-1} quanta] were determined from the response curves obtained with each shoot, assuming that chloroplastic (c_c) and substomatal (c_i) CO_2 mole fractions were equal within the needle. Using the formulation of photosynthesis proposed by Farquhar *et al.* (1980) and modified by subsequent authors (Harley *et al.* 1992; Lewis *et al.* 1994), V_{max} and R_d were estimated by non-linear regression using the data of the A - c_i curve for c_i < 200 μmol mol^{-1} according to following model,

$$A_v = V_{max} \frac{c_i - \Gamma^*}{[K_c(1 + O_2/K_o) + c_i]} - R_d \qquad (5.2)$$

where Γ^* is the CO_2 compensation mole fraction in the absence of dark respiration, given by,

$$\Gamma^* = 0.105 K_c O_2 / K_o \qquad (5.3)$$

and K_c [μmol mol^{-1}] and K_o [mmol mol^{-1}] are the Michaelis constants for CO_2 and oxygen, respectively, and O_2 is the intracellular oxygen mole fraction [210 mmol mol^{-1}] (Harley *et al.* 1985).

The temperature dependence of the parameters K_c and K_o were described according to Leuning (1995) in terms of their value at 20 °C (K_{c20} = 302, K_{o20} = 256) as follows,

$$parm_T = parm_{20} \exp\left[\frac{H_v}{293.15R}\left(1-\frac{293.15}{T_l}\right)\right] \quad (5.4)$$

where $parm_T$ and $parm20$ are the values of either parameter at T K and at 20 °C, respectively, H_v is the activation energy (K_c: H_v = 59,430 J mol^{-1} K^{-1}; K_o: H_v = 36,000 J mol^{-1} K^{-1}), T_l is the needle temperature in Kelvin and R is the gas constant (8.314 J mol^{-1} K^{-1}).

J_{max} was estimated from the values of A measured in saturating PFD and at 1500 µmol mol^{-1} CO_2 according to,

$$J_{max} = \frac{(A+R_d)\cdot 4(c_i+2\Gamma^*)}{(c_i-\Gamma^*)} \quad (5.5)$$

The apparent quantum efficiency of electron transport, α, the day respiration rate, R_d, and the convexity coefficient for the light dependence of electron transport, θ, were estimated from the PFD response curve by least squares adjustment to the following non-linear equation,

$$A_j = \frac{J}{4}\left(\frac{c_i-\Gamma^*}{c_i+2\Gamma^*}\right)-R_d \quad (5.6)$$

where J, the electron transport rate, was expressed according to Farquhar and Wong (1984) as,

$$J = \frac{\alpha Q + J_{max} - \sqrt{(\alpha Q + J_{max})^2 - 4\theta\alpha Q J_{max}}}{2\theta} \quad (5.7)$$

The temperature dependence of V_{max} and J_{max} were described according to Walcroft *et al.* (1997) in terms of their value at 20 °C as follows,

$$parm = \frac{parm_{20}\exp[(H_v/293.15R)(1-293.15/T_l)]}{1+\exp[(S_vT_l-H_d)/(RT_l)]} \quad (5.8)$$

where H_v and H_d are the activation and deactivation energies respectively. Activation and deactivation energies for V_{max} were determined for *P. mariana* by D. Loustau, INRA, Bordeaux, (H_v = 52,200 J mol^{-1} K^{-1} H_d = 205,600 J mol^{-1} K^{-1}). Values for the activation and deactivation energies of J_{max} for coniferous trees were obtained from the literature (H_v = 46,337 J mol^{-1} K^{-1} H_d = 198,924 J mol^{-1} K^{-1}, Walcroft *et al.* 1997). S_v is an entropy term (650 J mol^{-1}, Walcroft *et al.* 1997).

Branch measurements

Branch bag data were excluded from the analysis when the regression line through the concentration measurements from which the flux was calculated fitted the data with an r^2 value of less than 0.95. Additionally, photosynthetic models were only fitted to data collected in the daytime, defined as the period when incident PFD was above 3 μmol m^{-2} s^{-1}.

To obtain the PFD and temperature responses of photosynthesis, daytime branch bag data were classified into 5 °C leaf temperature classes, and data from each class were fitted to the simple non-rectangular hyperbolic PFD response as described above (eq. 5.1). R_d and ϕ were first estimated from the *y*-intercept and slope, respectively, of the A - Q response at PFD < 50 μmol m^{-2} s^{-1}. P_{max} and Θ were then determined by fitting eq. 5.1 to all daytime data.

The von Caemmerer and Farquhar model of photosynthesis (above) describes the rate of carbon assimilation as the minimum of two potential limitations, the carboxylation limited rate, A_v, and the RuBP regeneration (electron transport) limited rate, A_j. The parameters V_{max}, J_{max} and θ are typically determined through analysis of the response of photosynthetic uptake to changes in the substomatal CO_2 mole fraction (c_i) as described for the shoot measurements above, but may, with care, be extracted from data measured under conditions of natural environmental variation. Despite there having been only a limited natural variation in c_i in this study, (330 μmol mol^{-1} < c_i < 400 μmol mol^{-1} for all branches) it was possible to determine, analytically, environmental criteria under which the photosynthetic rate could be guaranteed to be limited by one or other of carboxylation or RuBP regeneration. Figure 5.1(a) shows an analysis of a part of the Farquhar model. It is clear that for the

range of c_i experienced, photosynthesis proceeds at the carboxylation-limited rate, A_v, when both needle temperature is below 25 °C and PFD is above 500 μmol m^{-2} s^{-1}. Similarly, Figure 5.1(b) illustrates a set of conditions when photosynthesis will proceed at the RuBP-regeneration limited rate, A_j, that is when c_i is between 330 and 400 μmol mol^{-1}, PFD is less than 170 μmol m^{-2} s^{-1} and needle temperature is above 15 °C. These criteria were got iteratively, i.e. the Farquhar model was initially parameterised using parameters from the literature, data were then selected according to criteria based on this parameterisation, from these data parameters were obtained and re-entered into the model, and the process was repeated. Day respiration, R_d, and the apparent quantum efficiency of electron transport, α, were estimated from the A - Q response at PFD < 50 μmol m^{-2} s^{-1}.

These conditions provided a large enough number of data points from which the parameter V_{max} could be determined accurately through non-linear regression. The more severely restricting conditions imposed to ensure RuBP regeneration limitation (high temperature plus low light) resulted in fewer data being available to estimate the parameters describing this limitation. Also, when environmental conditions were such that photosynthesis was limited by A_j (i.e. high temperature plus low light), rates were a long way short of J_{max} (see Figure 5.1(a)), and estimates of this parameter were by necessity extrapolations. These two factors resulted in very broad confidence intervals for J_{max} and θ. Moreover, the parameters J_{max} and θ are highly correlated when obtained by fitting the model to measurements made at normal environmental conditions. Therefore θ was fixed at the value found at the shoot level (0.677) and J_{max} was determined by finding a value for V_{max} (using the criteria described above) then prescribing this parameter in a procedure to fit the full Farquhar model to all the daytime data. The temperature response parameters for V_{max}, J_{max} and R_d were set equal to the values determined at the shoot level (D. Loustau in preparation). In order to investigate changes in these parameters over time, the data were grouped into twenty-day periods.

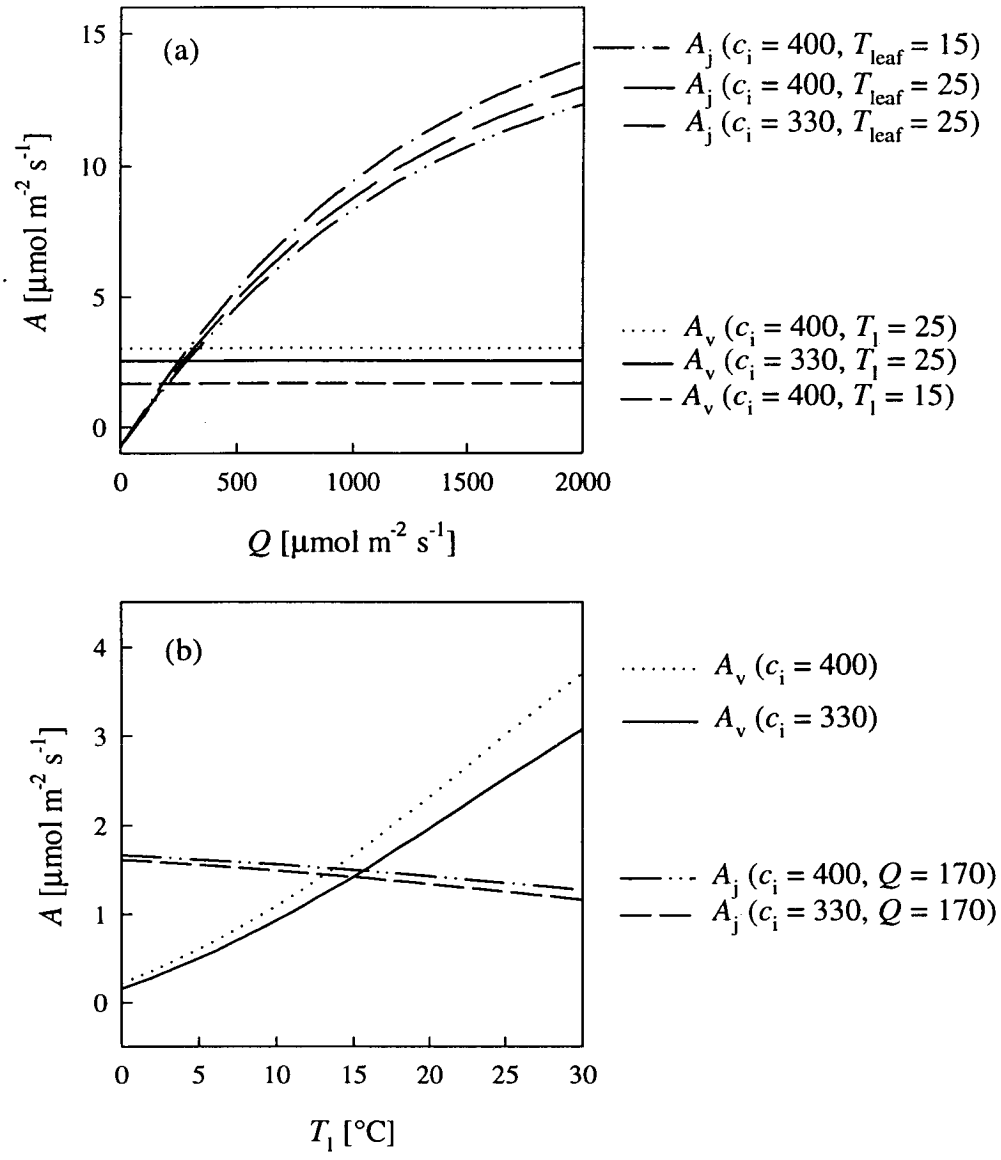

Figure 5.1. The relation between the carboxylation rate, A_v [µmol CO_2 m^{-2} s^{-1}], and the potential electron transport rate, A_j [µmol e^- m^{-2} s^{-1}], and (a) PFD, Q [µmol m^{-2} s^{-1}], and (b) needle temperature, T_l [°C], calculated from the Farquhar model. V_{max}, and J_{max} were determined iteratively from data, values of other parameters are given in the text.

Canopy measurements

The effects of changes in the CO_2 concentration of the air column below the eddy covariance sensor (the "storage" flux) were removed from the eddy covariance data to yield the "biotic" flux. From this biotic flux the forest floor CO_2 flux (measured with chambers, Chapter 3) was subtracted, resulting in a measure of the gas exchange of the canopy. The canopy exchange data were classified into 5 °C air temperature classes, and data from each class was fitted to a non-rectangular hyperbolic light

response as described above for shoot measurements. Parameters for the Farquhar model of photosynthesis were extracted from the canopy data by the same process as for the branch data, that is by iteratively setting criteria under which photosynthesis was limited by carboxylation in order to determine V_{max}, then prescribing this parameter and θ (0.677) and fitting the full Farquhar model to all daytime data to determine J_{max}. As for the branch data, the canopy data were grouped into twenty-day periods. The temperature response parameters for V_{max}, J_{max} and R_d were set equal to the values determined at the shoot level and R_d and α were estimated from the A - Q response at PFD < 50 μmol m^{-2} s^{-1}.

MODEL PARAMETERISATION – RESPIRATION

An Arrhenius "activation energy" temperature response (e.g Lloyd and Taylor, 1994) was fitted to the shoot, branch and canopy data collected when PFD = 0 μmol m^{-2} s^{-1}. The model was of the form,

$$R_T = R_{20} \exp\left(\frac{E_0}{293.15R}\left(1-\frac{293.15}{T}\right)\right) \qquad (5.9)$$

where R_T is the CO_2 efflux rate [μmol CO_2 m^{-2} s^{-1}] at needle temperature T (K), R_{20} is the efflux rate at 20 °C, R is the gas constant (8.314 J mol^{-1} K^{-1}) and E_0 is the activation energy (56,734 J mol^{-1} K^{-1}) (D. Loustau in preparation)

Needle temperature was used as the driving variable for the shoot and branch flux measurements, air temperature was used for the eddy covariance measurements. For both the branch and canopy scale measurements, the data were grouped into periods of twenty days, and the respiration models were fitted to the data when incident PFD was zero. The canopy data were further screened to exclude periods when turbulence was considered too low for the eddy covariance technique to produce reliable data, thus the models were only fitted to data when the friction velocity, U_*, was above 0.35 m s^{-1}. Since the larger part of the night-time respiration derives from soil efflux (Rayment 1995), and the estimate for the spatially integrated rate of soil efflux was itself derived from a model in which the main driving variable was temperature

(Chapter 3), the net ecosystem flux data were used uncorrected for the soil CO_2 efflux to avoid the circularity of fitting a model to model-derived data.

MODEL PARAMETERISATION – CONDUCTANCE

Two conductance models were fitted to the data, a Jarvis type "response surface" model (Jarvis 1976) and the Leuning (1995) modification of the Ball, Woodrow and Berry (1987) model (BWBL).

Specifically, the functions included in the Jarvis model were,

$$g_w = g_{w0} + (g_{wmax} - g_{w0})(1 - [k_{PFD}]^Q)\left(1 - \frac{D_s}{D_0}\left(\frac{(T_l - T_{min})(T_{max} - T_l)^\beta}{(T_{opt} - T_{min})(T_{max} - T_{opt})^\beta}\right)\right) \quad (5.10)$$

where g_{w0} is the minimum conductance, i.e. the conductance remaining in the darkness [mmol H_20 m^{-2} s^{-1}] when the stomata are fully "shut", and g_{wmax} is the maximum conductance when the stomata are fully "open" [mmol H_20 m^{-2} s^{-1}]. The PFD (Q) response was described as an exponential rise to a maximum, with parameter k_{PFD}. The humidity response was described as a linear decrease in conductance with increasing D_s, where D_s is the mole fraction humidity deficit [mmol H_20 mol^{-1} air] at the needle surface (equal to the difference between the saturation water vapour mole fraction at the needle temperature and the water vapour mole fraction of the surrounding air assuming a negligible aerodynamic resistance). The parameter D_0 is the leaf surface humidity deficit [mmol H_20 mol^{-1} air] at which conductance would be g_{w0}. The temperature response was described as a beta function with three parameters, the temperature at which conductance is at a maximum, T_{opt}, and the high and low temperatures (T_{max} and T_{min}, respectively) at which conductance would be equal to g_{w0}. β is given by $(T_{max} - T_{opt})/(T_{opt} - T_{min})$. The dark conductance, g_{w0}, was determined from the y-axis intercept of conductance against Q where $Q < 200$ µmol m^{-2} s^{-1} and g_{wmax} was simply the maximum conductance measured. The parameters k_{PFD}, T_{opt}, T_{max} and T_{min} were got from boundary analysis of the data, that is the values used described an envelope containing all the data. The parameter D_0 was found by fitting eq. 5.10 to all the data once the other parameters had been prescribed.

The BWBL model used incorporated a hyperbolic response to humidity deficit of air at the needle surface (Lohammar *et al.* 1980), as follows,

$$g_w = g_{w0} + a_1 \frac{A}{(c_s - \Gamma^*)(1 + D_s/D_0)} \qquad (5.11)$$

where g_{w0} is as described above, A and Γ^* are as described in the photosynthesis section above, c_s is the CO_2 mole fraction at the needle surface (equal to the ambient CO_2 mole fraction assuming a negligible aerodynamic resistance) and D_s is as described above. The empirical coefficients a_1 and D_0 were determined through a least squares fit of the model to the entire shoot measurement dataset.

To construct a fully predictive, dynamic, model of branch and canopy conductance in the field, a time-constant term, τ, was added to accommodate the response time of stomatal conductance to changing environmental conditions. The transient response is given by,

$$g_w = g_w(\varepsilon_{t-20}) + (g_w(\varepsilon_t) - g_w(\varepsilon_{t-20}))(1 - \exp(-20/\tau)) \qquad (5.12)$$

where g_w is the instantaneously measured conductance, the function $g_w(\varepsilon)$ expresses the steady state value of conductance (Jarvis or BWBL) under current environmental conditions, ε_t, and under the conditions twenty minutes previously, ε_{t-20}. τ is the time-constant, i.e. the time taken for the stomata to achieve 63.2 % (i.e. 1 - exp[-1]) of its total response to a step change in environmental conditions (Fischbeck & Fischbeck 1987). The time-constant, τ, was determined by fitting eq 5.12 to the entire branch and canopy datasets, using the parameters estimated from the "elite" datasets (see below), and adjusting τ by least squares analysis.

Apart from the envelope parameters which were fitted by eye, all model parameters were extracted from the data by least squares analysis using the SAS NLIN or REG procedures.

Shoot measurements

The parameters describing the irradiance and temperature responses of stomatal conductance included in the Jarvis model were fitted individually to those data

obtained when PFD and temperature were controlled variables. A single value for the BWBL humidity response parameter, D_0, was determined for all shoots by fitting the model to the combined data from all shoots. g_0 and a_1 were determined for each shoot by fitting eq. 5.11 after prescribing this value of D_0.

Branch measurements

Data for parameterisation of the two conductance models were first screened to exclude data for which the slope of the regression line through the water vapour concentration measurements from which the water vapour flux, E, was calculated, was not significantly different from zero (typically when $E < 0.025$ mmol $m^{-2}s^{-1}$). Measurements for which D_s was less than 1 μmol mol^{-1} and the relative humidity inside the bag was above 90% were also excluded to avoid calculating spuriously high values of conductance when the humidity gradient was small. An "elite" dataset was then extracted from these data using only those measurements where A, E, Q, T_l, D_s, relative humidity and calculated conductance were all within 10% of their previous value, i.e. that measured 20 minutes before. This eliminated any problems associated with the long time-constants of stomatal responses to changes in environmental conditions, and ensured that only those data in which stomatal aperture was fully adjusted to current conditions were included in the estimation of the steady-state response parameters.

Canopy measurements

Net canopy water vapour flux data were screened in exactly the same way as the branch bag data, with the exception that there was no requirement that the flux be significantly larger than zero and that the data were 30 minute averages.

RESULTS

Shoot photosynthesis

Parameter values for the simple PFD response model are given in Table 5.1. There were no significant differences between the values obtained from shoots at different heights in the canopy for any of the parameters of the simple irradiance response

model. Values for R_d, ϕ, P_{max} and Θ measured on shoots are superimposed on the branch derived estimates of these parameters in Figure 5.2.

Table 5.1. Mean values (± 95% confidence intervals) of the parameters R_d, ϕ, P_{max} and Θ of the simple model of the PFD response of photosynthesis (eq. 5.1). Values estimated from gas exchange measurements made on 14 shoots at the BOREAS SSA OBS site, July 1996 at CO_2 = 1500 µmol mol^{-1}. The P_{max} values at CO_2 = 350 µmol mol^{-1} was recalculated using the response of photosynthesis to CO_2.

Shoot location	R_d µmol CO_2 m^{-2} s^{-1}	ϕ mol CO_2 mol quanta^{-1}	P_{max} µmol CO_2 m^{-2} s^{-1}	Θ
Upper (n = 6)	0.87 ± 0.38	0.044 ± 0.013	6.0 ± 2.3	0.67 ± 0.21
Mid (n = 5)	0.63 ± 0.29	0.031 ± 0.014	4.0 ± 1.4	0.73 ± 0.10
Lower (n = 3)	0.68 ± 2.42	0.048 ± 0.044	4.1 ± 2.9	0.70 ± 0.86

Table 5.2 shows the values of the parameters V_{max}, J_{max}, θ, R_d and α measured on shoots in July and October. There was no relation between the value of V_{max} and the position of the shoot in the canopy, however there was a significant difference (p < 0.05) in the values of J_{max} found in the upper canopy compared with those found lower down within the canopy. Between July and October there was a decrease in V_{max} measured on shoots from the middle of the canopy. Because of the small number of measurements, however, this decrease was not statistically significant. Values of J_{max}, θ and α measured on the same shoots were significantly (p < 0.05) reduced over the same period. Average values for V_{max}, J_{max}, R_d and α measured on shoots at the three canopy positions are superimposed on the branch-derived estimates of these parameters in Figure 5.3, and parameters values averaged for all shoots are superimposed on canopy-derived estimates in Figure 5.5.

Table 5.2. Mean values (± 95% confidence intervals) of the parameters V_{max}, J_{max}, θ, R_d and α of the Farquhar model of photosynthesis (eq. 2 to 8). Values estimated from A-c_i and A-Q response curves made on 14 shoots at the BOREAS SSA OBS site in July (Upper, Mid, Lower) and October (Oct) 1996.

Period	Location (n)	V_{max} µmol CO_2 m^{-2} s^{-1}	J_{max} µmol e$^-$ m^{-2} s^{-1}	θ	R_d µmol CO_2 m^{-2} s^{-1}	α mol e$^-$ mol^{-1} quanta
July	Upper (6)	16.0 ± 5.5	64.1 ± 15.6	0.64 ± 0.10	0.72 ± 0.27	0.24 ± 0.07
July	Mid (5)	15.8 ± 4.1	47.1 ± 6.5	0.73 ± 0.09	0.53 ± 0.55	0.21 ± 0.03
July	Lower (3)	23.7 ± 9.5	46.6 ± 10.9	0.66 ± 0.13	0.75 ± 0.92	0.24 ± 0.08
Oct	Mid (6)	13.5 ± 2.6	26.9 ± 12.8	0.43 ± 0.28	0.45 ± 0.21	0.06 ± 0.04

Neither the nitrogen nor the phosphorus contents of the sample of needles used for gas exchange measurements were significantly different between the crown levels (Table 5.3). In contrast, there was a significant effect ($p < 0.05$) of needle age class on P content, with the highest concentration being found in the youngest needles. This effect was also almost significant ($p = 0.078$) for N content. A parallel result was found for specific needle area which was not different between crown levels but was significantly higher ($p < 0.05$) in the current year needles, i.e. age class 1996. The N and P-content distribution pattern was not accounted for by the differences in specific needle area, i.e. differences found were still significant when N and P contents were expressed on a surface area basis.

Table 5.3. Specific needle area and needle nutrient contents values averaged with respect to age class and vertical position in the canopy in 1996 at the BOREAS OBS site. In July 1996, needles were sampled on shoots collected at three heights in the canopy (Upper, Mid, Lower), from five trees, and total sample size was $n = 61$. In October 1996, 15 shoots were collected from the mid canopy level only, and total sample size was $n = 59$.

	Shoot	Needle age class					
	position	1992	1993	1994	1995	1996	All
N content	Upper	5.2	6.3	7.3	7.2	7.6	7.1
[mg g^{-1}]	Mid	5.8	6.3	6.8	6.1	11.0	7.5
	(Oct)	-	6.4	7.4	7.5	7.8	-
	Lower	-	6.6	6.8	7.0	6.8	6.8
P content	Upper	0.47	0.63	0.66	0.64	0.92	0.72
[mg g^{-1}]	Mid	0.51	0.50	0.54	0.51	1.32	0.71
	(Oct)	0.49	0.59	0.60	0.62	1.01	-
	Lower	-	0.56	0.59	0.59	1.03	0.64
Specific	Upper	39.6 ± 0.3	42.6 ± 1.7	38.7 ± 3.6	43.8 ± 2.9	42.2 ± 2.9	-
needle area	Mid	39.7 ± 0.8	42.4 ± 3.7	40.6 ± 1.9	43.7 ± 1.0	44.7 ± 2.9	-
[cm^2 g^{-1}]	Lower	41.2 ± 0.9	40.5 ± 1.8	42.0 ± 0.4	44.8 ± 3.8	48.6 ± 4.1	-

Branch photosynthesis

Parameter values for the non-linear rectangular hyperbolic response of photosynthesis to incident PFD and temperature class are given in Figure 5.2. Daytime "dark" respiration increased with temperature (Figure 5.2(a)), branches in the upper canopy appeared to follow an exponential increase whereas in the lower canopy the increase appeared linear. Differences between the branches were, however, slight and not statistically significant ($p > 0.05$). The apparent quantum efficiency also increased with temperature (Figure 5.2(b)). For the lower branches,

this increase continued up to the highest temperatures found under natural conditions; however, for the upper branches there appeared to be a slight reduction in apparent quantum efficiency at temperatures above 15 °C. Again, in most cases, differences between the branches were not statistically significant. The asymptotic maximum photosynthetic rate was consistently, and in most cases significantly ($p < 0.05$), higher for the branches on the easternmost tree than for those on the westernmost tree (Figure 5.2(c)). Differences between the heights were less pronounced but in general, maximum photosynthetic rates were higher for the branches in the lower canopy. For both trees the transition between PFD-limited and PFD-saturated photosynthesis became less abrupt at high temperatures for the lower branches only (Figure 5.2(d)).

Figure 5.3 shows the parameters V_{max}, J_{max}, R_d and α derived for each branch for each period of twenty days. There was a pronounced seasonality found in the values of both V_{max} and J_{max} for all branches. V_{max} was close to zero at the start of the measurement period, reached a maximum during the summer and declined later in the year (Figure 5.3). A similar seasonal pattern was observed for J_{max}. Values of V_{max} and J_{max} estimated for the East tree were consistently higher than those estimated for the West tree, although these differences were only significant for the upper branches. (Figure 5.3). R_d and α were both zero at the beginning and end of the measurement period, R_d reached a maximum in mid-summer and α reached a maximum at around day 220. The value of α estimated for the upper west branch was significantly lower than for all other branches for most of the year. Average values for V_{max}, J_{max}, R_d and α measured on branches are superimposed on the canopy-derived estimates of these parameters in Figure 5.5.

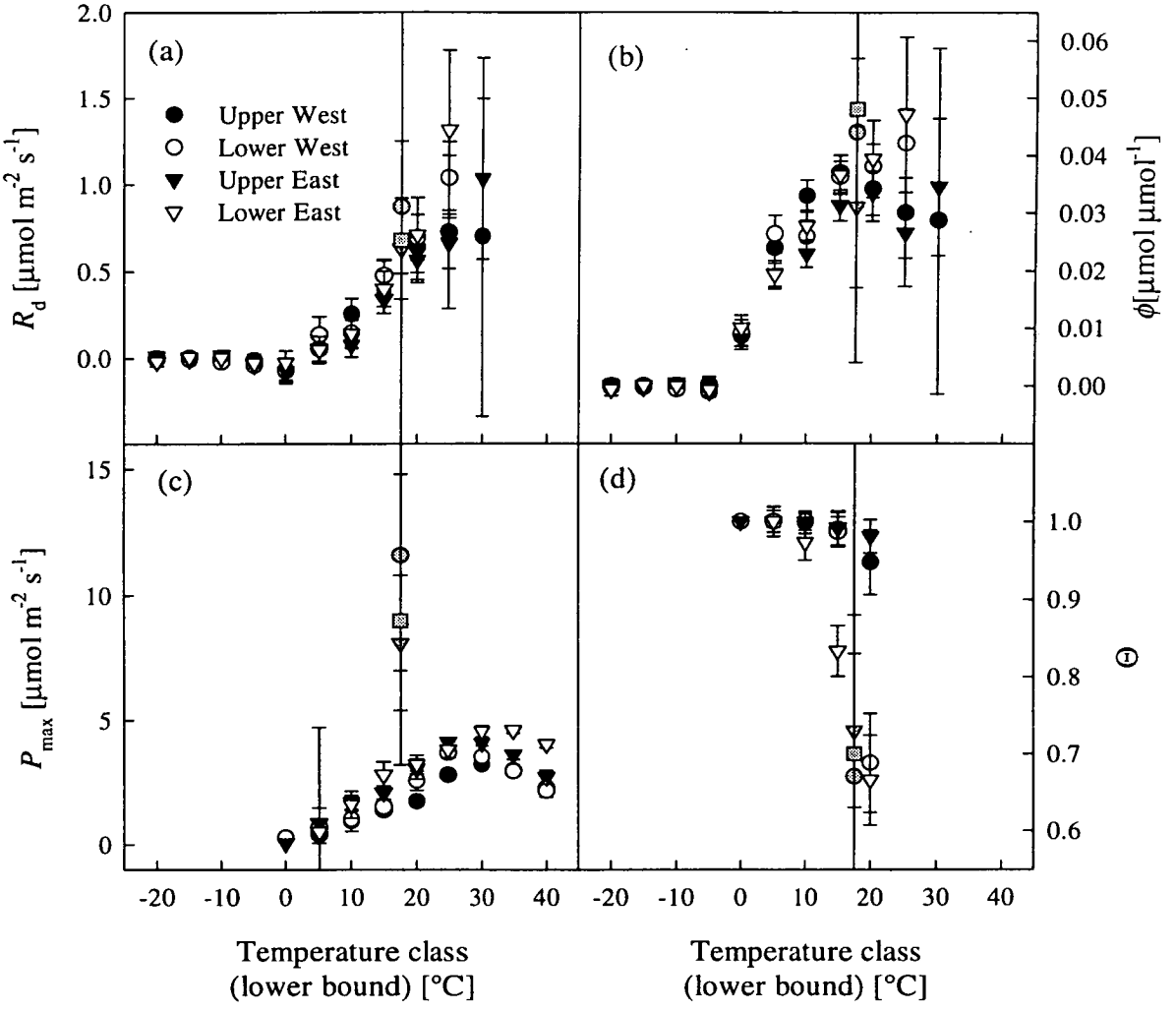

Figure 5.2. Change in the parameters values of the model of the response of branch photosynthesis to PFD at different temperatures. Measurements made on four black spruce branches at the BOREAS SSA OBS site from April to December 1996, and averaged over twenty-day periods. Closed symbols are branches in the upper canopy, open symbols are branches in the lower canopy. Circles– West tree, triangles – East tree. Grey symbols are the parameters estimated from shoot measurements made in July, circle, triangle and square – upper, mid and lower canopy, respectively. Error bars represent 95% confidence limits for the parameter estimates. (a) Day respiration, R_d. (b) Apparent quantum efficiency of photosynthesis, ϕ. (c) Asymptotic maximum photosynthetic rate, P_{max} at ca = 350 µmol mol^{-1}. (d) Convexity coefficient for the irradiance dependence of photosynthesis, Θ.

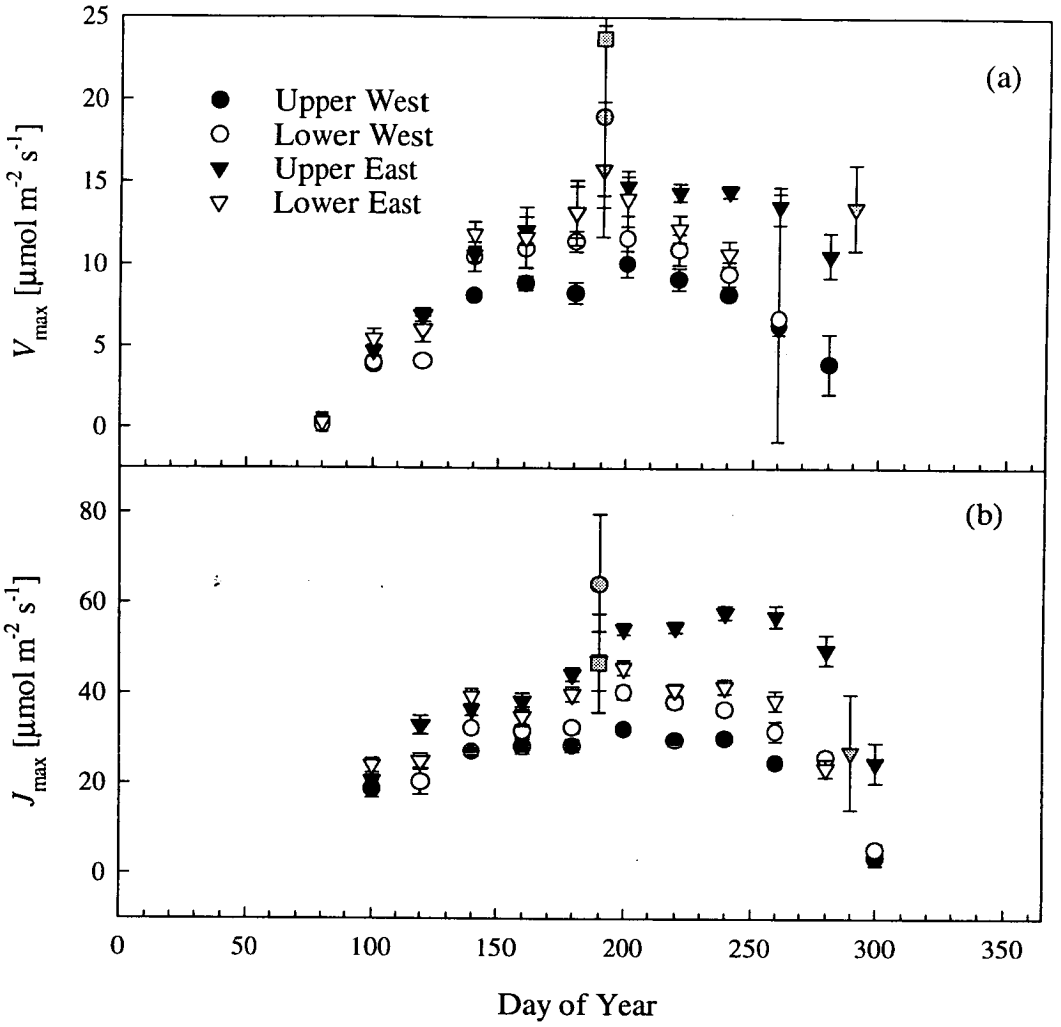

Figure 5.3 (a) & (b). Seasonal course of the photosynthetic parameters of the Farquhar model of photosynthesis at the BOREAS SSA OBS site from April to December 1996. Parameters values were calculated from branch bag measurements and averaged over twenty-day periods. Closed symbols: upper canopy, open symbols: lower canopy. Circles – West tree, triangles – East tree. Grey symbols are the parameters estimated from shoot measurements: circles, triangles and squares – upper, mid and lower canopy, respectively. Error bars represent 95% confidence limits for the parameter estimates. (a) Maximum rate of carboxylation, V_{max}. (b) PFD saturated rate of electron transport, J_{max}.

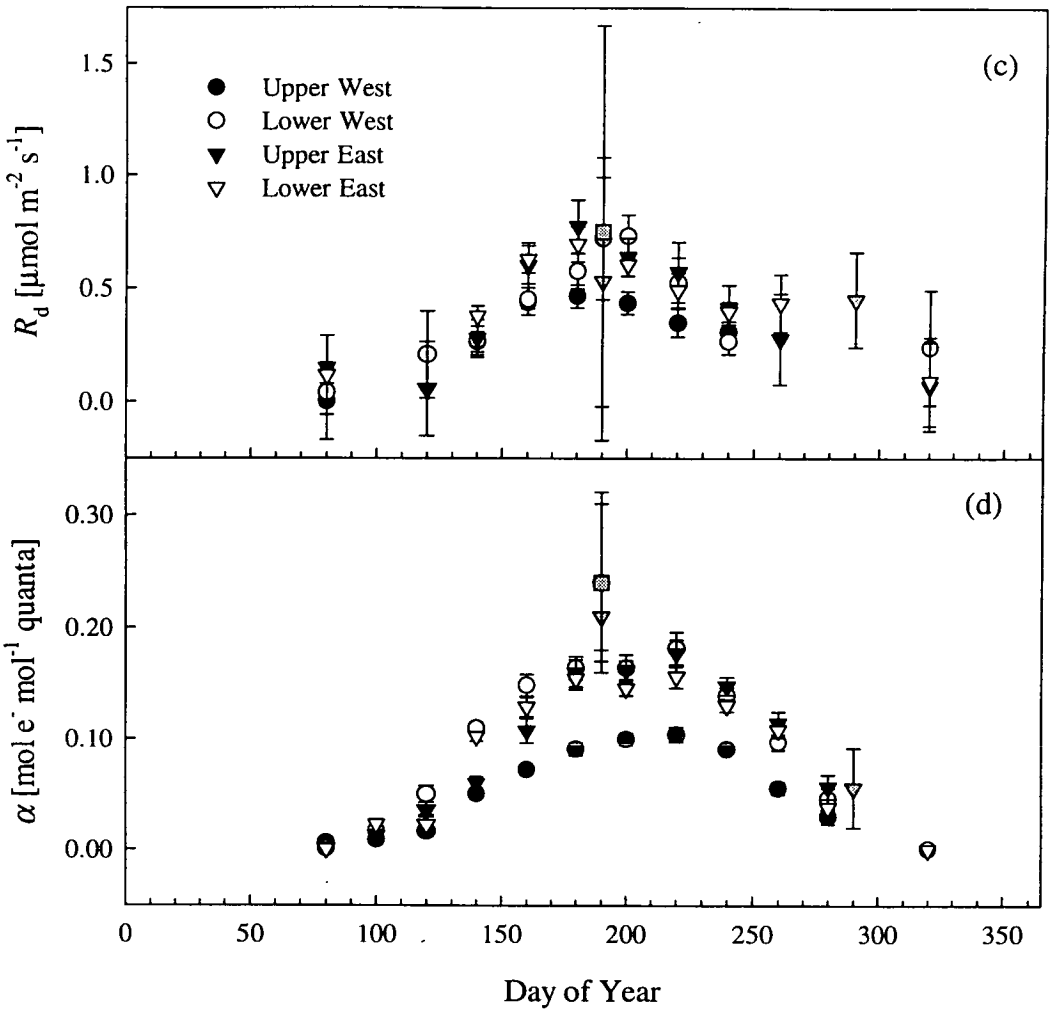

Figure 5.3 (c) & (d). Seasonal course of the photosynthetic parameters at the BOREAS SSA OBS site (1996). Parameters values were calculated from branch bag measurements and averaged over twenty-day periods. Closed symbols: upper canopy, open symbols: lower canopy. Circles – West tree, triangles – East tree. Grey symbols are the parameters estimated from shoot measurements: circles, triangles and squares – upper, mid and lower canopy, respectively. Error bars represent 95% confidence limits for the parameter estimates. (c) Daytime "dark" respiration, R_d. (d) apparent quantum efficiency of electron transport, α.

Canopy photosynthesis

Parameter values for the hyperbolic response of canopy photosynthesis to incident PFD for each temperature class are given in Figure 5.4. Day respiration exhibited no significant variation with temperature (Figure 5.4(a)). The apparent quantum efficiency showed a general increase from zero at temperatures above 0 °C, but these differences were not statistically significant ($p > 0.05$) (Figure 5.4(b)). The maximum photosynthetic rate of the canopy increased rapidly and significantly ($p < 0.05$) at temperatures above 0 °C, reaching a maximum around 15 °C, and dropped off

significantly at temperatures higher than this (Figure 5.4(c)). There was no variation in the convexity coefficient with temperature at temperatures below 15 °C, but a significant reduction at higher temperatures (Figure 5.4(d)).

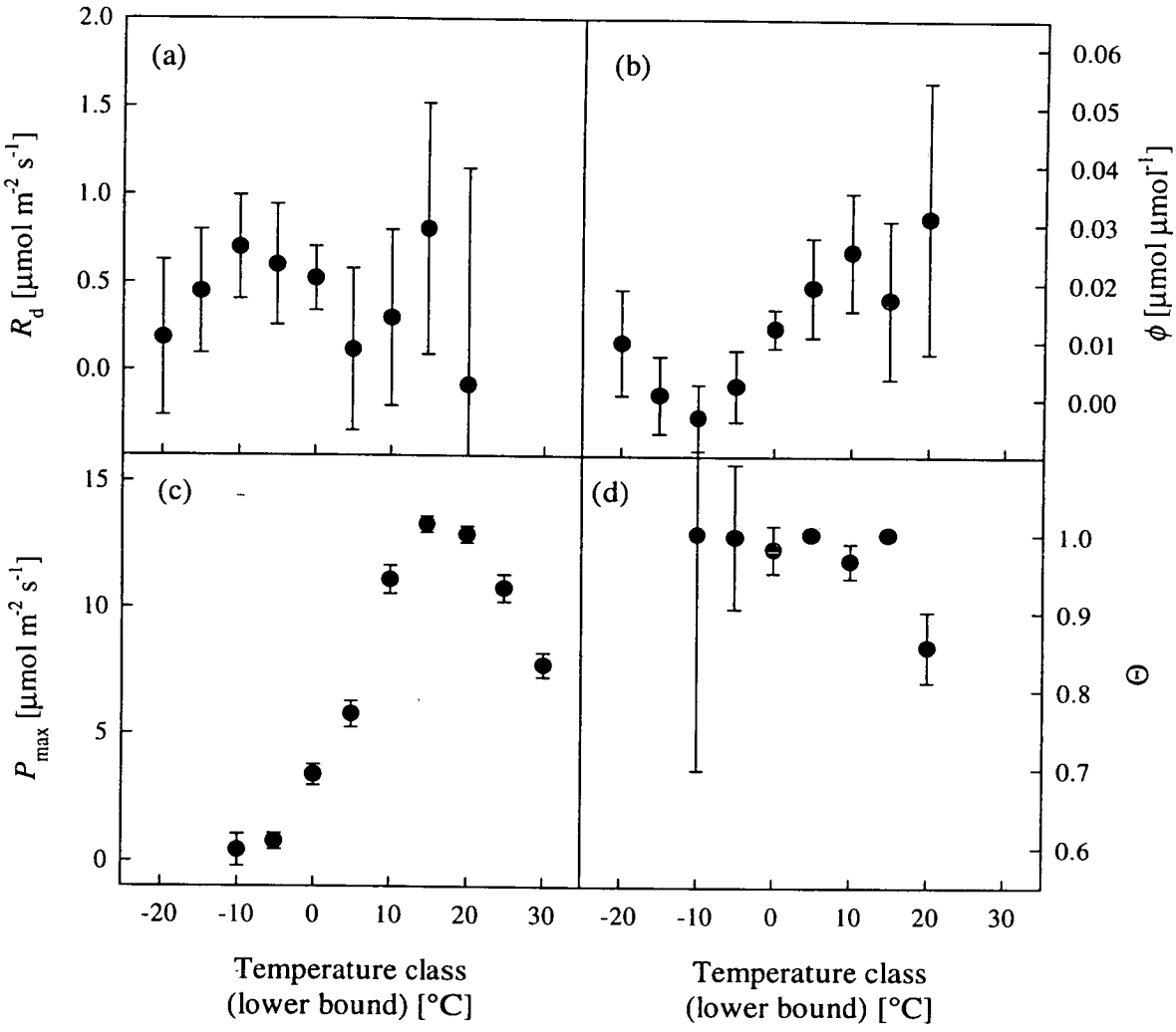

Figure 5.4. Change in the parameters values of the model of the response of canopy photosynthesis to PFD at different temperatures. Measurements made at the BOREAS SSA OBS site from April to December 1996 and averaged over twenty-day periods. Error bars represent 95% confidence limits for the parameter estimates. (a) Day respiration, R_d. (b) Apparent quantum efficiency, ϕ. (c) Asymptotic maximum photosynthetic rate, P_{max}. (d) Convexity coefficient for the irradiance dependence of photosynthesis, Θ.

The model parameters V_{max}, J_{max} and α derived for the canopy for each period of twenty days are shown in Figure 5.5. Both V_{max} and J_{max} started at low values at the start of the measurement period, reached maxima in late summer and declined later in the year (Figure 5.5(a)). α followed a similar seasonal time-course to V_{max} and

J_{max}, There was a marked reduction in α in the middle of the year, but the 95 % confidence interval for these estimates were large.

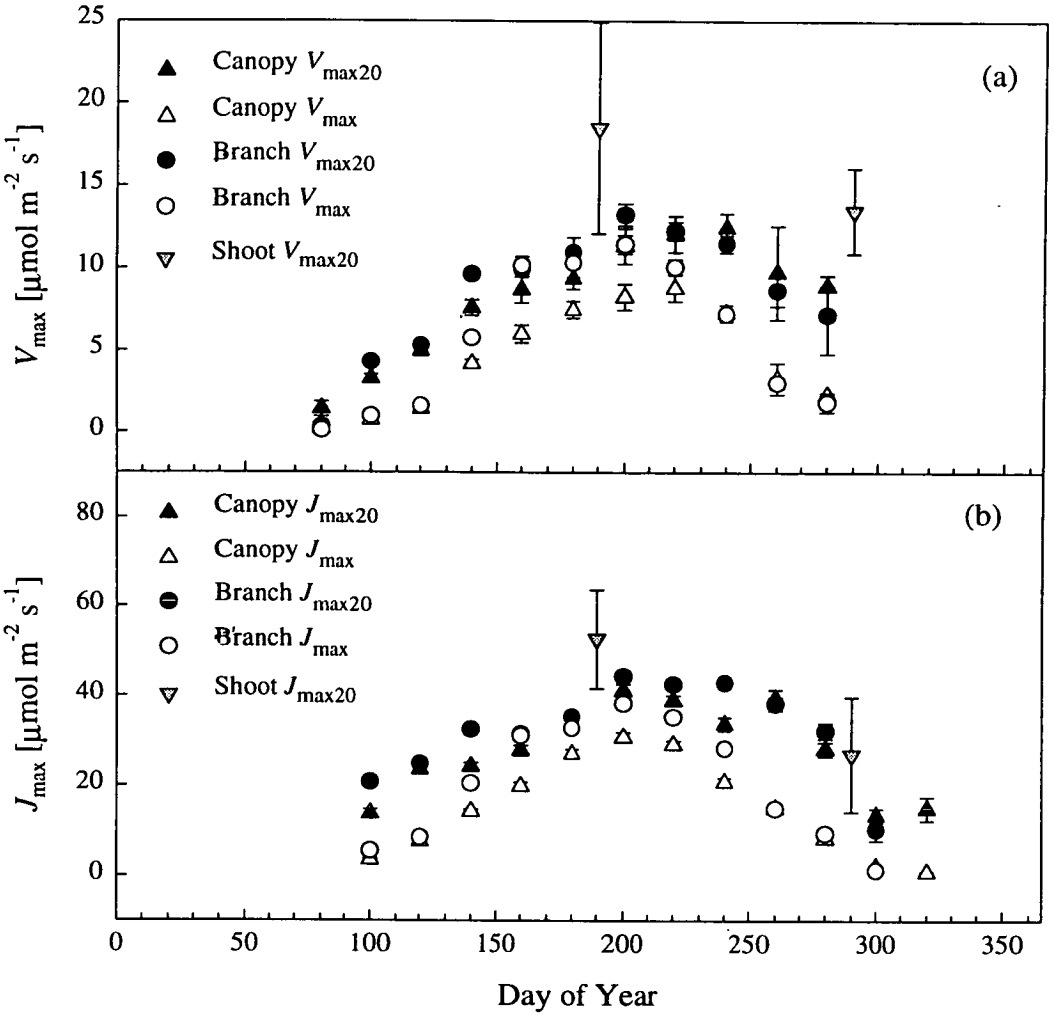

Figure 5.5 (a) & (b). Seasonal course of the parameters of the Farquhar model of photosynthesis for shoots (down triangles), branches (circles) and canopy (up triangles) at the BOREAS SSA OBS site from April to December 1996. Each value was calculated from measurements averaged over a 20-day period. Error bars represent 95% confidence limits for the parameter estimates. (a) Maximum rate of carboxylation, V_{max}. (b) Light saturated rate of electron transport, J_{max}. Two values are given, the rate corrected to 20 °C (closed symbols) and the actual rate measured (open symbols). Note that canopy values have been divided by the leaf area index, such that all parameters are expressed on an illuminated area basis.

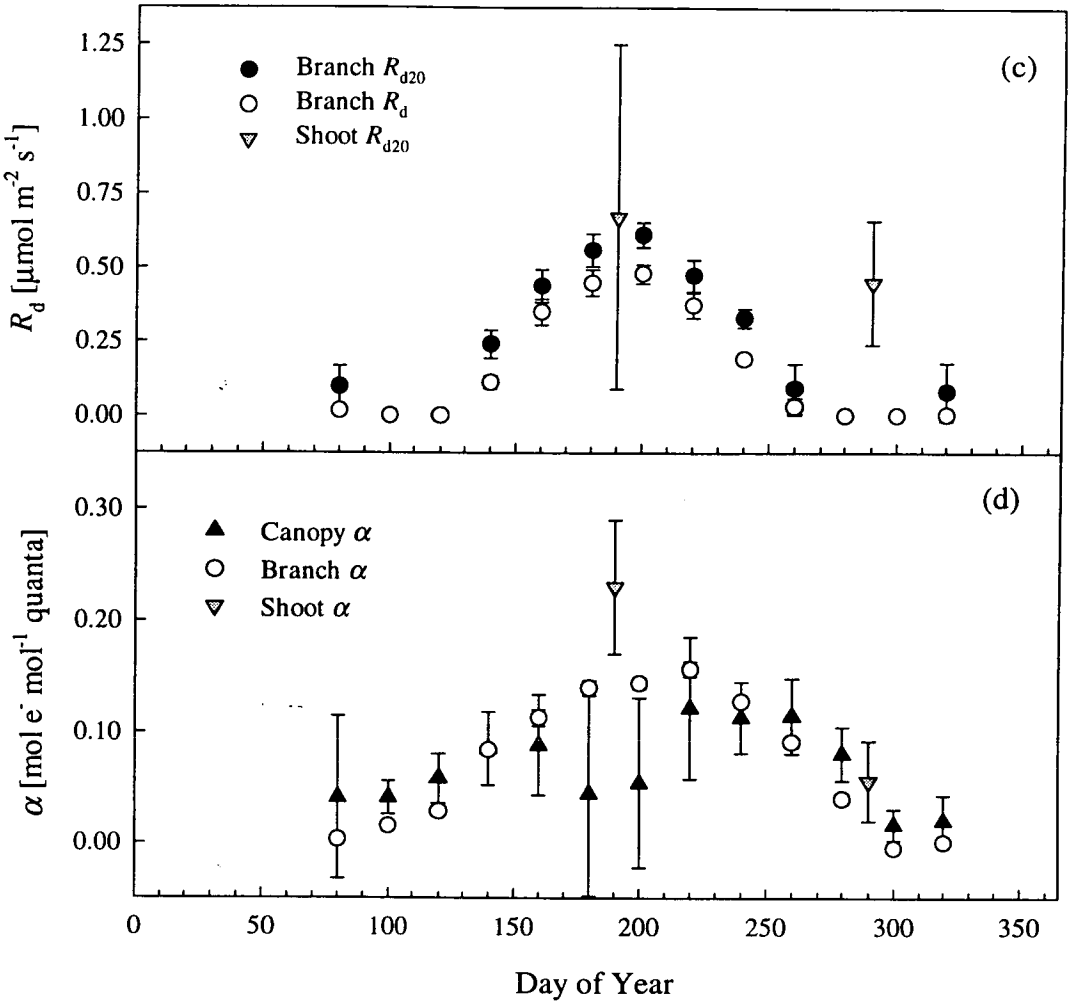

Figure 5.5 (c) & (d). Seasonal course of the parameters of the Farquhar model of photosynthesis for shoots (down triangles), branches (circles) and canopy (up triangles) at the BOREAS SSA OBS site from April to December 1996. Each value was calculated from measurements averaged over a 20-day period. Error bars represent 95% confidence limits for the parameter estimates. (c) Daytime "dark" respiration, R_d. (d) apparent quantum efficiency of electron transport, α. Two values of R_d are given, the rate corrected to 20 °C (closed symbols) and the actual rate measured (open symbols).

Shoot night-time respiration

Parameter values for the respiration model (eq. 5.9) fitted to the shoot data are given in Table 5.4. There were no significant differences ($p > 0.05$) between the values obtained from shoots at different heights in the canopy for any of the parameters. Although not statistically significant ($p > 0.05$) in view of the small sample size, the rate of respiration at 20 °C, R_{20}, was reduced by half between July and October. A small increase in the temperature sensitivity was observed over the same period. Average values for R_{20} and E_0 measured on shoots at the three canopy positions are

superimposed on the branch-derived estimates of these parameters in Figure 5.6, and parameter values averaged for all shoots are superimposed on canopy-derived estimates in Figure 5.7.

Table 5.4. Mean values (± 95% confidence limits) of the parameter estimates of an Arrhenius "activation energy" model of the response of shoot respiration to temperature. Values estimated from gas exchange measurements made on 11 shoots at the BOREAS SSA OBS site in July and October 1996.

Period	Shoot location (n)	R_{20} $\mu mol\ m^{-2}\ s^{-1}$	E_0 $J\ mol^{-1}\ K^{-1}$
July	Upper (1)	0.08 ± 0.10	68842 ± 23676
	Mid (3)	0.24 ± 0.30	48847 ± 24147
	Lower (1)	0.15 ± 0.05	47515 ± 6155
October	Mid (6)	0.11 ± 0.03	57568 ± 5186

Branch night-time respiration

Figure 5.6 shows the seasonal time courses of the branch-derived parameters for the temperature response of night-time respiration. R_{20} was significantly higher ($p < 0.05$) around day 100 and around day 300 than in the middle of the year, although the highest actual respiration rates, R, were observed in the middle of the year. Following a gradual increase in temperature sensitivity until day 140, E_0 varied little through the year until temperature sensitivity decreased after day 300. There were no consistent differences between the respiration parameters obtained from the different branches, although differences between individual twenty day periods were significant. Average values for R_{20} and E_0 measured on branches are superimposed on the canopy-derived estimates of these parameters in Figure 5.7.

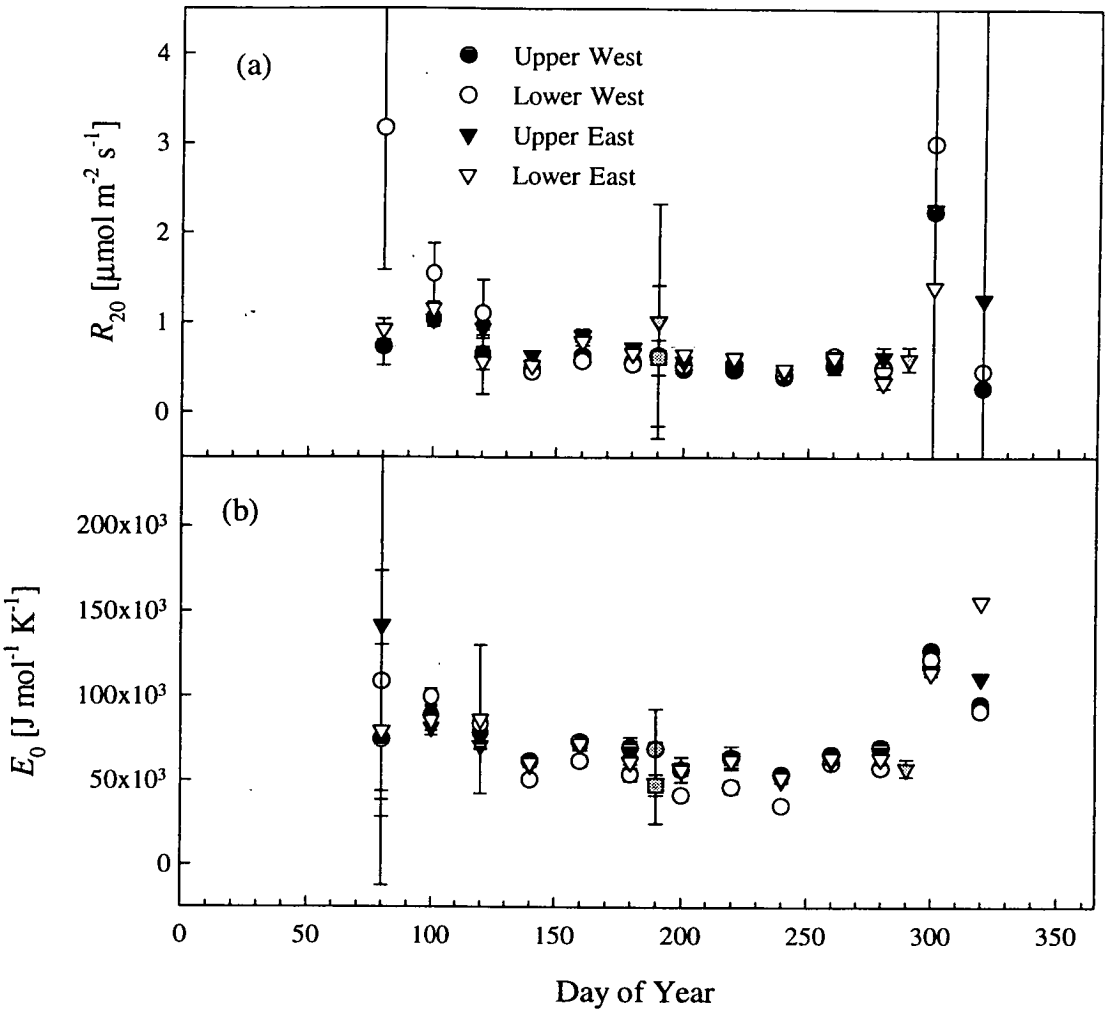

Figure 5.6. Seasonal course of the parameters of the Arrhenius "activation energy" model of night-time respiration temperature response at the BOREAS SSA OBS site from April to December 1996. Parameters values were calculated from branch bag measurements and averaged over twenty-day periods. Closed symbols: upper canopy, open symbols: lower canopy. Circles – West tree, triangles – East tree. Grey symbols are the parameters estimated from shoot measurements: circles, triangles and squares – upper, mid and lower canopy, respectively. Error bars represent 95% confidence limits for the parameter estimates. (a) Respiration rate at 20 °C, R_{20}. (b) Activation energy, E_0.

Canopy respiration

The seasonal time courses of the model parameters for the net ecosystem response to temperature are given in Figure 5.7. After an initial decline, R_{20} increased until the middle of the year, then decreased to close to zero by the end of the measurement period. The actual rates of night-time respiration measured at the start and end of the measurement period were similar. There was considerable variation in E_0 throughout the year, although the 95% confidence limits for the parameter estimates were large.

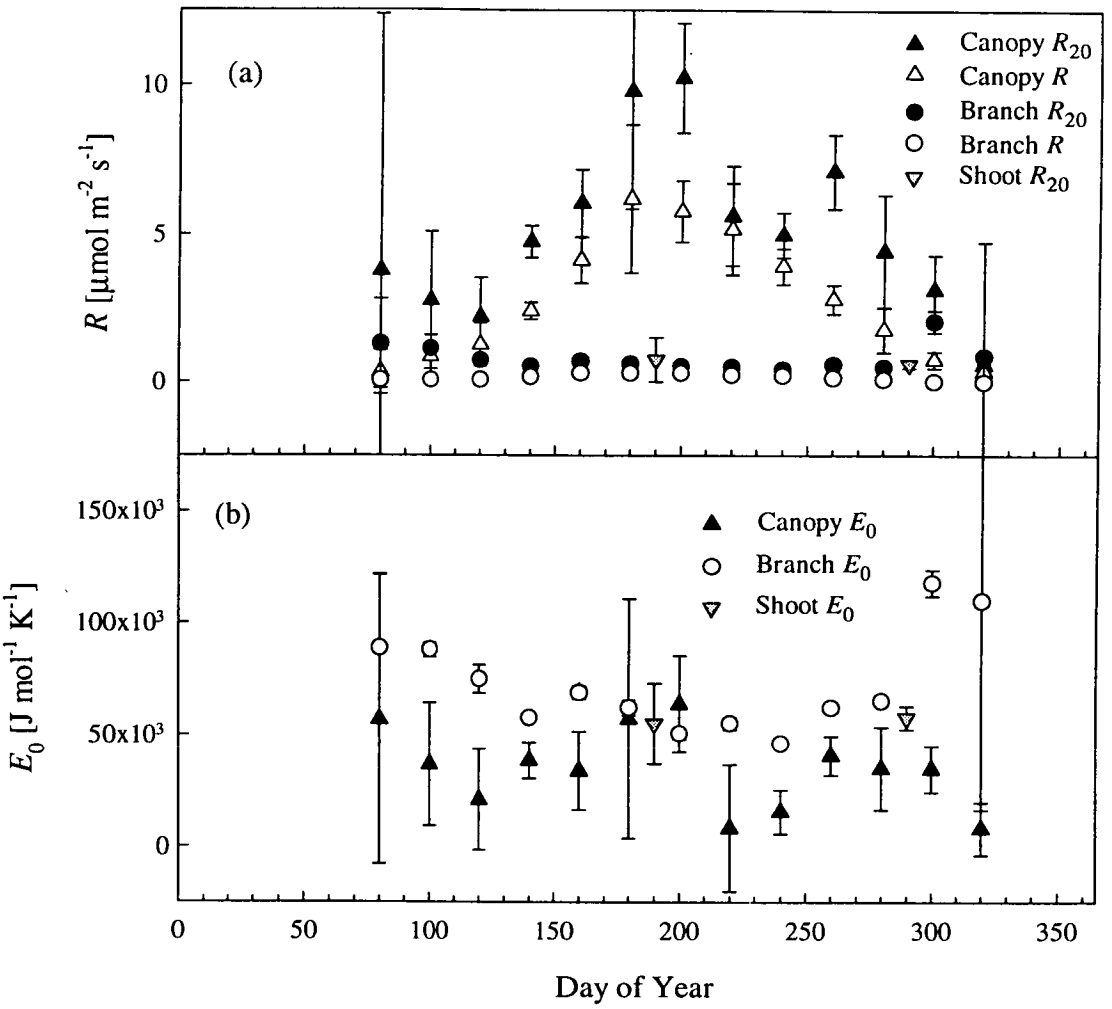

Figure 5.7. Seasonal course of the parameters of the an Arrhenius "activation energy" model of respiration temperature response for shoots (down triangles), branches (circles) and canopy (up triangles) at the BOREAS SSA OBS site from April to December 1996. Each value was calculated from measurements averaged over 20-day periods. Error bars represent 95% confidence limits for the parameter estimates. (a) Respiration rate. (b) Activation energy, E_0. Two values of R_d are given, the rate corrected to 20 °C, R_{20} (closed symbols), and the actual rate measured, R (open symbols). Note that shoot and branch parameters are expressed on an needle area basis and canopy parameters are expressed on a ground area basis.

Conductance

Values for the parameters of the Jarvis model of stomatal conductance fitted to the shoot measurements are given in Table 5.5. The data presented are the mean parameters for each canopy position. Since measurements were made at a constant dew point temperature, any effect of changing temperature was confounded with the effects of changing humidity deficit. Consequently only two shoots presented realistic temperatures response parameters, and therefore the results are not included

here. Shoots in the upper canopy had significantly higher minimum (g_{w0}) and maximum (g_{wmax}) conductances than shoots in the mid canopy. Confidence intervals were large for the parameters derived from the small sample of shoots in the lower canopy and the parameters were not significantly different ($p > 0.05$) to either the upper or mid-canopy shoots.

Table 5.5. Mean parameters (± 95% confidence intervals) of the Jarvis model of stomatal conductance. Values were derived from the *A* - *Q* response curves measured in July 1996 on a sample of 14 shoots (T_{air} = 17.5 °C, $T_{dew\ point}$ = 8 °C, CO_2 = 1500 µmol mol^{-1}).

Shoot location	g_{w0} [mmol m^{-2} s^{-1}]	g_{wmax} [mmol m^{-2} s^{-1}]	k_{pfd}
Upper (n = 6)	22.7 ± 14.0	58.9 ± 21.4	0.995 ± 0.003
Mid (n = 5)	16.4 ± 8.9	26.7 ± 10.4	0.988 ± 0.009
Lower (n = 3)	35.5 ± 73.2	50.4 ± 90.3	0.992 ± 0.019

The parameter values for the BWBL model of stomatal conductance fitted to the shoot measurements are given in Table 5.6. There were no statistically significant ($p > 0.05$) differences between any of the branches for either the minimum conductance, g_0, or the assimilation rate response parameter, a_1.

Table 5.6. Parameters (± 95% confidence intervals) of the BWBL model of stomatal conductance. Values were derived from the *A* - *Q* response curves measured in July 1996 on a sample of 14 shoots (T_{air} = 17.5 °C, $T_{dew\ point}$ = 8 °C, CO_2 = 1500 µmol mol^{-1}).

Shoot location	g_{w0} [mmol m^{-2} s^{-1}]	a_1	D_0 [mmol mol^{-1}]
Upper (n = 6)	30.5 ± 16.3	11426 ± 7465	4.6 ± 5.1
Mid (n = 5)	12.8 ± 7.4	5982 ± 3246	4.6 ± 5.1
Lower (n = 3)	8.7 ± 25.1	7830 ± 4862	4.6 ± 5.1
All (n = 14)	12.7 ± 3.8	7832 ± 5485	4.6 ± 5.1

Values for the parameters of the Jarvis model of conductance applied to the branch measurements are given in Table 5.7, together with confidence intervals where appropriate. No confidence intervals were estimated for the "envelope" parameters k_{pfd}, T_{min}, T_{opt} and T_{max} since these were fitted by eye and were therefore not susceptible to objective statistical analysis. Also no confidence interval was attached to g_{wmax} since this was simply the maximum conductance value observed. There was no significant difference between the minimum conductance, g_{w0}, observed for each

branch. Maximum conductance, g_{wmax}, was observed to be very highly correlated with minimum conductance according to $g_{wmax} = 1.4\ g_{w0} + 20.2$ ($r^2 = 0.97$), therefore it was considered that there was also no significant difference between the values of g_{wmax} for each branch. The PFD response of stomata, k_{pfd}, was similar for branches at the same position in the canopy, but was noticeably different between the upper and lower canopy positions, with the branches lower in the canopy reaching PFD saturation at lower PFD than those in the upper canopy. Conductance in the lower branch of the East tree was significantly less sensitive to humidity deficit than the other branches. There were no significant differences ($p > 0.05$) between the transient response time-constants for each branch.

Table 5.7. Parameter estimates (± 95% confidence limits where appropriate) of the Jarvis model of conductance. Values estimated from gas exchange measurements made on four branches at the BOREAS SSA OBS site between April and December 1996.

Branch location	g_0 mmol m^{-2} s^{-1}	g_{wmax} mmol m^{-2} s^{-1}	k_{pfd}	D_0 mmol mol^{-1}	T_{min} °C	T_{opt} °C	T_{max} °C	τ min
Upper West	3.8 ± 2.5	25.4	0.995	57.8 ± 4.2	2	32	52	16.4 ± 3.3
Lower West	7.8 ± 3.6	31.7	0.99	45.4 ± 8.0	-4	24	53	13.1 ± 3.4
Upper East	9.2 ± 10.5	32.5	0.995	61.0 ± 5.3	-5	30	52	4.5 ± 7.4
Lower East	5.9 ± 3.2	28.0	0.99	162.7 ± 88.7	2	21	50	13.5 ± 2.7
All	6.5 ± 2.1	32.5	0.995/ 0.99	53.2 ± 2.8	-5	27	55	11.9 ± 1.5

The parameter values for the BWBL model of conductance derived from the branch measurements are given in Table 5.8. There were no statistically significant differences ($p > 0.05$) between any of the branches for either parameter a_1, or response parameter D_0. The fitted values of the transient response time-constants calculated for the entire dataset were zero for three of the four branches.

Table 5.8. Parameters (± 95% confidence intervals) of the BWBL model of conductance. Values estimated from gas exchange measurements made on branches at the BOREAS SSA OBS site from April to December 1996.

Branch location	g_0 [mmol m^{-2} s^{-1}]	a_1	D_0 [mmol mol^{-1}]	τ [min]
Upper West	3.8 ± 2.5	1270 ± 396	93 ± 148	0
Lower West	7.8 ± 3.6	1201 ± 654	354 ± 3125	0
Upper East	9.2 ± 10.5	1361 ± 255	141 ± 210	0
Lower East	5.9 ± 3.2	1955 ± 494	54 ± 65	16.0 ± 5.6
All	6.5 ± 2.1	1536 ± 204	69 ± 42	-

Values for the parameters of the Jarvis model of conductance derived from the net ecosystem water vapour flux measurements are given in Table 5.9, together with confidence intervals where appropriate. Confidence intervals were not estimated for g_0 since this was simply the minimum conductance value observed, or the "envelope" parameters k_{pfd}, T_{min}, T_{opt} and T_{max} since these were fitted by eye.

Table 5.9. Parameters (± 95% confidence intervals where appropriate) of the Jarvis model of conductance. Values estimated from eddy covariance measurements of net ecosystem water vapour flux made at the BOREAS SSA OBS site from April to December 1996.

g_0 mmol m^{-2} s^{-1}	g_{wmax} mmol m^{-2} s^{-1}	k_{pfd}	D_0 mmol mol^{-1}	T_{min} °C	T_{opt} °C	T_{max} °C	τ min
14.7	192.4 ± 19.3	0.99	21.1 ± 2.4	-8	10	28	13.8 ± 12.1

The parameter values for the BWBL model of conductance derived from the net ecosystem water vapour flux measurements are given in Table 5.10.

Table 5.10. Parameters (± 95% confidence intervals) of the BWBL model of conductance. Values estimated from eddy covariance measurements of net ecosystem water vapour flux at the BOREAS SSA OBS site from April to December 1996.

g_0 [mmol m^{-2} s^{-1}]	a_1	D_0 [mmol mol^{-1}]	τ [min]
36.4 ± 10.6	1468 ± 313	50.8 ± 64.5	0

DISCUSSION

Temporal variation

The large variation over time observed in the photosynthesis and respiration parameters is an important characteristic of this boreal forest and contrasts with the temporally homogeneous behaviour of, say, tropical forest canopies. This highlights the need for making measurements of these processes throughout the growing season if these parameters are to be used for modelling purposes. Despite the large seasonal variation in V_{max} and J_{max}, the temperature responses of these parameters remained constant between summer and winter, i.e. there was no evidence of photosynthetic acclimation to seasonal temperature change (D. Loustau in prep.). For the branches and the canopy too, most of the annual variations in V_{max} are closely associated with changes in V_{max20}. Consequently any direct effects of temperature on V_{max} must be mainly limited to short-term variations, and the observed seasonality in V_{max} must reflect a seasonal change in photosynthetic activity at the biochemical, rather than at the environmental level. Thus there was a clear "ramping-up" of the parameters describing biochemical activity, V_{max}, J_{max} and α, from the time that air temperature first rose above zero at the start of the season (Figure 5.5). This steady rise in activity continued even after air temperature had reached its seasonal maximum and daily incident PFD had started to decrease. V_{max} only stopped increasing as it started to decline following a severe drop in air temperature around day 250.

Several environmental variables such as the timing of the soil thaw and freeze, the seasonal pattern of soil temperature and moisture availability, the occurrence of spring and autumn frosts and a late summer reduction in atmospheric humidity, may contribute to the seasonality in photosynthetic capacity in the boreal forest, and all these factors were observed to co-vary with photosynthetic capacity at the OBS site in 1996. Given only one year's physiological observations, however, it is impossible to make generalisations from these data alone.

The high values of R_{20} around day 100 coincided with the time of bud burst and subsequent rapid shoot extension, and it is probable that the observed increase in respiration was a reflection of this. The high values of R_{20} late in the year, around day 300, followed the first night-time frosts, and again it is likely that these high

respiration rates result from increased repair and biosynthesis demands. The seasonal change in the respiration temperature response is contrary to the assumption made by Ryan *et al.* (1997) that the sensitivity of black spruce respiration to temperature is constant over the year for trees at this site. Respiration was most sensitive to temperature around days 100 and 300, the times when construction demands dominate over maintenance costs, suggesting that the temperature sensitivity of growth respiration is higher than that of maintenance respiration.

The values of P_{max} estimated from the shoot photosynthesis irradiance response curves are slightly higher than the values measured by Middleton *et al.* (1997) for black spruce at the same site in 1994 (3.10 ± 0.22 μmol m^{-2} s^{-1}). This difference presumably stems from the difference in illumination system used, which was bilateral in the present study and unilateral in the measurements made by Middleton *et al.* (1997), since bilateral illumination reduces mutual shading within a shoot (Wang & Jarvis 1990). The observed values of V_{max} and J_{max} as derived from shoot measurements were broadly typical of the values found by other authors for other *Picea* species (Wullschleger 1993), apart from the anomalously high values of 412 and 210 μmol m^{-2} s^{-1} reported for black spruce by Bonan (1993).

These low values of P_{max} are readily explained by the very poor nutrient status of the trees at the site. Needle nitrogen concentrations were very low (Table 5.3), about half the value typically found in plantation-grown black spruce at similar latitudes (Lamhamedi & Bernier 1994). Needle phosphorus content lower than 1 mg g^{-1} is considered a sign of phosphorus deficiency (Lamhamedi & Bernier 1994). The average P-content of the needles at this site was below this level (Table 5.3), and was found to correlate with differences between the maximum photosynthetic rates observed for the branches (Chapter 4) indicating a possible phosphorus limitation to photosynthesis. However, there was a pronounced sensitivity of photosynthesis to ambient oxygen concentration, suggesting that despite the low phosphorus content, photosynthesis was not in fact limited by the triose phosphate utilisation rate (D. Loustau in preparation) and that most nutrient deficiency effects on photosynthesis were mediated through carboxylation activity and electron transport rate. This is consistent with studies of the effects of nitrogen fertilisation in northern latitude

forests where photosynthetic capacity was significantly increased after application of additional nitrogen (Mitchell & Hinckley 1993; Teskey, Gholz & Cropper 1994, Roberntz & Stockfors 1997).

Spatial variation

Given the low level of nitrogen and phosphorus availability, it is perhaps surprising that there was little or no significant difference in the shoot- or branch-derived values of V_{max} or P_{max} according to height. As a consequence, despite the branches in the upper canopy receiving almost exactly twice as much light over the year as those in the lower canopy, total carbon uptake of branches in the upper canopy was only 38% higher than in the lower canopy (Chapter 4). This result is consistent with the almost uniform vertical distribution of specific needle area, nitrogen and phosphorus contents in the canopy (Table 5.3), and is in contrast to the vertical stratification of photosynthetic capacity and nitrogen content observed in many plant species (Field & Mooney 1986; Pearcy & Sims 1994; Hollinger 1996). This apparent lack of photosynthetic acclimation to PFD may be the result of the highly aggregated structure of the canopy where the tall narrow, dense tree crowns do not form a closed canopy. The strongest gradient of light occurs horizontally along the branches, from the needles at the ends of the branches that are nearly always in sunlight, to those in the interior of the crown that are always shaded. Any optimisation of nitrogen/photosynthetic capacity allocation is therefore likely to be in the horizontal, rather than the vertical, direction, and the branch bag technique, because it integrates gas exchange over the whole of the branch, would therefore tend to obscure differences due to nitrogen allocation patterns in this instance.

Indeed current year needles, growing at the ends of the branches, had, on average, a 13% higher nitrogen and phosphorus contents than older needles (Table 5.3). Although separate measurements of photosynthetic parameters according to needle age were not made, it is reasonable to assume that current year needles may also have the highest photosynthetic capacity since a reduction in photosynthetic activity in needles older than one year has previously been observed in black spruce (Hom and Oechel 1983). Concomitant reductions in nutrient content and photosynthetic capacity have been also observed in other coniferous species (*e.g.* Porté and Loustau

1998). Thus the growth of new needles at the shoot tips, which results in the formation of an outer shell of new foliage, may therefore be regarded as the main mechanism by which this species allocates its photosynthetic capacity to the most illuminated part of the canopy, and nutrient reallocation between mature needles may play a only a minor part in acclimation.

Canopy photosynthesis

Several others workers have attempted to treat whole canopies as equivalent to a big leaf and to estimate parameters for a simple light response model of photosynthesis for the canopy (Ruimy *et al.* 1995). When calculated on a leaf area basis, the maximum rate of photosynthetic uptake by the canopy, P_{max}, estimated in this study (Table 5.11) was lower than that found for maritime pine (16.4 μmol m^{-2} s^{-1} Brunet, Berbigier & Daudet 1992), Douglas-fir (8.2 μmol m^{-2} s^{-1} Price & Black 1990) and Sitka spruce (5.5 μmol m^{-2} s^{-1} Jarvis 1994), but similar to that found in black spruce at a more northerly latitude (*ca.* 3.8 μmol m^{-2} s^{-1} Goulden *et al.* 1997). Estimated day respiration too was lower in this study (Table 5.11) than in maritime pine (0.35 μmol m^{-2} s^{-1}), Douglas-fir (0.71 μmol m^{-2} s^{-1}) and Sitka spruce (1.27 μmol m^{-2} s^{-1}), but slightly higher than in a more northerly black spruce stand (0.126 μmol m^{-2} s^{-1}) (references as above). The apparent quantum efficiency of photosynthesis, ϕ, for this stand (Table 5.11) was very similar to the 0.018 μmol μmol^{-1} found in maritime pine (Brunet *et al.* 1992) and the 0.02 μmol μmol^{-1} found in Douglas-fir (Price & Black 1990), lower than the 0.04 μmol μmol^{-1} found in a more northerly black spruce stand (Goulden *et al.* 1997), and lower than the 0.051 μmol μmol^{-1} found in Sitka spruce (Jarvis 1994). In comparison with other coniferous ecosystems, therefore, this boreal ecosystem displays rather low photosynthetic activity.

Lloyd *et al.* (1995b) estimated values for V_{max} (15.5 μmol m^{-2} s^{-1}), J_{max} (29.5 μmol m^{-2} s^{-1}) and R_d (0.16 μmol m^{-2} s^{-1}) for a tropical rainforest canopy (all values expressed on a leaf area basis), remarkably similar to the values found in this study of a boreal forest canopy (Table 5.11). This similarity is particularly striking in view of the theoretical difficulties in determining V_{max} and J_{max} at higher organisational scales. Notably, the canopy consists of many foliage elements subject to a wide variety of environmental conditions, such that while some may be operating under

carboxylation limited conditions, photosynthesis in others may be limited by electron transport.

Variation in parameters between organisational scales

Not all the physiological parameters describing the functioning of this forest ecosystem could be extracted at each organisational scale. For instance, the canopy daytime respiration rate, R_d, calculated from the *y*-axis intercept of the PFD response curve of canopy uptake, was particularly sensitive to any error in the corrections applied for the soil and understorey CO_2 exchanges and consequently reliable estimates of canopy daytime respiration using this method were not possible.

In Table 5.11 average model parameter values estimated for each of the three organisational scales for the period day 180 to day 200, between 15 and 20 °C are compared. Parameters estimated for the canopy that were calculated on a ground area basis have been divided by the estimated leaf area index (Chen *et al.* 1997) such that all parameters are expressed on a leaf area basis.

Table 5.11. Comparison between model parameters (± 95% confidence intervals where appropriate) as estimated from measurements at three organisational scales at the BOREAS SSA OBS site. Measurements were made between 15 and 20 °C in July 1996. The values of temperature sensitive parameters are given at 20 °C. Parameters are expressed on an illuminated leaf area basis.

Model	Parameter	Shoot	Branch	Canopy
Photosynthesis	R_d	0.73 ± 0.79	0.42 ± 0.09	0.18 ± 0.16
Simple light	ϕ	0.041 ± 0.017	0.035 ± 0.003	0.017 ± 0.014
response	P_{max}	4.7 ± 2.1	1.94 ± 0.29	3.02 ± 0.07
	Θ	0.70 ± 0.31	0.95 ± 0.024	1.00 ± 0.0004
Photosynthesis	V_{max}	18.5 ± 5.9	13.2 ± 0.7	11.3 ± 1.1
Farquhar *et al.*	J_{max}	52.6 ± 9.2	44.3 ± 0.8	41.1 ± 1.5
	R_d	0.67 ± 0.51	0.61 ± 0.04	-
	α	0.23 ± 0.06	0.14 ± 0.005	0.054 ± 0.077
Respiration	R_{20}	0.16 ± 0.15	0.54 ± 0.01	2.33 ± 0.42
	E_0	55068 ± 17993	50445 ± 2485	63742 ± 21412
Conductance	g_0	24.9 ± 11.3	6.5 ± 2.1	3.3
Jarvis	D_0	-	53.2 ± 2.8	21.1 ± 2.4
	g_{wmax}	45.3. ± 32.2	29.4 ± 32.5	43.7 ± 4.4
	k_{pfd}	0.992 ± 0.009	0.993	0.990
	T_{min}	-	-5	-8
	T_{opt}	-	27	10
	T_{max}	-	55	28
	τ	-	11.9 ± 1.5	13.8 ± 12.1

Nearly all the estimated parameters were found to vary with organisational level. Day respiration per unit leaf area, estimated by the simple light response model of photosynthesis decreased as the observational scale increased, despite the fact that a branch and a canopy, as organisational units, clearly have increasing respiratory overheads in terms of supporting, non-photosynthesising, biomass than does a shoot. The converse, i.e. respiration increasing with organisational level, was observed in a study of needle, shoot and canopy photosynthesis in Sitka spruce (Jarvis 1994). Differences between estimates of R_d for the different scales were, however, not significantly different ($p > 0.05$), and the difficulties estimating the daytime respiration of the canopy alone have been discussed above. There was a reduction in the apparent quantum efficiency of photosynthesis, ϕ, at larger scales, presumably as a result of more mutual shading of needles in branches than in shoots and more mutual shading in the canopy than in the branches – something that was not observed in Sitka spruce (Jarvis 1994). P_{max} estimated from the simple light response model was significantly lower ($p < 0.05$) for the branches than for the shoots or the canopy, the values for which were not significantly different ($p > 0.05$). Jarvis (1994) observed an increase in P_{max} as they scaled from needles to shoots to canopy, but this may have been largely a consequence of the rates being expressed on a total, silhouette and ground area basis respectively. The convexity of the PFD response was observed to increase with organisational scale, contrary to expectation (and contrary to the behaviour of Sitka spruce needles, shoots and canopy - Jarvis 1994), since this implies that all the leaves of the canopy were reaching light saturation at a single incident irradiance and suggests that there was no mutual shading at the canopy scale.

Parameter estimates for both V_{max} and J_{max} decreased at increasing organisational scales, although in no cases were the differences statistically significant ($p > 0.05$). Values reported by Meir (1996) for V_{max} (26 - 59 μmol m^{-2} s^{-1}) and J_{max} (40 - 105 μmol m^{-2} s^{-1}) measured on the leaves of tropical rainforest trees were typically three times higher than values of V_{max} (15.5 μmol m^{-2} s^{-1} expressed on leaf area basis) and J_{max} (29.5 μmol m^{-2} s^{-1} expressed on leaf area basis) for the whole canopy at the same

site (Lloyd *et al.* 1995b). Values of R_d for the shoots and branches were similar. There was a significant reduction in values of α in the branches compared to the shoots, and in the canopy compared to the branches. Again it is likely that this is the result of more mutual shading of needles in branches compared to shoots and in the canopy compared to branches.

Night-time respiration showed a significant ($p < 0.05$) increase between branches and shoots and between the canopy and branches, reflecting the increased respiration "overheads" in an increasing amount of supporting biomass. The temperature sensitivity of respiration is higher in the shoots and branches than for the canopy as a whole, since for the canopy an increased proportion of autotrophic respiration takes place in the woody stem, where it is less well coupled to short-term changes in air temperature, and consequently apparent temperature sensitivity is reduced. The difference is not, however, statistically significant ($p > 0.05$).

Comparison of the parameters of the conductance models is limited because it was not possible to estimate either temperature or humidity response parameters for the shoots. Values of the maximum conductance, g_{wmax}, varied little between the shoot, branch and canopy, but the residual conductance, g_0, decreased with increasing organisational scale. A possible explanation for this reduction in g_0 might be that branches and the canopy consist of an increasing proportion of older needles, whose stomata have become blocked with wax plugs (Jeffree *et al.* 1971), however the lack of a similar reduction in g_{wmax} does not support this. The canopy as a whole was more sensitive to changes in humidity deficit, PFD and temperature than were the branches. This is probably a consequence of the fact that the wide tree spacing ensured good coupling between the canopy and the atmosphere (Jarvis & McNaughton 1986), but the lack of turbulent penetration to the foliage in the densely packed tree crowns meant that the branches were effectively de-coupled from the atmosphere.

Conclusion

The order of magnitude agreement between parameter values found at the three organisational scales suggests that at least in the case of aerodynamically rough,

largely mono-specific, forest canopies, physiological parameters may be estimated from eddy covariance flux measurements with a reasonable degree of accuracy. The small differences between V_{max} and J_{max} at the different scales also suggests that the overall spatial organisation of photosynthetic capacity is more or less optimised for carbon uptake at each of the scales, and contrasts strongly with the three fold reduction of photosynthetic capacity found for tropical rainforests. It is interesting to note that despite the very different spatial organisations of boreal and tropical forests, there is a remarkable similarity between the values of V_{max} and J_{max} estimated for the whole canopy.

SUMMARY

To gain insight into the function of photosynthesis, respiration and evapotranspiration as processes operating within a globally important ecosystem, gas exchange measurements were made on mature black spruce (*Picea mariana*) trees at three organisational scales: individual shoots, whole branches, and a forest canopy. Empirical and biochemical models were fitted to these data, and physiological parameters were extracted. Pronounced seasonal variation was found in the estimated model parameters at all three organisational scales, highlighting the need for making physiological measurements throughout the year. Good agreement found between parameter values estimated for the different organisational scales suggests that physiological parameters could be estimated from eddy covariance flux measurements. The small differences between photosynthetic parameters estimated at the different scales also suggests that the overall spatial organisation of photosynthetic capacity is nearly optimised for carbon uptake at each of the scales.

Chapter Six – Estimating the Net Biotic Flux of Carbon from a Boreal Forest Ecosystem

This chapter considers three different means of estimating the net biotic flux (NBF) of carbon from a boreal forest ecosystem. NBF is defined as the net flux resulting from the various biotic fluxes, such as photosynthesis, autotrophic respiration and heterotrophic respiration, that occur within an ecosystem. NBF is distinct from the net ecosystem exchange (NEE) measured by the eddy covariance technique in that NEE is the NBF moderated by the abiotic processes, such as turbulence and advection, which control the transport of carbon between the ecosystem and the atmosphere.

METHODS

Component summation estimate of NBF

The component summation estimate of the net biotic flux (NBF) of CO_2 (SUMMATION) was arrived at from the separate measurements of CO_2 fluxes to/from the tree foliage, the tree woody biomass, the moss layer and the soil. Foliage photosynthesis, P_f, and respiration, R_f, were measured on four whole branches, using a closed gas exchange "branch bag" technique. The fluxes were then "scaled" to provide an estimate for the whole canopy by multiplying the instantaneous average flux by the leaf area index of the canopy (Chapter 4). Above-ground woody tissue respiration, R_w, was derived from measurements made on the trunks of 16 trees using an open gas exchange system (details in Lavigne & Ryan 1997). Moss gross photosynthesis, P_m, was measured *in situ* and under laboratory conditions using open and closed gas exchange systems (Dr. L.B. Flanagan, Carlton University, Ottawa, ONT.). Soil gas exchange, R_h, was measured with open system gas exchange chambers at eight locations, positioned to provide a stratified sample of spatial heterogeneity (Chapter 3). Gaps in the branch bag data caused by instrument failure were filled using multiple linear regression (Chapter 4), producing a continuous dataset for the growing season. Winter-time CO_2 fluxes to/from the foliage were considered to be zero (Chapter 4). Winter-time soil CO_2 flux was estimated from the observed relationship between soil CO_2 efflux and 10 cm depth soil temperature

(Chapter 3), and soil temperature data which were continuous from November 1995 until December 1996.

MAESTRA estimate of NBF

MAESTRA is a forest canopy radiation absorption, photosynthesis and respiration model (developed by Dr. B. Medlyn, University of Edinburgh, from the MAESTRO model of Wang & Jarvis 1990) in which the forest canopy is represented as an array of distinct tree crowns, whose positions, dimensions and physiological and structural characteristics are specified explicitly. The model uses the Farquhar, von Caemmerer and Berry (1980) formulation of photosynthesis and a Jarvis-type "response surface" model of stomatal conductance (Jarvis 1976). Foliage and woody biomass respiration (growth and maintenance) are treated as exponential functions of biomass temperature. Full details of the parameter values used, their sources, and modifications made to the standard MAESTRA model are given in an Appendix. MAESTRA models the tree component of the ecosystem, therefore the output of the model was combined with the chamber-based estimates of moss and soil gas exchange (above) to give an estimate of NBF.

BIG-LEAF estimate of NBF

The Eddy covariance data were screened to remove any data when turbulence was insufficient for the eddy covariance technique to be considered reliable (i.e. when the friction velocity, U_*, was less than 0.35 m s^{-1}, J. Massheder, University of Edinburgh) Daytime canopy CO_2 exchange was derived from this NEE data by subtracting the flux from the soil measured with chambers, as described above. The photosynthesis model proposed by Farquhar *et al.* (1980) and modified by subsequent authors (Harley *et al.* 1992; Lewis *et al.* 1994), was then fitted to these data, and estimates of the parameters V_{max}, J_{max}, θ, H_v, H_d, R_d and α were obtained. An Arrhenius activation energy function, driven by 5 cm soil temperature, was fitted to the night-time data, and the parameters E_0 and R_0 were estimated. Details of these models and of the additional model parameters used are given in Chapter 4. Thus the BIG-LEAF model of NBF consisted of a Farquhar-type photosynthesis sub-model during the daytime, and an activation energy respiration sub-model at night. The NBF for the entire year was estimated by driving these models with the

meteorological data obtained at the site. Fluxes to/from the foliage were considered to be zero through the deep winter (Chapter 4), so that during this time the BIG-LEAF model consisted simply of the respiration model.

Sensitivity of eddy covariance measurements to method of filling in gaps

Eddy covariance data obtained during low turbulence conditions (i.e. when $U_* < 0.35$ m s^{-1}, J. Massheder, University of Edinburgh) were replaced with estimates of NBF obtained by the three approaches, SUMMATION, MAESTRA and BIG-LEAF, described above. The BIG-LEAF approach is equivalent to the commonly used strategy of replacing low turbulence data with data estimated from a relationship between NEE and soil temperature, obtained during conditions of high turbulence (e.g. Jarvis *et al.* 1997).

In addition, the NBF for the winter period before eddy covariance measurements were started was estimated by three methods, (1) by assuming that the NBF at the start and end of the measurement period (found to be approximately the same) was maintained at a constant level throughout the winter, (the ENDS approach), (2) by applying the same BIG-LEAF respiration sub-model used for estimating night-time NBF to soil temperatures measured through the winter, and (3) from the relationship between the chamber based soil CO_2 efflux measurements and soil temperatures measured through the winter as in the SUMMATION method.

RESULTS

Comparison of NBF with eddy covariance data

Figure 6.1 shows a comparison between the three estimates of **half-hourly** NBF and direct measurement of NEE (eddy covariance plus the storage flux, EC + ΔS) for daytime and night-time periods. Table 6.1 summarises the results. The SUMMATION approach tended to overestimate the magnitude of the NBF compared to the eddy covariance estimate, predicting higher fluxes into the ecosystem during the day (a), and out of the ecosystem during the night (b). The MAESTRA approach underestimated measured NBF when there was a net uptake by the ecosystem during the day (c), but overestimated the net efflux at night (d). The BIG-LEAF approach gave a bias-free prediction of the NBF compared to the eddy covariance data during the day (e), but tended to underestimate measured NBF at times of high night-time efflux (f). At night, when direct measurement of NBF by eddy covariance indicated no net exchange between the ecosystem and the atmosphere, both the SUMMATION and the MAESTRA approach tended to predict net effluxes of CO_2 from the ecosystem (b) & (d). These differences between the half-hourly estimates of NBF and NEE were carried through into the estimates of total NBF for the day and the night-time periods (Figure 6.2).

Table 6.1. Correlation between three estimates of net biotic flux and measured net ecosystem exchange measured at half-hourly intervals at the BOREAS SSA OBS site for the period day 91 to day 332 of 1996.

Estimation method	Day (n = 5595) r^2	Night (n = 3904) r^2
SUMMATION	0.68	0.12
MAESTRA	0.64	0.06
BIG-LEAF	0.64	0.39

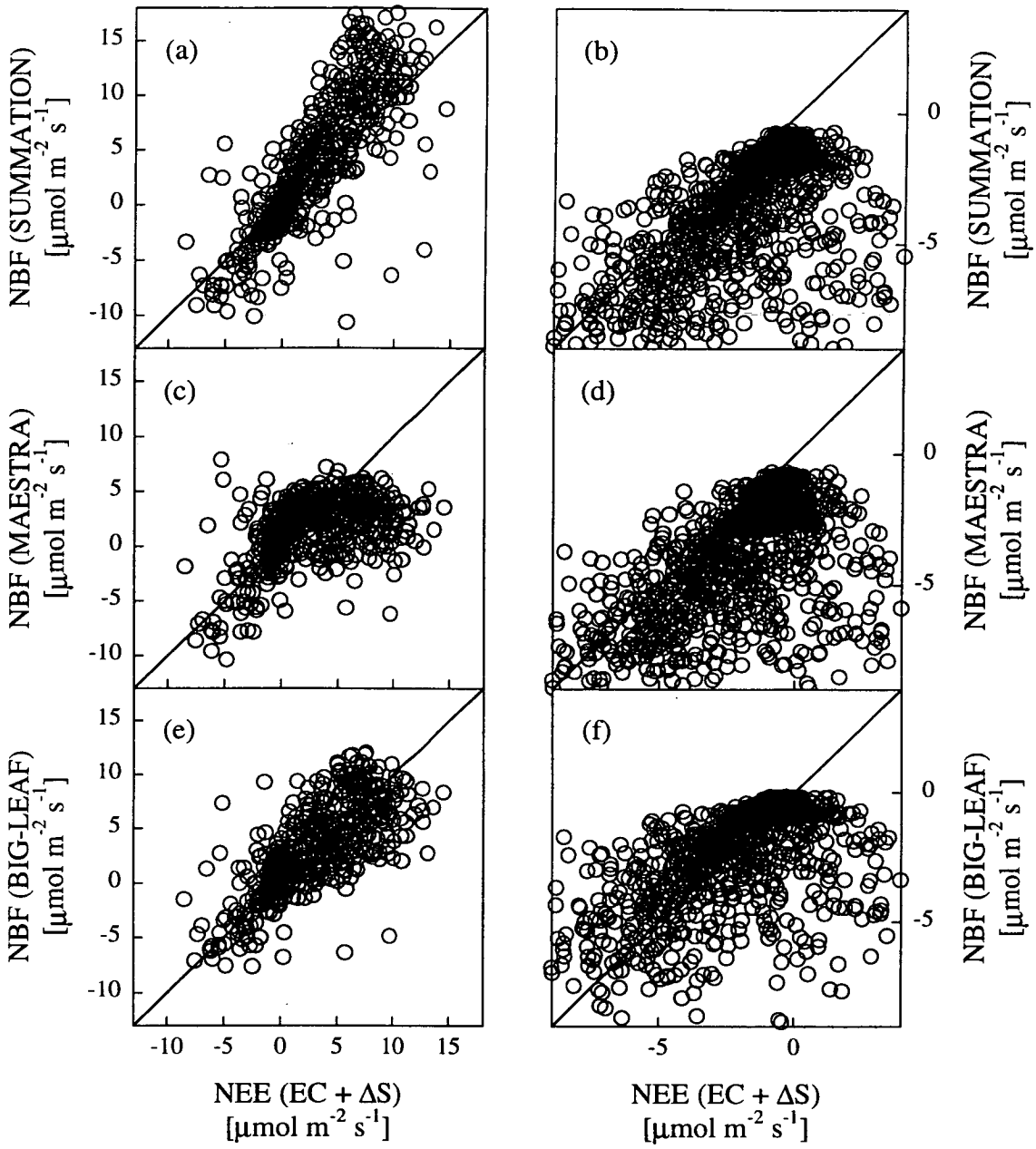

Figure 6.1. Comparison between estimated net biotic flux (NBF) and measured net ecosystem exchange (NEE) measured at **half-hourly** intervals at the BOREAS SSA OBS site for the period day 91 to day 332 of 1996. Graphs on the left hand side (a, c & e) are for daytime periods, those on the right hand side (b, d & f) for night-time periods. For clarity only every tenth point is plotted on the daytime graphs, every third point on the night-time graphs. Measured NEE data (EC + ΔS) are the eddy covariance measurements of net ecosystem exchange plus the "storage" fluxes as described in the text. Fluxes are positive into the ecosystem. Fluxes were estimated by (a) & (b) a SUMMATION of the component fluxes, (c) & (d) a detailed canopy model MAESTRA, and (e) & (f) an aggregated BIG-LEAF model.

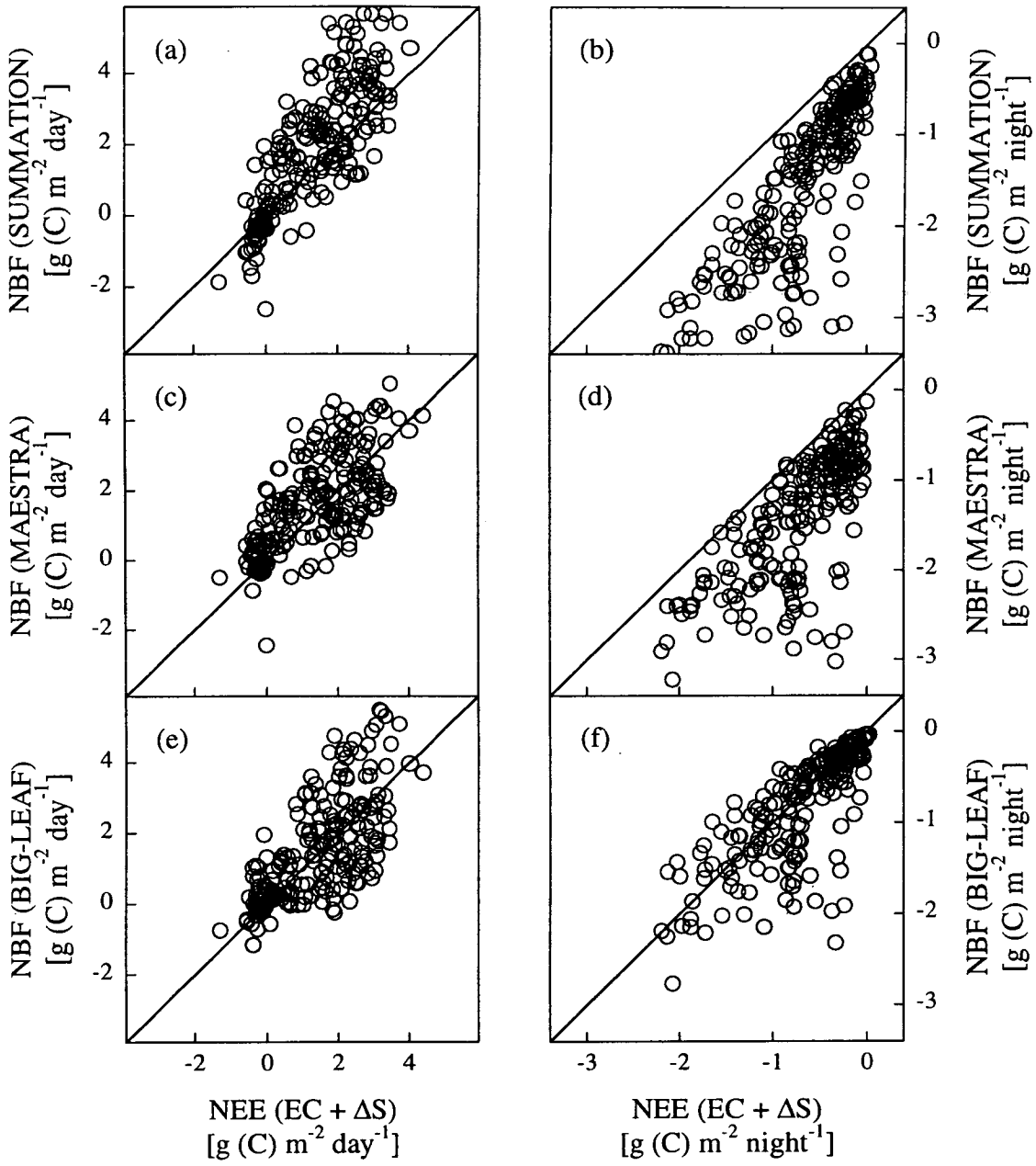

Figure 6.2. Comparison between estimated **daily** net biotic flux (NBF) and measured **daily** net ecosystem exchange (NEE) for daytime (left hand side) and night-time (right hand side) periods at the BOREAS SSA OBS site for the period day 91 to day 332 of 1996. Measured NEE data (EC + ΔS) are the eddy covariance measurements of net ecosystem exchange plus the "storage" fluxes as described in the text. Fluxes are positive into the ecosystem. Fluxes were estimated by (a) & (b) a SUMMATION of the component fluxes, (c) & (d) a detailed canopy model MAESTRA, and (e) & (f) an aggregated BIG-LEAF model.

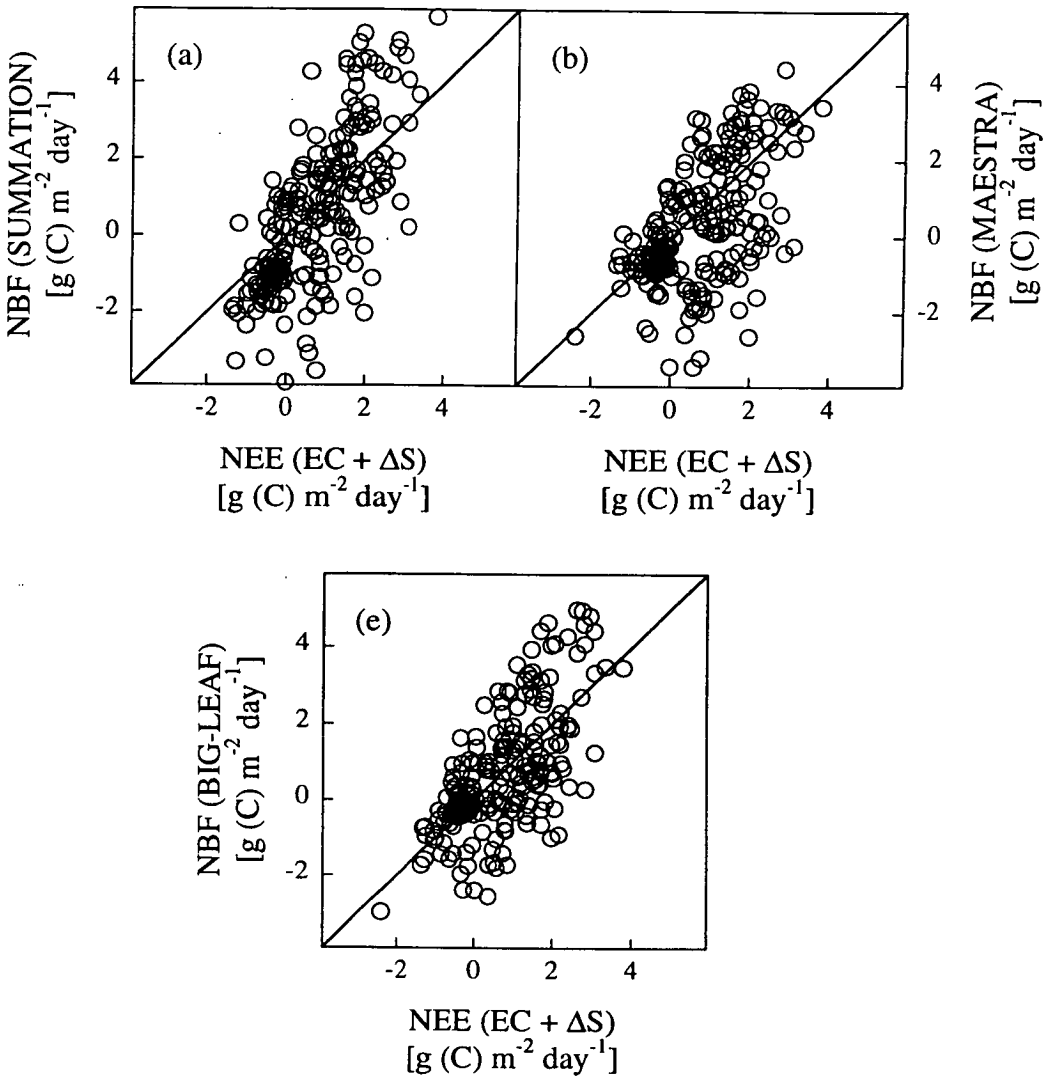

Figure 6.3. Comparison between estimated **24-hour** net biotic flux (NBF) and measured **24-hour** net ecosystem exchange (NEE) for the BOREAS SSA OBS site for the period day 91 to day 332 of 1996. Measured NEE data (EC + ΔS) are the eddy covariance measurements of net ecosystem exchange plus the "storage" fluxes as described in the text. Fluxes are positive into the ecosystem. Fluxes were estimated by (a) a SUMMATION of the component fluxes, (b) a detailed canopy model MAESTRA and (c) an aggregated BIG-LEAF model.

Figure 6.3 shows the same data, combined to give estimates of the **24-hour** NBF (i.e. daytime plus night-time). Again, on a daily basis there was a trend for the magnitude of the SUMMATION estimate of daily total NBF to be larger than that measured, regardless of whether the ecosystem was a net source or a net sink for CO_2 on that day. Similar, but less pronounced trends were also apparent for the 24-hour NBF estimated by the MAESTRA and the BIG-LEAF approaches.

Table 6.2 presents the total NBF for the period day 91 to day 332 of 1996, by direct measurement and estimated by the three approaches. All approaches agree that over this period the ecosystem was a net sink for CO_2, but the estimates vary considerably. All three estimation approaches produced lower values for the NBF over this period than did eddy covariance.

Table 6.2. Comparison of estimated carbon balance for the BOREAS SSA OBS site for the period day 91 to day 332 of 1996. Data were estimated by eddy covariance with no correction for periods of low turbulence (EC + ΔS), SUMMATION of the component fluxes, a detailed canopy model MAESTRA and an aggregated BIG-LEAF model.

Estimation method	Total [Mg (C) ha^{-1} yr^{-1}]	Day	Night
EC + ΔS	1.61	3.22	-1.61
SUMMATION	1.03	4.76	-3.73
MAESTRA	0.73	3.98	-3.25
BIG-LEAF	1.46	3.39	-1.93

Sensitivity of eddy covariance measurements of NEE to method of filling in gaps

Figure 6.4 and Table 6.3 illustrate the sensitivity of the total measured NEE for the period day 91 to day 332 of 1996 to the method of correcting the eddy covariance plus storage flux data for periods of low turbulence. Correcting with the BIG-LEAF model imposes the smallest change to the estimated total NBF from the direct measurement, correcting with MAESTRA reduces the estimated net ecosystem uptake to less than one third of the directly measured uptake, and correcting with the SUMMATION estimate changes the estimated net ecosystem uptake to negative from positive.

Table 6.3. Comparison of estimated carbon balance for the BOREAS SSA OBS site for the period day 91 to day 332 of 1996. Eddy covariance plus storage data were replaced with values "corrected" by one of the three approaches when $U_* < 0.35$ m s^{-1}. The sources of the "corrected" data were a SUMMATION of the component fluxes, a detailed canopy model MAESTRA and an aggregated BIG-LEAF model.

Correction method	Total [Mg (C) ha^{-1} yr^{-1}]	Day	Night
No correction	1.61	3.22	-1.61
SUMMATION	-0.24	3.11	-3.36
MAESTRA	0.50	3.54	-3.04
BIG-LEAF	1.29	3.31	-2.02

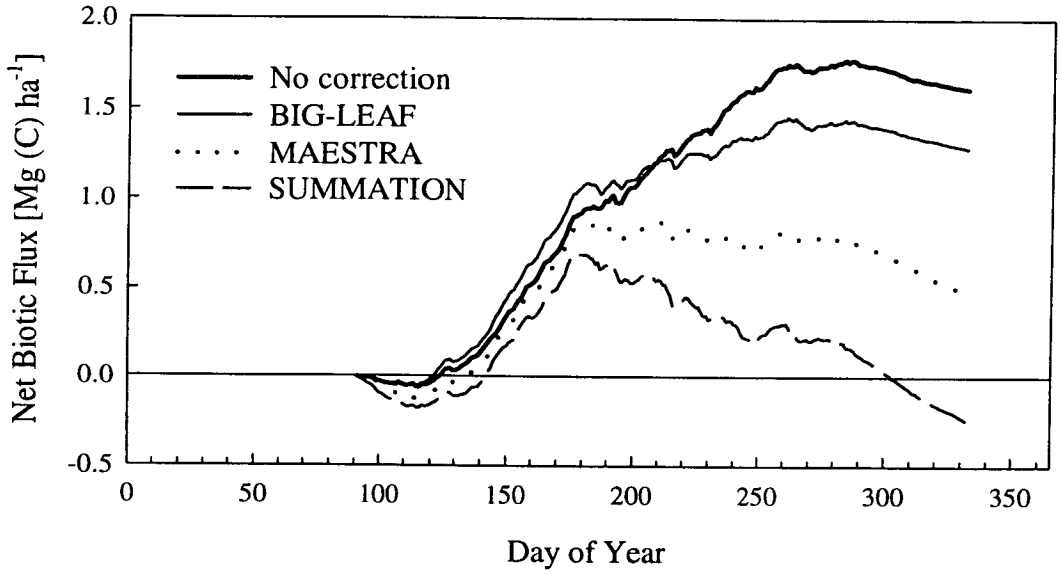

Figure 6.4. Cumulative net biotic flux (NBF) for the BOREAS SSA OBS site for the period day 91 to day 332 of 1996. Direct measurements were made by eddy covariance corrected for the storage flux (No correction). Low turbulence data ($U_* < 0.35$ m s^{-1}) were replaced with data from a SUMMATION of the component fluxes, a detailed canopy model MAESTRA and an aggregated BIG-LEAF model.

Figure 6.5 and Table 6.4 illustrate the sensitivity of the estimated annual total NBF to the method of filling in the winter-time gap (day 333 1995 to day 90 1996) in the eddy covariance dataset. Filling the gap with the average flux obtained under turbulent conditions during the first and last ten days of the measurement period (ENDS) resulted in a reduction in the estimated annual carbon uptake below that measured during the measurement period (day 91 to day 332 1996) of over one quarter. Using the BIG-LEAF model to fill the winter-time gap reduced the estimated carbon uptake by over one third and using the chamber-based SUMMATION estimate of winter-time soil CO_2 efflux reduced the estimated annual net ecosystem uptake to less than one fifth of the directly measured uptake during the measurement period.

Table 6.4. Comparison of estimated annual carbon balance for the BOREAS SSA OBS site for the year ending day 332 of 1996. Measurements from day 91 to day 332 were made by eddy covariance corrected for the storage flux and uncorrected for low turbulence periods. Fluxes before day 91 were estimated by one of three methods, a SUMMATION of the modelled component fluxes, an extrapolation of the first and last ten days of the measurement period (ENDS) and an aggregated BIG-LEAF model.

Correction method	Total [Mg (C) ha^{-1} yr^{-1}]
No correction	1.61
SUMMATION	0.33
ENDS	1.19
BIG-LEAF	1.03

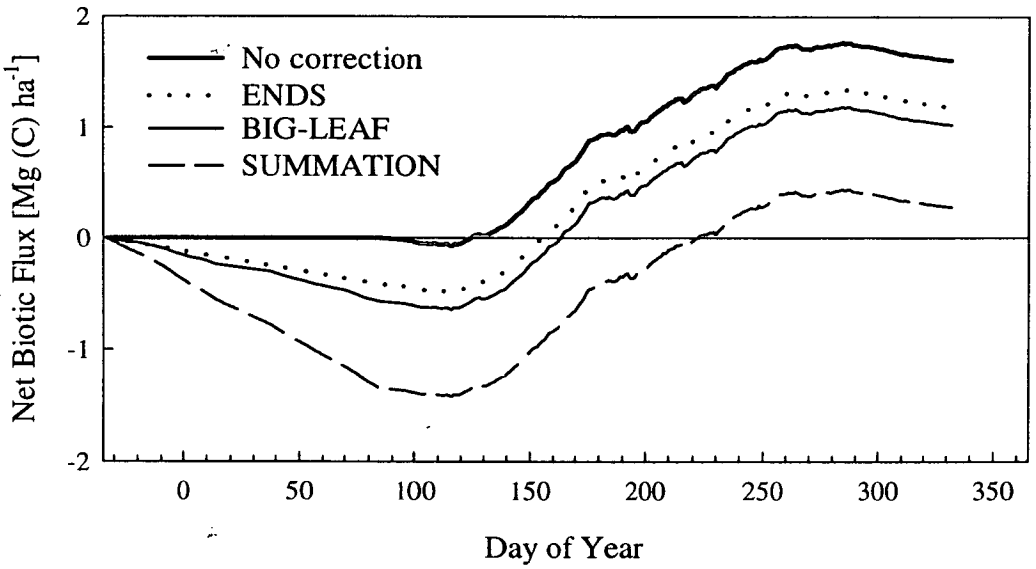

Figure 6.5. Estimated cumulative net biotic flux (NBF) for the BOREAS SSA OBS site for the year ending day 332 of 1996. Measurements from day 91 to day 332 were made by eddy covariance corrected for the storage flux and uncorrected for low turbulence periods. Fluxes before day 91 were estimated by one of three methods, a SUMMATION of the modelled component fluxes, an extrapolation of the first and last ten days of the measurement period (ENDS) and an aggregated BIG-LEAF model. The cumulative NBF assuming no flux before the measurement period is also shown (No correction).

DISCUSSION

Comparison of model estimates with data

Considering that they were obtained totally independently of the eddy covariance data, both the chamber-based component flux SUMMATION estimate and the detailed radiation absorption, photosynthesis and respiration model (MAESTRA) based estimate of NBF agreed well with the direct measurements on a half-hourly

and a 24-hour basis. This is especially true given that MAESTRA was parameterised with photosynthetic parameters from the black spruce trees only, and no account was made of the moss photosynthesis and respiration. The underestimation by the MAESTRA model of the daytime fluxes during periods of high uptake was similar to, but more pronounced than, that observed in a comparison of the output from another detailed canopy model (CANOAK) with eddy covariance data for a temperate deciduous forest (Baldocchi and Harley 1995) and the output of a big-leaf model with eddy covariance data for a tropical forest (Lloyd *et al.* 1995b).

The tendencies of the chamber-based SUMMATION method to overestimate the magnitude of the net ecosystem flux both during the day and the night need to be considered separately. The overestimation of the daytime photosynthetic uptake of the ecosystem is most likely the consequence of the simplistic scheme used to scale the measurements of photosynthesis made on four individual branches to the whole canopy. The method used was to multiply the photosynthetic rate, averaged over the branches, by the total leaf area for the canopy, i.e. assuming that the behaviour of each branch was representative of an equal portion of the canopy. The validity of this assumption is certainly questionable and it is reasonable to suppose that the branches lower in the canopy, where the photosynthetic rate was lower, were in fact representative of a larger fraction of the canopy than the branches near the top of the canopy and should have been weighted accordingly. Confounding this, all four branches measured were located on the south-facing side of the trees and in the highly clumped canopy of the OBS site it is probable that the photosynthetic uptake of north-facing branches was significantly less.

The tendency of both the chamber-based SUMMATION method and MAESTRA to overestimate the night-time efflux of carbon from the ecosystem is, in part, because the data shown in Figure 6.1 (right hand side) represent all the eddy covariance measurements made, including those for which turbulence was considered insufficient ($U_* < 0.35$ m s^{-1}), so therefore many of the measured data points close to zero are from times when it is likely that NEE measured by eddy covariance is an underestimation of NBF. Thus the very low r^2 values found in this comparison are, at least in part, a result of the large scatter in the eddy covariance data. The BIG-LEAF

model, being derived entirely from the eddy covariance data, would be expected to produce fluxes unbiased with respect to the measured fluxes.

Low U_* corrections

Corrections for periods of low turbulence were an important component of the final estimate of the annual net carbon balance for the ecosystem, constituting more than half of the final dataset, and almost three quarters of the night-time measurements (Table 6.6). The choice of method used to make this correction, and indeed, whether to make any correction at all, is therefore of considerable importance.

Table 6.6. Frequency of "good" ($U_* \geq 0.35$ m s^{-1}) and "bad" ($U_* < 0.35$ m s^{-1}) eddy covariance data for the BOREAS SSA OBS site for the period day 91 to day 332 of 1996.

	All	Day	Night
$U_* \geq 0.35$ m s^{-1}	5711	4575	1136
$U_* < 0.35$ m s^{-1}	5860	2631	3229

The BIG-LEAF estimate of NBF, derived from measured data, appeared the best means of providing an unbiased means of interpolating measured data to fill in short gaps in a long term dataset, although this is only true when these gaps are randomly occurring, e.g. the result of instrument failure etc. Data gaps resulting from low turbulence are, however, not random, but occur systematically with respect to environmental conditions. For example, during day-time at the OBS site there was a highly significant ($p < 0.0001$) positive correlation between U_* and incoming photon flux density (Figure 6.6(a)). Since there is a strong mechanistic relationship between incoming PFD and photosynthetic uptake, the observed reduction in the net ecosystem exchange in low U_* conditions during the daytime must be, at least in part, the result of PFD reduced NBF at these times. Despite this clear and systematic bias towards higher flux values in the high turbulence data from which the BIG-LEAF model was derived, the correlation between high NEE and highly turbulent conditions appeared to be accounted for in the model's PFD response function, and model estimates of daytime NBF showed a similar "response" to U_* as do eddy covariance data corrected for the storage flux (Figure 6.6(b)).

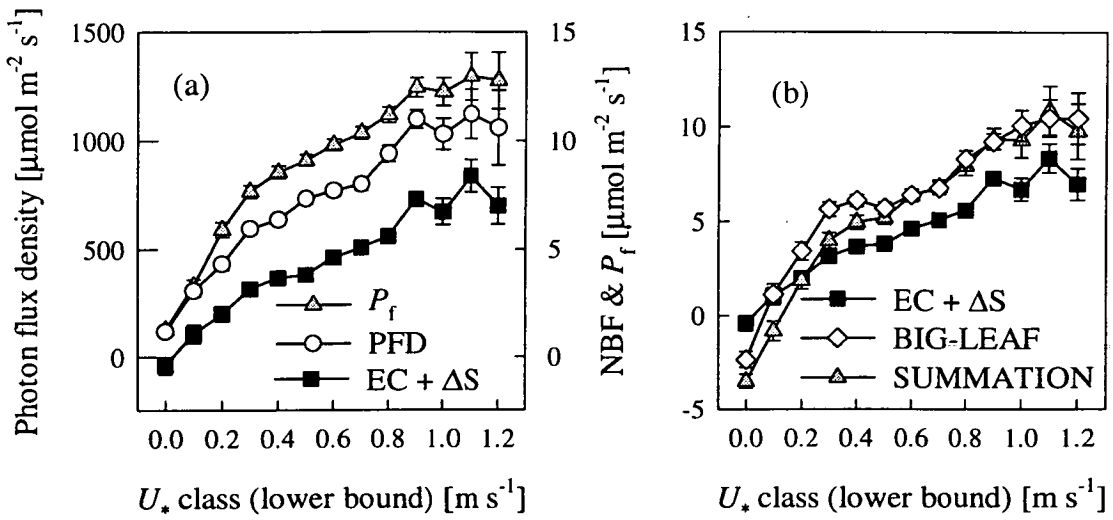

Figure 6.6. (a) Correlation between friction velocity (U_*) and incoming photon flux density (PFD), measured **daytime** NBF (i.e. EC + ΔS) and branch gross photosynthesis (P_f). (b) Correlation between friction velocity (U_*) and measured (EC + ΔS) and modelled daytime NBF (SUMMATION & BIGLEAF). Data are for the period day 150 to day 250 1996 at the BOREAS SSA OBS site. Data were binned by U_*, and the means (± 95 % confidence limits) plotted.

During the night-time period, a there is a similar reduction in the measured NBF (i.e. eddy covariance plus the storage flux) under conditions of low turbulence ($U_* < 0.35$ m s^{-1}) (Figure 6.7(a)). It is common to make the assumption that the main environmental variable controlling CO_2 efflux at night is temperature, through the effect of temperature on the rate of respiration in the soil and trees. Since there is no clear positive correlation between U_* and temperature (Figure 6.7(a)), it is commonly supposed that the observed reduction in the net ecosystem exchange under low U_* conditions at night is purely a consequence of a reduction in turbulent transport of CO_2 out of the ecosystem, and that the inability of the storage flux correction to provide a measurement of net ecosystem exchange that is independent of turbulence points to an advective loss of CO_2 from the system. (e.g. Goulden *et al.* 1996a; Grace *et al.* 1996). However, direct measurements of the component fluxes of the net ecosystem flux at night-time, reveal that there is also a definite reduction in the efflux of CO_2 from the canopy and from the soil at these times (Figure 6.7(a)). Thus at least a part of the reduction in the NBF, observed as eddy covariance plus the storage flux under low U_* conditions is the consequence of a reduction in the actual NBF at these times, rather than a measurement artefact.

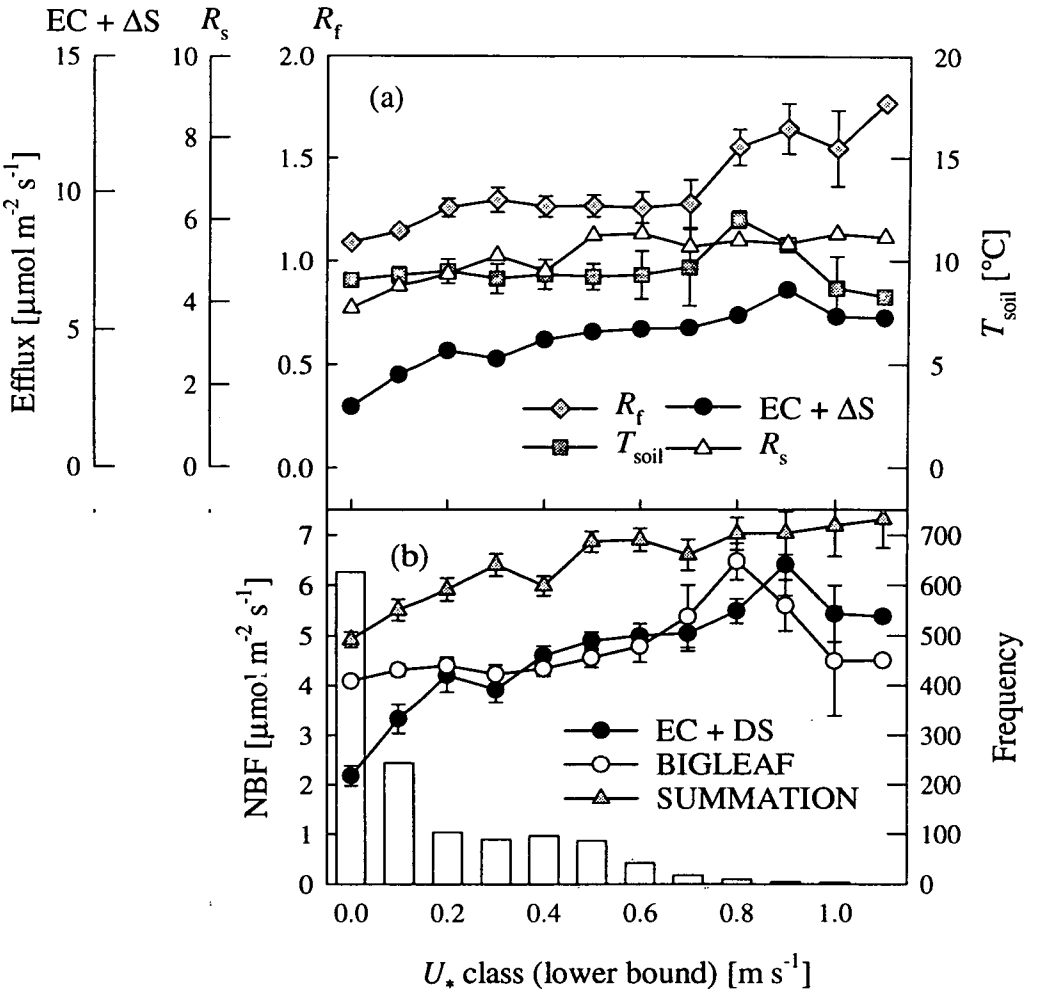

Figure 6.7. (a) Correlation between friction velocity (U_*) and measured night-time NBF (i.e. EC + ΔS), **night-time** foliage respiration (R_f), night-time soil CO_2 efflux (R_s), and night-time 10 cm depth soil temperature (T_{soil}) (b) Correlation between friction velocity (U_*) and measured (EC + ΔS) and modelled (BIGLEAF & SUMMATION) night-time NBF, and frequency of each U_* class. Data are for the period day 150 to day 250 1996 for the BOREAS SSA OBS site. Data were binned by U_*, and the means (± 95 % confidence limits) plotted.

The question arises as to why the soil and foliage respiration rates should be positively correlated with U_*. In the case of soil respiration, a reduced rate of soil CO_2 efflux under conditions of low turbulence has been found at this site (Chapter 3) and observations elsewhere support the hypothesis that there is a mechanistic relationship between turbulence-induced pressure fluctuations at the soil surface and the exchange of CO_2 between air within the soil volume and the atmosphere (Kimball & Lemon 1971; Baldocchi & Meyers 1991). Thus it is not the actual generation of CO_2 by respiration in the soil that is affected by turbulence, but rather the process by which CO_2 is transported between the soil and the atmosphere, i.e. the

coupling between soil respiration and soil CO_2 efflux is affected by turbulence. We might expect, therefore, that if we were able to extend our calculation of the storage flux to include CO_2 stored in the soil volume, addition of the storage flux to the eddy covariance measure of net ecosystem exchange would indeed provide a net biotic flux independent of turbulence.

In the case of foliage, however, the correlation between respiration rate measured inside branch enclosures and atmospheric turbulence is neither direct nor causal. Figure 6.6 illustrates the strong correlation that exists during the daytime between incident PFD and U_*, and daytime photosynthetic uptake by the foliage clearly increases as incident PFD increases (until light saturation occurs). At this site there was also a highly significant ($p < 0.0001$) positive correlation between mean night-time U_* and the mean daytime U_* on the preceding day, and a significant ($p < 0.05$) positive correlation between the mean night-time foliage respiration rate (measured on whole branches) and the total photosynthetic uptake by the foliage on the previous day (also measured on whole branches). Thus it follows that there will be a tendency for nights when atmospheric turbulence is lowest, to be nights when foliage respiration is also lowest (Figure 6.7).

From these considerations, it is clear that, at this site, there are physical and biological variables that contribute to a reduced NBF under low U_* conditions. Because soil temperature is not correlated with U_* (Figure 6.7(a)), a big-leaf model that is driven by soil temperature will not predict this low turbulence reduction in NBF, and is likely to overestimate the efflux of CO_2 from the ecosystem at these times (Figure 6.7(b)). Since the majority of night-time measurements of net ecosystem exchange are made under low turbulence conditions (Table 6.6, Figure 6.7(b)), replacing directly measured data with estimates predicted by a big-leaf model leads to a substantial increase in estimated night-time carbon loss (Figure 6.4), and the final estimate of the annual net carbon balance of the ecosystem is underestimated. Furthermore, if it is the case that some of the "missing" CO_2 efflux is not being "lost" from the system by advection, but is rather remaining within the soil volume, "trapped" by the lack of turbulence, there is a strong likelihood of double counting, i.e. when turbulence increases to a level such that eddy covariance

data are considered reliable, the "trapped" CO_2 will be released from the soil volume and will be measured as an efflux, even if displaced in time from when it was produced.

It is by no means clear, therefore, that eddy covariance data, once corrected with the storage flux, should be further "corrected" to exclude periods of low turbulence, since the low fluxes measured in these conditions are probably the result of temporary phenomena, for which subsequent fluxes adequately compensate. Nevertheless, eddy covariance actually measures turbulent transport, and measures net ecosystem exchange only on the condition that turbulent transport dominates over diffusive transport. The technique cannot measure net ecosystem exchange when this assumption is violated. Therefore two things are required. Firstly, more consideration must be given to the turbulence cut-off point, i.e. the point below which turbulent transport is not the dominant means of exchange between the ecosystem and the atmosphere. This point is certainly below the value of 0.35 m s^{-1} that has been used as the cut-off point for measurements made at this site (e.g. Jarvis *et al.* 1997). Secondly, a source of information other than a big-leaf model based on the flux data themselves is needed for filling in these systematic gaps in the data. Chamber measurements, because they are independent of eddy covariance measurements, should provide a more suitable unbiased dataset.

In practice, however, at least at this site, the chamber-based flux measurements do not seem to be unbiased with respect to the eddy covariance measurements (Figures 6.1, 6.2 & 6.3), and therefore direct use of these data in replacing low turbulence data ($U_* < 0.35$ m s^{-1}) also substantially affects the estimated net ecosystem carbon balance (Figure 6.4, see also Figure 6.7). The most likely reason for the discrepancy between the chamber summation and eddy covariance estimates of NBF is in the "scaling-up" scheme that is used to estimate the total ecosystem fluxes from individual chamber measurements. Thus the position of soil CO_2 efflux chambers, necessarily restricted in spatial extent, may not actually be representative of the whole area that forms the "footprint" of eddy covariance measurements. Likewise, an error in the estimation of the total leaf area of the canopy will result in errors when scaling-up foliage fluxes. A reasonable solution to this problem might be to

"calibrate" the chamber summation estimates with good eddy covariance data ($U_* >$ 0.35 m s^{-1}), separately for the day and night periods, by simply dividing the chamber-based SUMMATION estimate by the slope of the relationship between the SUMMATION estimate of NBF and such eddy covariance measurements of NBF. These calibrated data could then be used to fill in any systematically occurring gaps in the data.

Use of eddy covariance in long term studies of ecosystem function

In this study, the estimated net carbon balance for the BOREAS SSA OBS site for 366 days ending on day 332 of 1996 measured by eddy covariance ranged from a net uptake of 1.19 Mg (C) ha^{-1} yr^{-1} using the data uncorrected for low turbulence or deep winter periods, to a net loss of 1.15 Mg (C) ha^{-1} yr^{-1} using the chamber measurements directly to fill in low turbulence and deep winter gaps in the dataset. Using the BIG-LEAF approach to filling in periods of low turbulence and deep winter, the estimated annual net carbon uptake for 1996 was 0.70 Mg (C) ha^{-1} yr^{-1}. If, rather than using the chamber measurements directly, we use the "calibrated" chamber measurements to fill in low turbulence and deep winter gaps in the eddy covariance data, the site is estimated to be a net sink of 0.23 Mg (C) ha^{-1} yr^{-1}. Interestingly, "calibrating" the chamber measurements to the eddy covariance measurements makes very little difference to the chamber summation estimate of the net carbon balance for the site; a net uptake of 0.33 Mg (C) ha^{-1} yr^{-1} using the uncalibrated measurements and a net uptake of 0.39 Mg (C) ha^{-1} yr^{-1} using the calibrated measurements. These estimates compare to IPCC's current estimate of the annual net carbon balance of the region, based on process-based ecological models, as being a net carbon uptake of 0.5 - 1.0 Mg (C) ha^{-1} yr^{-1} (page 467, Houghton *et al.* 1995).

Combining the eddy covariance data from all the BOREAS sites for 1996, the estimated annual net carbon balance, weighted by the proportion of each ecosystem type investigated, is 0.5 - 0.8 Mg (C) ha^{-1} yr^{-1}, equivalent to a net sequestration by the global boreal forest of around 1 Gt (C) yr^{-1} (T.A. Black in prep). This is a significant proportion of the 1 to 3 Gt (C) yr^{-1} unaccounted for in the global carbon budget (e.g. Schimel 1995). Goulden *et al* (1996b), however, estimated 90% confidence limits for long term eddy covariance measurements at the Harvard forest

of ± 0.3 Mg (C) ha^{-1} yr^{-1} and Moncrieff *et al.* (1996) calculated that a reasonable estimate of the total uncertainty arising from both random and systematic errors in eddy covariance measurements at a tropical forest was 53 % of the flux. If these confidence limits are transferable to other eddy covariance measurement sites, it is doubtful that using eddy covariance *alone* can make significant improvements to current estimates of the annual net carbon balance at the regional or global scale.

What eddy covariance measurements can do, however, is to provide an insight into the functioning of particular ecosystems and into the controls on the inter-annual variability of their source/sink behaviour (e.g. Goulden *et al.* 1998). These ecosystems might then be considered as models of how whole biomes function. Chamber measurements, because they facilitate a deeper understanding of the mechanisms underlying ecosystem function, should be considered as an essential and integral part of ecosystem studies.

SUMMARY

Three estimates of the net biotic flux of carbon for a boreal black spruce forest ecosystem were obtained from: (a) a summation of chamber-based foliage and moss photosynthesis and foliage, woody biomass and soil respiration fluxes scaled to be representative of the whole ecosystem; (b) a canopy light interception and carbon flux model (MAESTRA) parameterised for the site from canopy structure and shoot gas exchange data; and (c) a "big-leaf" model fitted to selected eddy covariance data. These estimates were compared to "direct" measurements of net biotic flux obtained from eddy covariance corrected for the storage flux. The "big-leaf" estimate produced good agreement with measured net biotic flux during both the daytime and the night-time. During the daytime, the chamber-based methods tended to overestimate the net biotic flux and MAESTRA tended to underestimate the net biotic flux compared to the eddy covariance measurements. During the night-time, both the chamber-based methods and MAESTRA overestimated the magnitude of the loss of carbon from the ecosystem compared to the measured flux.

In 1996, the annual net carbon uptake for the ecosystem estimated from chamber summation was 0.33 Mg (C) ha^{-1} yr^{-1}, the corresponding estimate from the big-leaf

model was 0.86 Mg (C) ha^{-1} yr^{-1}. Once corrections had been made for gaps in the continuous record resulting from periods of low turbulence and the fact that no measurements were made during the deep winter, the eddy covariance "direct" measurement of the annual net carbon uptake for 1996 was estimated to be 0.70 Mg (C) ha^{-1} yr^{-1}. This estimate was found to be sensitive to the choice of data used for filling in gaps in the dataset, and it is by no means clear which of the estimates of net biotic flux is the most reliable during these periods. Indeed evidence is put forward suggesting that the widely used method of using a relationship between night-time ecosystem efflux and temperature obtained during turbulent periods to estimate the "true" ecosystem efflux during periods of low turbulence may be flawed. If this "correction" is not made, the net carbon uptake of the ecosystem for 1996 is 1.19 Mg (C) ha^{-1} yr^{-1}.

Chapter Seven – The Carbon Balance of a Boreal Forest Ecosystem

This chapter draws together the various component carbon fluxes measured in a boreal forest ecosystem into a complete description of the annual carbon budget for the ecosystem. Using the temperature sensitivities of the component fluxes, the temperature sensitivity of the net carbon balance of the ecosystem is modelled.

METHODS

Annual carbon balance for 1996

A full annual carbon budget for the BOREAS SSA OBS site was constructed, using component flux data described in previous chapters for the foliage gross photosynthesis (P_f) and foliage respiration (day and night) (R_f), woody biomass respiration (R_w), moss gross photosynthesis (P_m) and soil efflux (R_h). Foliage gross photosynthesis was estimated by adding day respiration to the measured net photosynthesis. Foliage day respiration was estimated from night-time respiration measurements adjusted for temperature and assuming that respiration in the light is 60 % of the rate in the dark at the same temperature. The other fluxes necessary to create a full description of carbon exchanges within the ecosystem were above-ground biomass increase (net of above-ground detritus) (Δ_{ag}) and above-ground detritus (D_{ag}) (data from Gower *et al.* 1997), root respiration (R_r) (data from Ryan *et al.* 1997), moss turnover (D_m) (data from the BOREAS northern study area, Harden *et al.* 1997), root detritus and fine root turnover (D_r) and below-ground biomass increase (net of root detritus & fine root turnover) (Δ_r) (data from Steele *et al.* 1997). Additionally, four further fluxes were postulated; moss respiration (R_m), carbon allocation to below-ground parts (A_r), root exudation (D_{ex}), and the change in soil organic matter pool (Δ_s). Although these fluxes were not measured directly, their magnitudes were determined by the following carbon mass-balance constraints (directly measured fluxes in bold),

$$\boldsymbol{P_f = R_f + R_w + D_{ag} + \Delta_{ag} + A_r} \quad (7.1)$$

$$A_r = \boldsymbol{R_r + D_r} + \Delta_r + D_{ex} \quad (7.2)$$

$$\boldsymbol{D_{ag} + D_m + D_r + D_{ex} = R_h} + \Delta_s \quad (7.3)$$

$$P_m = R_m + D_m \quad (7.4)$$

Sensitivity of 1996 annual carbon balance to temperature

The temperature sensitivity of the 1996 annual ecosystem carbon balance was investigated by considering the temperature sensitivities of both the SUMMATION and BIG-LEAF methods of estimating the carbon balance of the ecosystem (Chapter 6). For the SUMMATION method, the annual net carbon balance flux of each of the component fluxes was considered separately. The temperature sensitivity of total annual foliage carbon uptake (P_f) was determined by adjusting the air temperature in the meteorological data used to drive a temperature-sensitive model of daily gas exchange (Chapter 4). No adjustment was made to the humidity deficit of the air. Similarly, adjustments were made to the soil temperatures used to drive the soil efflux sub-model (R_h and R_r)(Chapter 3). Respiration of the above-ground woody biomass (R_w) was partitioned into growth and maintenance respiration, and variation in total annual maintenance respiration with temperature was calculated using the temperature sensitivity of instantaneous respiration rate measured on the tree stems (Lavigne & Ryan 1997). The total annual growth respiration was set proportional to the total annual above-ground production, i.e. $\Delta_{ag} + D_{ag}$. Root respiration was partitioned into growth and maintenance respiration in the same proportion as measured for above-ground biomass. Root maintenance respiration was described with the same temperature sensitivity as total soil respiration and growth respiration was set proportional to total annual root production, i.e. $\Delta_r + D_r + D_{ex}$. Above- and below-ground biomass increase (net of detritus), Δ_{ag} and Δ_r, and the flux of carbon from above- to below-ground parts, A_r, were determined by assuming that any carbon left over after the plant had met its respiratory requirements and detritus loss would be allocated in the same ratio as at present, i.e. 11:3 above-ground:below-ground. The photosynthesis, P_m, and respiration, R_m, of the moss was modelled as responding to temperature change in the same way as the tree foliage. All detritus fluxes were considered to be proportional to the pool size, thus in this model of the carbon balance over one year, the detritus fluxes were insensitive to temperature. For the BIG-LEAF method, the temperature sensitivity was investigated by adjusting by a constant amount all the temperatures in the meteorological data used to force the model.

RESULTS

Best estimate of annual carbon balance for 1996

Figure 7.1 shows a best estimate of the carbon budget of the ecosystem for the year ending day 332 of 1996. Two estimates of the annual net ecosystem exchange are given: (1) in bold type, the direct measurement by eddy covariance corrected for missing data, for the winter period and for periods of low turbulence with the BIG-LEAF model as described in Chapter 6; (2) in normal type, the difference between the total gross photosynthetic uptake and the total respiratory efflux, both of these fluxes having been estimated from chamber-based measurements, i.e. the SUMMATION method described in the Chapter 6. The estimated total loss of carbon from the ecosystem was 94 % of the estimated total gross photosynthetic uptake, making the residual net gain of carbon by the system small in comparison with either of these fluxes.

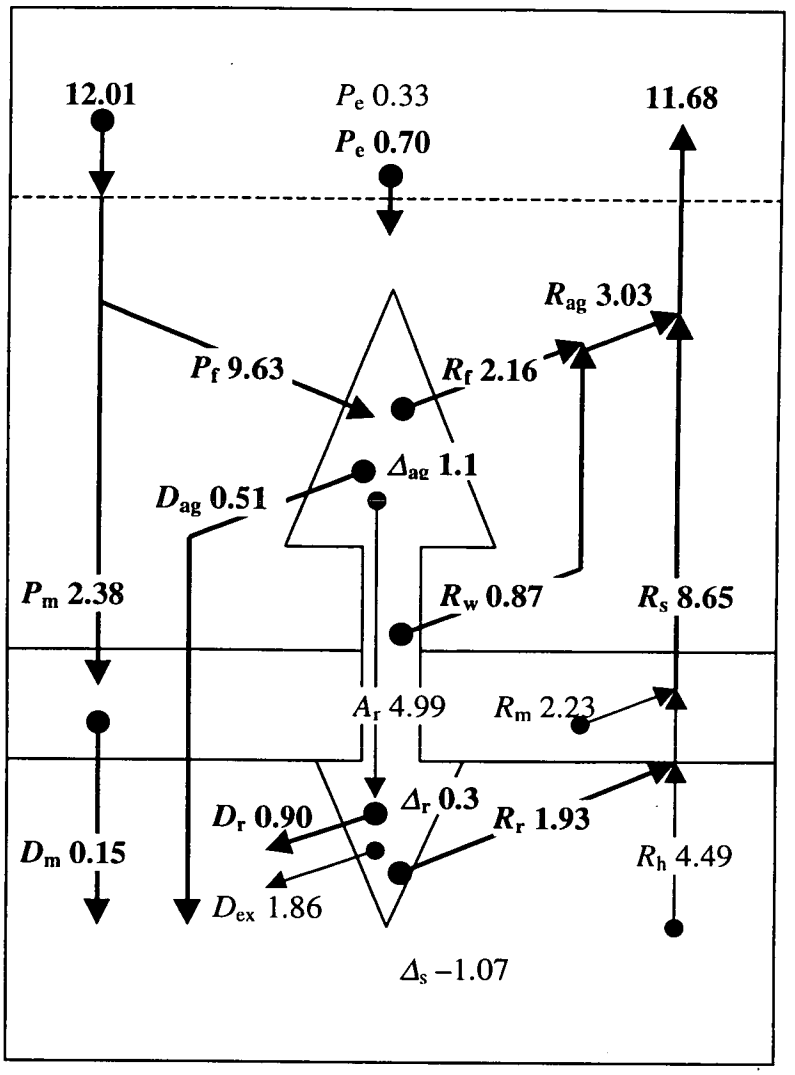

Figure 7.1. Estimated annual carbon balance for the BOREAS SSA OBS site for a period of 366 days, ending day 332 of 1996. Fluxes are in Mg (C) ha^{-1} yr^{-1}. Arrows and values in bold were measured directly, other fluxes were derived by mass balance. Two estimates of the net ecosystem exchange, P_e, are given, the direct measurement by eddy covariance (bold) and the difference between the total gross uptake and the total efflux (plain). The other fluxes are; P_f tree foliage gross photosynthesis (Chapter 4), P_m moss gross photosynthesis (Dr. L.B. Flanagan Carlton University, Ottawa, ONT.), R_f tree foliage total respiration (Chapter 4), R_w above-ground woody biomass respiration (Ryan *et al.* 1997; Lavigne & Ryan 1997), R_{ag} above-ground tree biomass respiration, R_m moss respiration, R_r root respiration (Ryan *et al.* 1997), R_h heterotrophic respiration in soil, R_s soil surface efflux (Chapter 3), D_{ag} above-ground detritus (Gower *et al.* 1997), D_m moss turnover (Harden *et al.* 1997), D_r root detritus & fine root turnover (Steele *et al.* 1997), D_{ex} root exudate, A_r carbon allocation to below-ground parts, Δ_{ag} above-ground NPP (Gower *et al.* 1997), Δ_r below-ground NPP (Steele *et al.* 1997), Δ_s change in soil organic matter pool.

Sensitivity of 1996 annual carbon balance to temperature

Figure 7.2 shows how the predicted annual net carbon balance of the ecosystem for 1996 varies with temperature. From the estimated temperature sensitivities of the individual fluxes considered in the chamber-based SUMMATION method, the ecosystem would have had a net carbon balance of zero in 1996 if the temperature had been around 0.4 °C warmer than it was. In contrast, the BIG-LEAF model suggested that temperatures would have needed to be 2.2 °C warmer in 1996 for the ecosystem to be neither a source nor a sink for carbon. Table 7.1 presents predicted values for the annual totals of the component carbon fluxes of the ecosystem for a selected number of temperatures.

Table 7.1. Predicted annual totals of the component carbon fluxes of the BOREAS SSA OBS ecosystem. All values are Mg (C) ha^{-1} yr^{-1}. Fluxes are as described in Figure 7.1, with the addition of total gross photosynthesis, P, above-ground woody biomass growth respiration, R_{wm}, above-ground woody biomass maintenance respiration, R_{wg}, root growth respiration, R_{rm}, root maintenance respiration, R_{rg}, and total ecosystem respiration, R. Detritus fluxes were independent of temperature (see text) $D_{ag} = 0.51$, $D_r = 0.90$, $D_{ex} = 1.86$ and $D_m = 0.15$. Arrows indicate how each flux is composed of its component fluxes.

	Temperature relative to 1996							
	-4 °C	-2 °C	-1 °C	0 °C	1 °C	2 °C	4 °C	6 °C
P_f	7.72	8.70	9.16	9.63	10.06	10.47	11.20	11.85
P_m	1.90	2.15	2.26	2.38	2.49	2.59	2.77	2.92
P ↵	9.62	10.85	11.43	12.01	12.55	13.06	13.97	14.77
R_f	1.51	1.81	1.98	2.16	2.35	2.55	3.00	3.54
R_{wm}	0.33	0.37	0.39	0.42	0.44	0.47	0.53	0.60
R_{wg}	0.32	0.40	0.43	0.45	0.47	0.47	0.45	0.36
R_w ↵	0.65	0.77	0.82	0.87	0.91	0.94	0.98	0.96
R_{ag} ↵	2.16	2.58	2.80	3.03	3.26	3.49	3.98	4.50
R_{rm}	0.60	0.74	0.83	0.93	1.05	1.20	1.58	2.12
R_{rg}	0.71	0.88	0.95	1.00	1.03	1.05	0.99	0.81
R_r ↵	1.30	1.62	1.78	1.93	2.08	2.25	2.57	2.93
R_m	1.76	2.00	2.11	2.23	2.34	2.44	2.62	2.78
R_h	2.48	3.23	3.79	4.49	5.37	6.45	9.48	14.05
R_s ↵	5.54	6.85	7.68	8.65	9.79	11.14	14.67	19.76
R ↵	7.70	9.43	10.48	11.68	13.05	14.63	18.65	24.26
Δ_{ag}	0.78	0.97	1.04	1.10	1.14	1.15	1.09	0.89
Δ_r	0.21	0.26	0.28	0.30	0.31	0.31	0.30	0.24
Δ_s	0.94	0.19	-0.37	-1.07	-1.95	-3.04	-6.07	-10.63
↓ A_r	4.27	4.64	4.82	4.99	5.16	5.32	5.62	5.94
P_e (SUMMATION)	1.92	1.42	0.95	0.33	-0.50	-1.57	-4.68	-9.49
P_e (BIG-LEAF)	1.02	1.10	1.03	0.86	0.58	0.15	-1.43	-5.33

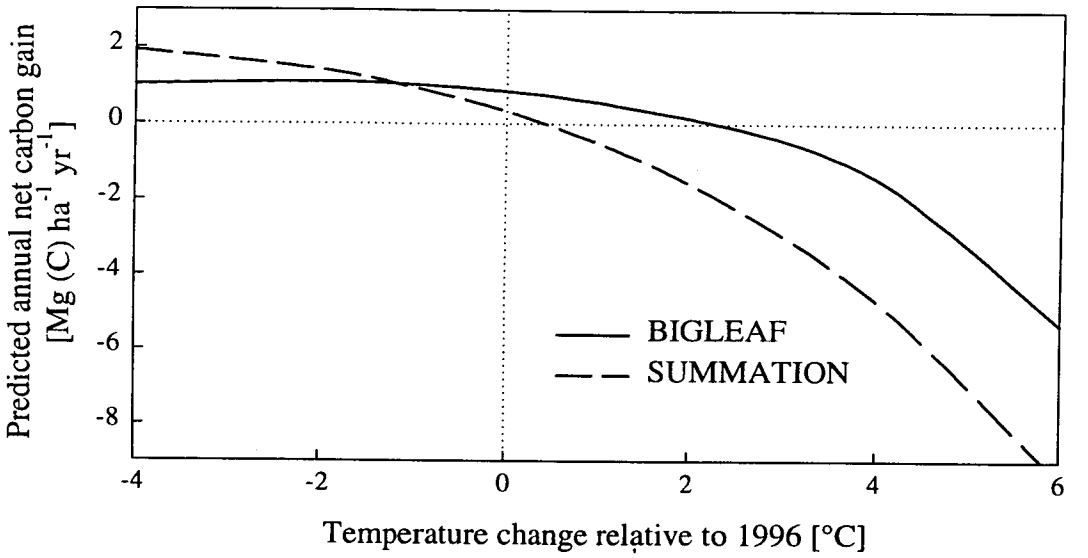

Figure 7.2. Temperature sensitivity of the predicted annual net carbon balance for the BOREAS SSA OBS site in 1996. Temperatures are described relative to temperatures in 1996.

DISCUSSION

Sensitivity of ecosystem carbon balance to temperature

Houghton *et al.* (1995) predict that global mean temperature will rise by between 1.5 °C and 2 °C by the year 2100. This warming is expected to be most pronounced in high northern latitudes, where temperatures are expected to increase by up to 5 °C over the next fifty years. Although this study does not, and cannot, make any statements concerning the effects this warming will have on the function, the structure and, ultimately, the net carbon balance of this ecosystem in the long term, the estimated sensitivity of the 1996 net carbon balance to temperature does give some indication of the ways in which this ecosystem might respond to a changing climate. The most striking feature of the estimated annual net carbon balance of this ecosystem is that gross photosynthetic carbon uptake is, under current temperature conditions, only slightly larger in magnitude than the total respiratory carbon loss (Figure 7.1). Photosynthesis, being a partly diffusive process, is less temperature sensitive than respiration, which is a wholly biological process, and consequently with increasing temperature, the estimated total respiratory carbon loss from this ecosystem will increase much more rapidly than will the estimated gross

photosynthetic carbon uptake (Table 7.1). Thus the ecosystem as a whole is predicted to switch very readily from being a net sink for carbon to being a net carbon source. This switch has been observed in arctic tundra ecosystems (Oechel *et al.* 1993), and if this were to be the case throughout the forests of this biome, it adds weight to the suggestion that the boreal region may be the location of a major positive feedback on global climate change (Lashof 1989; Houghton *et al.* 1995).

It is interesting to note that despite the predicted switch from carbon sink to carbon source at the ecosystem scale, net primary production (NPP) in the trees themselves is, at least for moderate temperature increases, predicted to increase with temperature (Δ_{ag} and Δ_r, Table 7.1). Underlying the prediction that the ecosystem may become a net carbon source is a net reduction in the pool of organic matter in the soil (Δ_s, Table 7.1). Consider the estimated carbon budget for this ecosystem under current conditions, Figure 7.1, the observed increase in annual NPP of the trees, and the calculated reduction in the soil organic matter pool arising from the predicted increase in temperature, suggests that this ecosystem is already responding to a climate that is different to the one in which it was established. For an ecosystem to be sustainable in the long term, one would expect that the soil organic matter pool would, at the very least, not decrease over time, but from the estimated temperature sensitivity of this ecosystem, we can see that the temperature would have to be around 1.6 °C cooler than at present for this to be the case. Thus it seems that even though the net carbon balance of this ecosystem is currently positive, its long term sustainability is questionable.

SUMMARY

Using chamber-based measurements, a carbon balance for the BOREAS Southern Study Area Old Black Spruce site was constructed. The annual net carbon uptake of the ecosystem was the small difference between a large inward flux, gross photosynthetic uptake (12.01 Mg (C) ha^{-1} yr^{-1}), and a large outward flux, total autotrophic plus heterotrophic respiration (11.68 Mg (C) ha^{-1} yr^{-1}). An investigation of the sensitivity of the component fluxes to temperature showed the ecosystem is likely to switch from a carbon sink to a carbon source in response to an increase in annual average temperature of between 0.4 and 2.2 °C.

Concluding Remarks

Understanding the nature of the interaction between the land surface and the atmosphere is one of the most important scientific pursuits of our time. Using chamber studies of the fluxes of carbon and water to and from the major sub-components of a globally important biome, the boreal forest, this thesis has sought to make a contribution to this understanding.

With care, chamber studies can provide estimates of both the instantaneous and the seasonal exchanges of CO_2 between the soil and the atmosphere (Chapters 2 and 3) and between the foliage and the atmosphere (Chapter 4), the two major sub-components of the net ecosystem flux (Figure 7.1). By parameterising physiologically meaningful models with these data (e.g. Chapter 5), I have attempted to "scale up" these chamber measurements to give estimates of these sub-component fluxes for the whole ecosystem (Chapters 3 and 6). Aggregating these sub-component fluxes gives an estimate of the net ecosystem flux, and this was found to compare favourably with direct measurement of the net ecosystem flux by eddy covariance (Chapter 6). The errors associated with the estimates of the sub-component fluxes are quite large (e.g. Figure 3.9), indeed for the two major sub-components the errors may be larger than the net uptake of the ecosystem, and larger than some of the smaller sub-component fluxes (Figure 7.1). If the errors in these estimates are random, this will have no effect on the estimated overall carbon balance, and on any conclusions about the sustainability of the ecosystem drawn from the carbon balance. If, however, there are systematic errors (for example in the estimation of soil CO_2 efflux) erroneous conclusions may be made about the carbon balance of the ecosystem.

Similar considerations about systematic errors need to be applied to eddy covariance data, and here chamber measurements can provide valuable supporting data (Chapter 6). The question of what, if any, low-turbulence corrections to make to eddy covariance data remains, and requires further consideration and experimentation. Nevertheless, the agreement between the whole canopy "physiological" gas-exchange parameters derived from eddy covariance measurements, and the leaf and branch scale gas exchange parameters (Chapter 5) emphasises that the eddy

covariance technique does provide biologically meaningful information that can be used to parameterise the biotic component of models of land surface-atmosphere interactions.

Two interesting scientific questions arising from this thesis stand out, and require immediate further investigation. Firstly, and most importantly, the exact nature of the effect of atmospheric turbulence on the efflux of CO_2 from the soil needs to be further studied. Evaluation of this effect is needed both to ascertain the veracity of chamber-based soil efflux measurements (particularly those measurements made with closed chamber techniques), and also to shed light on possible processes by which the reduction observed in the net ecosystem exchange under conditions of low turbulence may be an accurate description of ecosystem function, and may not necessarily point to a failing of the eddy covariance technique. Secondly, the biological processes governing ecosystem function are by nature dynamical, yet the models that we use to describe these processes are static, (for example the respiration models in Chapter 3 and the photosynthesis model in Chapter 5). The inclusion of dynamic responses in models of ecosystem component function should improve the predictive capacity of these models. For example, the inclusion of a time-constant term in models of stomatal conductance (eq. 5.14) improved the fit of these models in most cases, and there is evidence suggesting that the inclusion of a term relating to photosynthesis on the previous day might improve models of night-time respiration where the only driving variable is temperature (Chapter 6). A description of soil efflux that includes sensitivity to turbulence would also be likely to benefit from the inclusion of a dynamical term, since this sensitivity is very possibly a function of the transient build-up and subsequent turbulence-induced out-flushing of CO_2 from within the soil volume.

The remarkable similarity between the photosynthetic parameters obtained at the whole canopy scale for this boreal forest and for a tropical forest (Chapter 5) is also worth investigating further, since it would appear to suggest that at the canopy scale these two very different ecosystems behave similarly, and that differences in productivity between these ecosystems is essentially a function of the local climatic conditions experienced by each ecosystem.

References

Allen, S.E. (1989) *Chemical Analysis of Ecological Materials.* 2nd Edition edn. Oxford: Blackwell Scientific Publications.

Alvarez, R., Santanatoglia, O.J. and Garcia, R. (1995) Effect of temperature on soil microbial biomass and its metabolic quotient *in-situ* under different tillage systems. *Biology and Fertility of Soils* **19**, 227-230.

Baldocchi, D.D. (1997) Flux footprints within and over forest canopies. *Boundary Layer Meteorology* **85**, 273-292.

Baldocchi, D.D., Hicks, B.B. & Meyers, T.P. (1988) Measuring biosphere-atmosphere exchanges of biologically related gases with micrometeorological methods. *Ecology*, **69**, 1331-1340.

Baldocchi, D.D. and Meyers, T.P. (1991) Trace gas exchange above the floor of a deciduous forest. 1. Evaporation and CO_2 efflux. *Journal of Geophysical Research-Atmospheres* **96**, 7271-7285.

Baldocchi, D.D and Harley, P.C. (1995) Scaling carbon dioxide and water vapour exchange from leaf to canopy in a deciduous forest. II. Model testing and application. *Plant, Cell and Environment* **18**, 1157-1173.

Baldocchi, D., Valentini, R., Running, S., Oechel, W. and Dahlman, R. (1996) Strategies for measuring and modelling carbon-dioxide and water-vapor fluxes over terrestrial ecosystems. *Global Change Biology* **2**, 159-168.

Baldocchi, D.D., Verma, S.B., Matt, D.R. and Anderson, D.E. (1986) Eddy correlation measurements of carbon dioxide efflux from the floor of a deciduous forest. *Journal of Applied Ecology* **23**, 967-975.

Ball, J.T., Woodrow, I.E. and Berry, J.A. (1987) A model predicting stomatal conductance and its contribution to the control of photosynthesis under different environmental conditions. In: Biggins, I. (Ed.) *Progress in Photosynthetic Research*, pp. 221-224. Netherlands: Martinus Nijhoff Publishers

Bigras, F.J., Gonzalez, A., D'Aoust, A.L. and Hebert, C. (1996) Frost hardiness, bud phenology and growth of containerised *Picea mariana* seedlings grown at three nitrogen levels and three temperature regimes. *New Forests* **12**, 243-259.

Bigras, F.J. and Margolis, H.A. (1997) Shoot and root sensitivity of containerised black spruce, white spruce and jack pine seedlings to late fall freezing. *New Forests* **13**, 29-49.

Blanke, M.M. (1996) Soil respiration in an apple orchard. *Environmental and Experimental Botany* **36**, 339-348.

Bonan, G.B. (1992) Soil temperature as an ecological factor in boreal forests. In: Shugart, H.H., Leemans, R. and Bonan, G.B. (Eds.) *A Systems Analysis of the Global Boreal Forest*, pp. 126-143. Cambridge: Cambridge University Press

Bonan, G.B. (1993) Physiological controls of the carbon balance of boreal forest ecosystems. *Canadian Journal of Forest Research* **23**, 1453-1471.

BOREAS (1996) *Field operations in BOREAS*, Washington: NASA.

Brunet, Y., Berbigier, P. and Daudet, F.A. (1992) Carbon dioxide exchanges between a temperate pine forest and the atmosphere: Landes project. *Poster presentation at the first IGAC conference, April 1992.* (Referred to in Ruimy *et al.* 1995)

Chapin, F.S. and Kedrowski, R.A. (1983) Seasonal changes in nitrogen and phosphorus fractions and autumn retranslocation in evergreen and deciduous taiga trees. *Ecology* **64**, 376-391.

Chen, J.M., Rich, P.M., Gower, S.T., Norman, J.M. and Plummer, S. (1997) Leaf area index of boreal forests: theory, techniques, and measurements. *Journal of Geophysical Research-Atmospheres* **102**, 29429-29443.

Ciais, P., Tans, P.P., Trolier, M., White, W.C. and Francey, R.J. (1995) A large northern terrestrial CO_2 sink indicated by the $^{13}C/^{12}C$ ratio of atmospheric CO_2. *Science* **269**, 1098-1102.

Cihlar, J., Chen, J.M. and Li, Z.Q. (1997) Seasonal AVHRR multichannel data sets and products for studies of surface-atmosphere interactions. *Journal of Geophysical Research-Atmospheres* **102**, 29625-29640.

Denmead, O.T. and Raupach, M.R. (1993) Methods for Measuring Gas Transport in Agricultural and Forest Systems. In: Anonymous *Agricultural Ecosystem Effects on Trace Gases and Global Climate Change. ASA Special Publication no. 55.* pp. 19-43.

Denmead, O.T., Raupach, M.R., Dunin, F.X., Cleugh, H.A. and Leuning, R. (1996) Boundary layer budgets for regional estimates of scalar fluxes. *Global Change Biology* **2**, 255-264.

Dufrêne, E., Pontailler, J.-Y. and Saugier, B. (1993) A branch bag technique for simultaneous CO-2 enrichment and assimilation measurements on beech (*Fagus sylvatica* L.) *Plant Cell and Environment* **16**, 1131-1138.

Fang, C. and Moncrief, J.B. (1998) An open-top chamber for measuring soil respiration and the influence of pressure difference on CO_2 efflux measurement. *Functional Ecology* **12**, 319-325.

Farquhar, G.D., von Caemmerer, S. and Berry, J.A. (1980) A biochemical model of photosynthetic CO_2 assimilation in leaves of C_3 species. *Planta* **149**, 78-90.

Farquhar, G.D. and Wong, S.C. (1984) An empirical model of stomatal conductance. *Australian Journal of Plant Physiology* **11**, 191-210.

Field, C. and Mooney, H.A. (1986) The photosynthesis-nitrogen relationship in wild plants. In *On the Economy of Plant Form and Function* (ed. Givnish, T.J.), pp. 25-55. Cambridge University Press, Cambridge.

Fischbeck, H.J. and Fischbeck, K.H. (1987) Formulas Facts and Constants for Students and Professionals in Engineering, Chemistry and Physics, 2nd edn. Berlin: Springer-Verlag.

Frolking, S., Goulden, M.L., Wofsy, S.C., Fan, S.M., Sutton, D.J., Munger, J.W., Bazzaz, A.M., Daube, B.C., Crill, P.M., Aber, J.D., Band, L.E., Wang, X., Savage, K., Moore, T. and Harriss, R.C. (1996) Modelling temporal variability in the carbon balance of a spruce/moss boreal forest. *Global Change Biology* **2**, 343-366.

Goulden, M.L., Munger, J.W., Fan, S.M., Daube, B.C. and Wofsy, S.C. (1996a) Carbon dioxide exchange by a temperate deciduous forest: response to interannual changes in climate. *Science* **271**, 1576-1578.

Goulden, M.L., Munger, J.W., Fan, S. -M., Daube, B.C. and Wofsy, S.C. (1996b) Measurements of carbon sequestration by long-term eddy covariance - methods and a critical-evaluation of accuracy. *Global Change Biology* **2**, 169-182.

Goulden, M.L., Daube, B.C., Fan, S.M., Sutton, D.J., Bazzaz, A., Munger, J.W. and Wofsy, S.C. (1997) Physiological responses of a black spruce forest to weather. *Journal Of Geophysical Research-Atmospheres* **102**, 28987-28996.

Grace, J., Lloyd, J., Mcintyre, J., Miranda, A., Meir, P., Miranda, H., Moncrieff, J., Massheder, J., Wright, I. and Gash, J. (1995) Fluxes of carbon-dioxide and water-vapour over an undisturbed tropical forest in south-west amazonia. *Global Change Biology* **1**, 1-12.

Grace, J., Malhi, Y., Lloyd, J., McIntyre, J., Miranda, A.C., Meir, P. and Miranda, H.S. (1996) The use of eddy covariance to infer the net carbon dioxide uptake of Brazilian rain forest. *Global Change Biology* **2**, 209-217.

Goulden, M.L., Wofsy, S.C., Harden, J.W., Trumbore, S.E., Crill, P.M., Gower, S.T., Fries, T., Daube, B.C., Fan, S.-M., Sutton, D.J., Bazzaz, F.A. and Munger, J.W. (1998) Sensitivity of boreal forest carbon balance to soil thaw. *Science* **279**, 214-217.

Gower, S.T., Vogel, J.G., Norman, J.M., Kucharik, C.J., Steele, S.J. and Stow, T.K. (1997) Carbon distribution and aboveground net primary production in aspen, jack pine, and black spruce stands in Saskatchewan and Manitoba, Canada. *Journal of Geophysical Research-Atmospheres* **102**, 29029-29041.

Hale, S.E. (1997) Turbulent transport above and within a black spruce forest canopy. PhD Thesis, University of Edinburgh.

Halliwell, D.H. and Apps, M.J. (1997) *BOReal Ecosystem-Atmosphere Study (BOREAS) biometry and auxiliary sites: locations and descriptions.* Edmonton. Natural Resources Canada, Canadian Forest Service, Northern Forest Centre.

Hanson, P.J., Wullschleger, S.D., Bohlman, S.A. and Todd, D.E. (1993) Seasonal and topographic patterns of forest floor CO_2 efflux from an upland oak forest. *Tree Physiology* **13**, 1-15.

Harden, J.W., O'Neill, K.P., Trumbore, S.E., Veldhius, H. and Stocks, B.J. (1997) Moss and soil contributions to the annual carbon flux of a maturing boreal forest. *Journal of Geophysical Research-Atmospheres* **102**, 28805-28816.

Harley, P.C., Weber, J.A. and Gates, D.M. (1985) Interactive effects of light, leaf temperature, CO_2 and O_2 on photosynthesis in soybean. *Planta* **165**, 249-263.

Harley, P.C., Thomas, R.B., Reynolds, J.F. and Strain, B.R. (1992) Modelling photosynthesis of cotton grown in elevated CO_2. *Plant, Cell and Environment* **15**, 217-282.

Hollinger, D.Y. (1996) Optimality and nitrogen allocation in a tree canopy. *Tree Physiology* **16**, 627-632.

Hom, J.L. and Oechel, W.C. (1983) The photosynthetic capacity, nutrient content and nutrient use efficiency of different needle age-classes of black spruce (*Picea mariana*) found in interior Alaska. *Canadian Journal of Forest Research* **13**, 834-839.

Houghton, R.A. and Woodwell, G.M. (1989) Global climatic-change. *Scientific American* **260**, 36-44.

Houghton, J.T., Jenkins, G.J. and Ephraums, J.J. (1990) (Eds.) *Climate Change. The IPCC Scientific Assessment*, Cambridge: Cambridge University Press.

Houghton, J.T., Meira Filho, L.G., Callander, B.A., Harris, N., Kattenberg, A. and Maskell, K. (1995) (Eds.) *Climate Change 1995. The Science of Climate Change.* Cambridge: Cambridge University Press.

Jarvis, P.G. (1976) The interpretation of the variations in leaf water potential and stomatal conductance found in canopies in the field. *Philosophical Transactions of the Royal Society of London, Series B-Biological Sciences* **273**, 593-610.

Jarvis, P.G. (1994) Capture of carbon dioxide by a coniferous forest. In: Monteith, J.L., Scott, R.K. and Unsworth, M.H. (Eds.) *Resource capture by forest crops*, pp. 351-374. Nottingham: Nottingham University Press

Jarvis, P.G. and Leverenz, J.W. (1982) Productivity of temperate, deciduous and evergreen forests. In: Lange, O.L., Nobel, P.S., Osmond, C.B. and Ziegler, H. (Eds.) *Encyclopaedia of Plant Physiology*, pp. 233-280. Berlin: Springer-Verlag]

Jarvis, P.G. and McNaughton, K.G. (1986) Stomatal control of transpiration: scaling up from leaf to region. *Advances in Ecological Research* **15**, 1-49.

Jarvis, P.G., Massheder, J.M., Hale, S.E., Moncrieff, J.B., Rayment, M. and Scott, S.L. (1997) Seasonal variation of carbon dioxide, water vapour, and energy exchanges of a boreal black spruce forest. *Journal of Geophysical Research-Atmospheres* **102**, 28953-28966.

Jeffree, C.E., Johnson, R.P.C. and Jarvis, P.G. (1971) Epicuticular wax in the stomatal antechamber of Sitka spruce and its effects on the diffusion of water vapour and carbon dioxide. *Planta* **98**, 1-10.

Jury, W.A., Letey, J. and Collins, T. (1982) Analysis of chamber methods used for measuring nitrous oxide production in the field. *Journal of the Soil Science Society of America* **46**, 250-256.

Kanemasu, E.T., Powers, W.L. and Sij, J.W. (1974) Field chamber measurements of CO_2 flux from soil surface. *Soil Science* **118**, 233-237.

Keeling, R.F., Piper, S.C. and Heimann, M. (1996) Global and hemispheric CO_2 sinks deduced from changes in atmospheric O_2 concentration. *Nature* **381**, 218-221.

Kimball, B.A. and Lemon, E.R. (1971) Air turbulence effects upon soil gas exchange. *Proceedings of the Soil Science Society of America* **35**, 16-21.

Kirschbaum, M.U.F. (1995) The temperature dependence of soil organic matter decomposition, and the effect of global warming on soil organic C storage. *Soil Biology and Biochemistry* **27**, 753-760.

Lamhamedi, M.S. and Bernier, P.Y. (1994) Ecophysiology and field performance of black spruce (*Picea mariana*): a review. *Annals of Forest Science* **51**, 529-551.

Larsen, J.A. (1980) *The Boreal Ecosystem*, New York: Academic Press

Lashof, D.A. (1989) The dynamic greenhouse - feedback processes that may influence future concentrations of atmospheric trace gases and climatic-change. *Climatic Change* **14**, 213-242.

Lavigne, M.B. and Ryan, M.G. (1997) Growth and maintenance respiration rates of aspen, black spruce and jack pine stems at northern and southern BOREAS sites. *Tree Physiology* **17**, 543-551.

Leuning, R. (1995) A critical appraisal of a combined stomatal-photosynthesis model for C_3 plants. *Plant Cell and Environment* **18**, 339-355.

Lewis, J.D., Griffin, K.L., Thomas, R.B. and Strain, B.R. (1994) Phosphorus supply affects the photosynthetic capacity of loblolly-pine grown in elevated carbon dioxide. *Tree Physiology* **14**, 1229-1244.

LI-COR (1990) LI-6200 Primer. An Introduction to Operating the LI-6200 Portable Photosynthesis System. Revision 2. p. 2-7.

Lloyd, J. and Taylor, J.A. (1994) On the temperature dependence of soil respiration. *Functional Ecology* **8**, 315-323.

Lloyd, J., Chin Wong, S., Styles, J.M., Batten, D., Priddle, R., Turnbull, C. and McConchie, C.A. (1995a) Measuring and modelling whole-tree gas exchange. *Australian Journal of Plant Physiology* **22**, 987-1000.

Lloyd, J., Grace, J., Miranda, A.C., Meir, P.W., Wong, S.C., Miranda, B.S., Wright, I.R., Gash, J.H.C. and McIntyre, J. (1995b) A simple calibrated model of amazon rain-forest productivity based on leaf biochemical-properties. *Plant Cell and Environment* **18**, 1129-1145.

Lohammer, T., Larsson, S., Linder, S. and Falk, S.O. (1980) FAST-Simulation models of gaseous exchange in Scots Pine. *Ecological Bulletin* **32**, 505-523.

Lundegårdh, H. (1927) Carbon dioxide evolution of soil and crop growth. *Soil Science* **23**, 417-453.

Mariko, S., Bekku, Y. and Koizumi, H. (1994) Efflux of carbon dioxide from snow-covered forest floors. *Ecological Research* **9**, 343-350.

Meir, P.W. (1996) The exchange of carbon dioxide in tropical forest. PhD Thesis, University of Edinburgh.

Middleton, E.M., Sullivan, J.H., Bovard, B.D., Deluca, A.J., Chan, S.S. and Cannon, T.A. (1997) Seasonal variability in foliar characteristics and physiology for boreal forest species at the five Saskatchewan tower sites during the 1994 boreal ecosystem-atmosphere study. *Journal of Geophysical Research-Atmospheres* **102**, 28831-28844.

Mitchell, A.K. and Hinckley, T.M. (1993) Effects of foliar nitrogen concentration on photosynthesis and water use efficiency in Douglas-fir. *Tree Physiology* **12**, 403-410.

Moncrieff, J.B., Malhi, Y. and Leuning, R. (1996) The propagation of errors in long-term measurements of land-atmosphere fluxes of carbon and water. *Global Change Biology* **2**, 231-240.

Moncrieff, J.B., Massheder, J.M., deBruin, H., Elbers, J., Friborg, T., Heusinkveld, B., Kabat, P., Scott, S., Soegaard, H. and Verhoef, A. (1997a) A system to measure surface fluxes of momentum, sensible heat, water vapour and carbon dioxide. *Journal Of Hydrology* **189**, 589-611.

Moncrieff, J., Valentini, R., Greco, S., Seufert, G. and Ciccioli, P. (1997b) Trace gas exchange over terrestrial ecosystems: methods and perspectives in micrometeorology. *Journal of Experimental Botany* **48**, 1133-1142.

Monteith, J.L., Szeicz, G. and Yabuki, K. (1964) Crop photosynthesis and the flux of carbon dioxide below the canopy. *Journal of Applied Ecology* **1**, 321-337.

Moore, T.R. (1984) Litter decomposition in a sub-arctic, spruce-lichen woodland in eastern Canada. *Ecology* **65**, 299-308.

Nakane, K., Kohno, T., Horikoshi, T. and Nakatsubo, T. (1997) Soil carbon cycling at a black spruce (*Picea mariana*) forest stand in Saskatchewan, Canada. *Journal of Geophysical Research-Atmospheres* **102**, 28785-28793.

Nakayama, F.S. (1990) Soil respiration. *Remote Sensing Reviews* **5**, 311-321.

Nay, S. M., Mattson, K. G. and Bormann, B. T. (1994) Biases of chamber methods for measuring soil CO_2 efflux demonstrated with a laboratory apparatus. *Ecology* **75**, 2460-2463.

Norman, J.M., Garcia, R. and Verma, S.B. (1992) Soil surface CO_2 fluxes and the carbon budget of grassland. *Journal of Geophysical Research-Atmospheres* **97**, 18845-18853.

Norman, J.M., Kucharik, C. J., Gower, S. T., Baldocchi, D. D., Crill, P. M., Rayment, M., Savage, K. & Striegl, R. G. (1997) A comparison of six methods for measuring soil surface carbon dioxide fluxes. *Journal of Geophysical Research-Atmospheres* **102**, 28771-28778.

Oechel, W.C., Hastings, S.J., Vourlitis, G., Jenkins, M., Riechers, G. and Grulke, N. (1993) Recent change of arctic tundra ecosystems from a net carbon-dioxide sink to a source. *Nature* **361**, 520-523.

Ögren, E. and Evans, J.R. (1993) Photosynthetic light-response curves. 1. The influence of CO_2 partial pressure and leaf inversion. *Planta* **189**, 182-190.

Ogunjemiyo, S., Schuepp, P.H., MacPherson, J.I. and Desjardins, R.L. (1997) Analysis of flux maps versus surface characteristics from twin otter grid flights in BOREAS 1994. *Journal of Geophysical Research-Atmospheres* **102**, 29135-29146.

Oke, T.R. (1987) Boundary Layer Climates, 2nd edn. London: Routledge.

Parkinson, K.J. (1981) An improved method for measuring soil respiration in the field. *Journal of Applied Ecology* **18**, 221-228.

Pearcy, R.W. and Sims, D.A. (1994) Photosynthetic acclimation to changing light environments: scaling from the leaf to the whole plant. *Exploitation of environmental heterogeneity by plants* (eds. Caldwell M.M. & Pearcy R.W.), pp. 145-174, Academic Press, San Diego.

Porra, R.J., Thompson, W.A. and Kriedmann, P.E. (1989) Determination of accurate extinction coefficients and simultaneous equations for assaying chlorophylls *a* and *b* extracted with four different solvents: verification of the concentration of chlorophyll standards by atomic absorption spectroscopy. *Biochimica et Biophysica Acta* **975**, 384-394.

Porte A., Loustau D., 1998. Variability of photosynthetic parameters of mature needles within the crown of a 25-year old maritime Pine. *Tree Physiology* **18**, 223-232.

Price, D.T. and Black, T.A. (1990) Effect of short-term variation in weather on diurnal canopy CO_2 flux and evapotranspiration of a juvenile Douglas-fir stand. *Agricultural and Forest Meteorology* **50**, 139-158.

Raich, J.W. and Schlesinger, W.H. (1992) The global carbon dioxide flux in soil respiration and its relationship to vegetation and climate. *Tellus* **44B**, 81-90.

Rayment, M.B. (1995) Sub-canopy scale carbon fluxes in BOREAS. *Poster presentation at the XXth EGS conference, April 1995.* Hamburg.

Rayment, M.B. and Jarvis, P.G. (1997) An improved open chamber system for measuring soil CO effluxes in the field. *Journal of Geophysical Research-Atmospheres* **102**, 28779-28784.

Roberntz, P. and Stockfors, J. (1997) Effects of elevated CO_2 concentration and nutrition on net photosynthesis, stomatal conductance and needle respiration of field-grown Norway spruce trees. PhD Thesis, Swedish University of Agricultural Sciences.

Ruimy, A., Jarvis, P.G., Baldocchi, D.D. and Saugier, B. (1995) CO_2 fluxes over plant canopies and solar radiation: a review. *Advances in Ecological Research* **26**, 1-68.

Ryan, M.G., Lavigne, M.B., Gower, S.T., Flanagan, L.B., Brooks, J.R. and Ehleringer, J.R. (1997) Annual carbon cost of autotrophic respiration in boreal forest ecosystems in relation to species and climate. Photosynthesis and carbon isotope discrimination in boreal forest ecosystems: a comparison of functional characteristics in plants from three mature forest types. *Journal of Geophysical Research-Atmospheres* **102**, 28861-28869.

Saugier, B., Granier, A., Pontailler, J.Y., Dufrene, E. and Baldocchi, D.D. (1997) Transpiration of a boreal pine forest measured by branch bag, sap flow and micrometeorological methods. *Tree Physiology* **17**, 511-519.

Schimel, D.S. (1995) Terrestrial ecosystems and the carbon-cycle. *Global Change Biology* **1**, 77-91.

Schlentner, R.E. and Van Cleve, K. (1985) Relationships between CO_2 evolution from soil, substrate-temperature, and substrate moisture in 4 mature forest types in interior Alaska. *Canadian Journal of Forest Research* **15**, 97-106.

Sellers, P.J., Hall, F.G., Baldocchi, D.D., Cihlar, J., Crill, P., den Hartog, J., Goodison, B., Kelly, R.D., Lettenmaier, D., Margolis, H., Ranson, J. and Ryan, M. (1994) Experiment Plan: Boreal Ecosystem-Atmosphere Study. NASA, Washington.

Sellers, P.J., Hall, F.G., Margolis, H., Kelly, R.D., Baldocchi, D.D., den Hartog, J., Cihlar, J., Ryan, M., Goodison, B., Crill, P., Ranson, J., Lettenmaier, D. and Wickland, D.E. (1995) The Boreal Ecosystem-Atmosphere Study (BOREAS): An Overview and Early Results from the 1994 Field Year. *Bulletin of the American Meteorological Society* **76**, 1549-1577.

Sellers, P.J., Hall, F.G., Kelly, R.D., Black, A., Baldocchi, D., Berry, J., Ryan, M., Ranson, K.J., Crill, P.M., Lettenmaier, D.P., Margolis, H., Cihlar, J., Newcomer, J., Fitzjarrald, D., Jarvis, P.G., Gower, S.T., Halliwell, D., Williams, D., Goodison, B., Wickland, D.E. and Guertin, F.E. (1997) Boreas in 1997: experiment overview, scientific results, and future directions. *Journal of Geophysical Research-Atmospheres* **102**, 28731-28769.

Šesták, Z., Catsky, J. and Jarvis, P. G. (1971) Plant Photosynthetic Production Manual of Methods. Junk, The Hague.

Somerfeld, R.A., Mosier, A.R. and Musselman, R.C. (1993) CO_2, CH_4 and N_2O flux through a Wyoming snow-pack and implications for global budgets. *Nature* **361**, 140-142.

Son, Y. and Kim, H.-W. (1996) Soil respiration in *Pinus rigida* and *Larix leptolepis* plantations. *Journal of Korean Forestry Society* **85**, 496-505.

Sprugel, D.G., Hinckley, T.M. and Schaap, W. (1991) The theory and practice of branch autonomy. *Annual Review of Ecology and Systematics* **22**, 309-334.

Steele, S.J., Gower, S.T., Vogel, C.A. and Norman, J.M. (1997) Root mass, net primary production and turnover in aspen, jack pine and black spruce forests in Saskatchewan and Manitoba, Canada. *Tree Physiology* **17**, 577-587.

Teskey, R.O., Gholz, H.L. and Cropper, Jr., W.P. (1994) Influence of climate and fertilisation on net photosynthesis of mature slash pine. *Tree Physiology* **14**, 1215-1227.

Tryon, P.R. and Chapin, F.S. (1983) Temperature control over root-growth and root biomass in taiga forest trees. *Canadian Journal of Forest Research* **13**, 827-833.

Van Cleve, K., Barney, R. and Schlentner, R. (1981) Evidence of temperature control of production and nutrient cycling in two interior Alaska black spruce ecosystems. *Canadian Journal of Forest Research* **11**, 258-273.

Van Cleve, K., Oechel, W.C. and Hom, J.L. (1990) Response of black spruce (*Picea-mariana*) ecosystems to soil-temperature modification in interior Alaska. *Canadian Journal of Forest Research* **20**, 1530-1535.

von Caemmerer, S. and Farquhar, G.D. (1981) Some relationships between the biochemistry of photosynthesis and the gas exchange of leaves. *Planta* 376-387.

Walcroft, A.S., Whitehead, D., Silvester, W.B. and Kelliher, F.M. (1997) The response of photosynthetic model parameters to temperature and nitrogen concentration in *Pinus radiata* D. Don. *Plant, Cell and Environment* **20**, 1338-1348.

Wang, Y.P. and Jarvis, P.G. (1990) Influence of crown structural properties on PAR absorption, photosynthesis, and transpiration in Sitka spruce - application of a model (MAESTRO). *Tree Physiology* **7**, 297-316.

Winkler, J.P., Cherry, R.S. and Schlesinger, W.H. (1996) The Q-10 relationship of microbial respiration in a temperate forest soil. *Soil Biology and Biochemistry* **28**, 1067-1072.

Wofsy, S.C., Goulden, M.L., Munger, J.W., Fan, S.M., Bakwin, P.S., Daube, B.C., Bassow, S.L. and Bazzaz, F.A. (1993) Net exchange of CO_2 in a mid-latitude forest. *Science* **260**, 1314-1317.

Wullschleger, S.D. (1993) Biochemical limitations to carbon assimilation in C_3 plants - a retrospective analysis of the A/C_i curves from 109 species. *Journal of Experimental Botany* **44**, 907-920.

Vowinckel, T., Oechel, W.C. and Boll, W.G. (1974) The effect of climate on the photosynthesis of *Picea mariana* at the subarctic tree line. 1. Field measurements. *Canadian Journal of Botany* **53**, 604-620.

Yue, D. and Margolis, H. (1993) Photosynthesis and dark respiration of black spruce cuttings during rooting in response to light and temperature. *Canadian Journal of Forest Research* **23**, 1150-1155.

Zine El Abidine, A., Stewart, J.D., Bernier, P.Y. and Plamondon, A.P. (1995) Diurnal and seasonal variation in gas exchange and water relations of lowland and upland black spruce ecotypes. *Canadian Journal of Botany* **73**, 716-722.

Appendix

Parameter values and switches used in the MAESTRA simulation and their sources.

Parameter	Description	Value	Notes
NOLAY	Number of canopy layers	6	
NZEN	Number of zenith angles	5	
NAZ	Number of azimuth angles	11	
MODELGS	Stomatal conductance model	1	Jarvis-type
MODELJM	Source of Farquhar parameters	0	Read from file
MODELRD	Source of leaf respiration parameters	0	Read from file
MODELRW	Source of wood respiration parameters	0	Read from file
MODELSS	Sun and shade leaf treatment	0	Leaves treated separately
XMAX	Plot length in x- direction (m)	30	*
YMAX	Plot length in y-direction (m)	30	*
NOTREES	Number of trees in the plot	250	*
BEARING	x-axis bearing of from south (°)	-90	*
XSLOPE	Slope of plot in x- direction (°)	0	*
YSLOPE	Slope of plot in y- direction (°)	0	*
LATHEM	Hemisphere	N	BOREAS (1996)
LAT	Latitude (°)	53° 59' 13"	BOREAS (1996)
LONHEM	Hemisphere	W	BOREAS (1996)
LONG	Longitude (°)	105° 7' 5"	BOREAS (1996)
TZLONG	Longitude of the meridian of the time zone (°)	90	BOREAS (1996)
DIFSKY	Distribution of diffuse radiation	0	Uniform (Default)
PRESS	atmospheric pressure (Pa)	94000	Standard pressure at site
JLEAF	Leaf area density distribution	1	Vertical beta distribution
NOAGEC	Number of age classes for which leaf area distribution specified	1	
BPT	Leaf area density distribution beta function parameters	105 2 4	P.G. Jarvis & B.Kruijt University of Edinburgh
RANDOM	Clumping factor	0.33	Ratio of projected shoot area to projected needle area
CSHAPE	Crown shape	CYL	Upright cylinder
ELP	Leaf angle distribution parameter	1.0	Spherical distribution

Parameter	Description	Value	Notes
NALPHA	Number of leaf angle classes	1	
EXTWIND	Exponential coefficient of wind speed decline within canopy	0.19	Hale 1997
COEFFT	Coefficient of allometric relationship between woody biomass and DBH	0.0000647	Derived from Gower *et al.* 1997
EXPONT	Exponent of above	1.39405	As above
ZPD	Zero-plane displacement (m)	4.5	Hale 1997
Z0HT	Roughness length (m)	1.03	Hale 1997
ZHT	Measurement height (m)	25.8	Jarvis *et al.* 1997
INDIVRADX	Individual crown radius in X direction (m)	*	
INDIVRADY	Individual crown radius in Y direction (m)	*	
INDIVHTCROWN	Individual crown height (m)	*	
INDIVHTTRUNK	Individual trunk height (m)	*	
INDIVDIAM	Individual DBH (m)	*	
INDIVLAREA	Individual crown leaf area (m^2 $tree^{-1}$)	*	
TAIR	Air temperature (°C)	†	
RH	Relative humidity (fraction)	†	
CA	Atmospheric CO_2 concentration (ppm)	†	
WIND	Wind speed above the canopy ($m\ s^{-1}$)	†	
TSOIL	Soil temperature (°C)	†	
PAR	Incident PAR ($\mu mol\ m^{-2}\ s^{-1}$)	†	
MFD	Humidity deficit (mmol H_2O mol^{-1} air)	†	Not standard in Maestra
NOAGEP	Number of age classes for which physiological parameters specified	1	
RHOSOL	Soil reflectance in three wavebands (PAR, NIR, thermal)	0.10 0.30 0.05	B. Kruijt University of Edinburgh
ATAU	Leaf transmittance in three wavebands (PAR, NIR, thermal)	0.05 0.30 0.01	B. Kruijt University of Edinburgh
ARHO	Leaf reflectance in three wavebands (PAR, NIR, thermal)	0.10 0.25 0.05	B. Kruijt University of Edinburgh

Parameter	Description	Value	Notes
JMAX	J_{max} (μmol e^- m^{-2} s^{-1})	0‡	20/03/96
		22‡	09/04/96
		70‡	19/05/96
		80‡	07/08/96
		60‡	06/11/96
		0‡	05/12/96
VMAX	V_{max} (μmol CO_2 m^{-2} s^{-1})	0‡	20/03/96
		18‡	19/05/96
		20‡	18/07/96
		18‡	16/09/96
		0‡	15/11/96
THETA	Curvature of the electron transport light-response curve	0.67	D. Loustau in prep.
EAVJ	Activation energy of J_{max} (J mol^{-1} K^{-1})	46337	D. Loustau in prep.
EDVJ	Deactivation energy of J_{max} (J mol^{-1} K^{-1})	198900	D. Loustau in prep.
DELSJ	Entropy term (J mol^{-1})	650	D. Loustau in prep.
EAVC	Activation energy of V_{max} (J mol^{-1} K^{-1})	52,200	D. Loustau in prep.
RD	Leaf dark respiration rate (μmol m^{-2} s^{-1})	0.9‡	20/03/96
		0.7‡	29/04/96
		0.4‡	27/08/96
		0.5‡	16/09/96
		0‡	26/11/96
RTEMP	Temperature at which RD specified (°C)	17.5‡	
Q10F	Foliage respiration temperature response exponent	0.069‡	
DAYRESP	Fraction by which dark respiration reduced in the light	0.4	B. Kruijt University of Edinburgh
GSREF	Maximum stomatal conductance (mol m^{-2} s^{-1})	0.0325‡	
GSMIN	Cuticular conductance (mol m^{-2} s^{-1})	0.0066‡	
PAR0	Stomatal conductance irradiance response parameter	0.995‡	Exponential rise to maximum, not standard in Maestra
D0	Stomatal conductance humidity response parameter (mmol H_2O mol^{-1} air)	53.2‡	Linear humidity deficit response, not standard in Maestra

Parameter	Description	Value	Notes
T0	Low temperature at which stomatal conductance = GSMIN (°C)	-2‡	Beta function temperature response, not standard in Maestra
TREF	Temperature at which stomatal conductance = GSREF (°C)	30‡	As above
TMAX	High temperature at which stomatal conductance = GSMIN (°C)	52‡	As above
WLEAF	Width of leaf (m)	0.001‡	
NSIDES	Number of sides of the leaf with stomata	1‡	
EFFY	Efficiency of woody biomass growth (mol CO_2 g^{-1} DW)	1.0875	Derived from Lavigne & Ryan 1997
RMW	Woody biomass maintenance respiration rate (nmol g^{-1} DW s^{-1})	0.142	Derived from Rayment unpublished data and Lavigne & Ryan 1997
Q10W	Woody biomass respiration temperature response exponent	0.059	As above
RTEMP	Temperature at which RMW specified	15	As above

* Data describing the stand structure for the simulated plot were created by a MS Visual Basic programme such that the model stand had the same distribution of size class, sapwood thickness, trunk height and crown height characteristics and the same total leaf area as the actual study area (stand characteristics derived from Gower *et al.* 1997; Chen *et al.* 1997; Halliwell & Apps 1997; Dr. R. Knox NASA/GSFC, Greenbelt, MD.).

† Meteorological data from automatic weather station at the OBS site.

‡ This study. Values are those obtained from measurements made on shoots wherever possible, or, when unavailable, from branch measurements.